



Copernicus Atmosphere Monitoring Service



Validation report of the CAMS near-real time global atmospheric composition service

System evolution and performance statistics Status up to 1 December 2015

Issued by: KNMI

Date: 29/02/2016

REF.: CAMS84_2015SC1_D.84.1.2-2016Q1_201602





This document has been produced in the context of the Copernicus Atmosphere Monitoring Service (CAMS). The activities leading to these results have been contracted by the European Centre for Medium-Range Weather Forecasts, operator of CAMS on behalf of the European Union (Delegation Agreement signed on 11/11/2014). All information in this document is provided "as is" and no guarantee or warranty is given that the information is fit for any particular purpose. The user thereof uses the information at its sole risk and liability. For the avoidance of all doubts, the European Commission and the European Centre for Medium-Range Weather Forecasts has no liability in respect of this document, which is merely representing the authors view.



Validation report of the CAMS near-real-time global atmospheric composition service.

System evolution and performance statistics.

Status up to 1 December 2015

Editors:

V. Huijnen (KNMI), H.J. Eskes (KNMI), M. Schulz (MetNo),
S. Chabrillat (BIRA-IASB)

Authors:

S. Basart (BSC), A. Benedictow (MetNo), A.-M. Blechschmidt (IUP-UB),
S. Chabrillat (BIRA-IASB), Y. Christophe (BIRA-IASB), H. Clark (CNRS-LA),
E. Cuevas (AEMET), H. Flentje (DWD), K. M. Hansen (AU), U. Im (AU),
J. Kapsomenakis (AA), B. Langerock (BIRA-IASB), A. Richter (IUP-UB),
M. Schulz (MetNo), N. Sudarchikova (MPI), V. Thouret (CNRS-LA),
A. Wagner (DWD), C. Zerefos (AA)

Report of the Copernicus Atmosphere Monitoring Service,
Validation Subproject (CAMS-84).

Date:

29 February 2016.

Status:

Final

Citation:

Validation report of the CAMS near-real-time global atmospheric composition service. System evolution and performance statistics; Status up to 1 December 2015. V. Huijnen, H.J. Eskes, S. Basart, A. Benedictow, A.-M. Blechschmidt, S. Chabrillat, Y. Christophe, H. Clark, E. Cuevas, H. Flentje, K.M. Hansen, U. Im, J. Kapsomenakis, B. Langerock, A. Richter, N. Sudarchikova, M. Schulz, V. Thouret, A. Wagner, C. Zerefos, Copernicus Atmosphere Monitoring Service (CAMS) report, CAMS84_1_D1.2_201602, February 2016.

Available at:

http://atmosphere.copernicus.eu/quarterly_validation_reports



Executive Summary

The Copernicus Atmosphere Monitoring Service (CAMS, <http://atmosphere.copernicus.eu>) is a component of the European Earth Observation programme Copernicus. The CAMS global near-real time (NRT) service provides daily analyses and forecasts of reactive trace gases, greenhouse gases and aerosol concentrations. The CAMS system was developed by a series of MACC research projects (MACC I-II-III) until July 2015. This document presents the validation statistics and system evolution of the CAMS NRT service for the period until 1 December 2015. Updates of this document appear every 3 months.

This summary is split according to areas of interest to users: Climate forcing, regional air quality, and stratospheric ozone. Specific attention is given to the ability of the CAMS system to capture recent events. We focus on the 'o-suite', which is based on the C-IFS (Composition-IFS) modelling system at ECMWF and which produces daily analyses and forecasts based on available meteorological and atmospheric composition observations using the ECMWF 4D-Var assimilation system. For analyses and forecasts of trace gases the CB05 tropospheric chemistry is used, while for aerosol this is the CAMS prognostic aerosol module. We furthermore assess the impact of the composition observations by comparing the validation results from the 'o-suite' to a 'control' configuration without assimilation.

The o-suite data delivery for the period September-November 2015 was reliable, with 95% of the forecasts delivered before 22:00 UTC. Since December 2012 on average 96% of the forecasts were delivered on time.

Climate forcing

Tropospheric ozone (O₃)

Model ozone is validated with respect to surface and free tropospheric ozone observations from the GAW and ESRL networks, IAGOS airborne data and ozone sondes. For free tropospheric ozone against sondes the o-suite modified normalized mean biases (MNMBs) are on average between -20 and +10% over the Northern Hemisphere (NH), and with MNMBs ranging between -30% and +40% for Tropics Antarctic stations (Fig. S1). This is an improvement compared to the control experiment without the assimilation of composition observations. For September-November 2015 good agreement is found over the NH mid latitudes, which is confirmed with IAGOS evaluations over Frankfurt and Dusseldorf. Larger biases are found over the southern hemisphere mid-latitudes and Antarctica by up to +30% in January 2015.

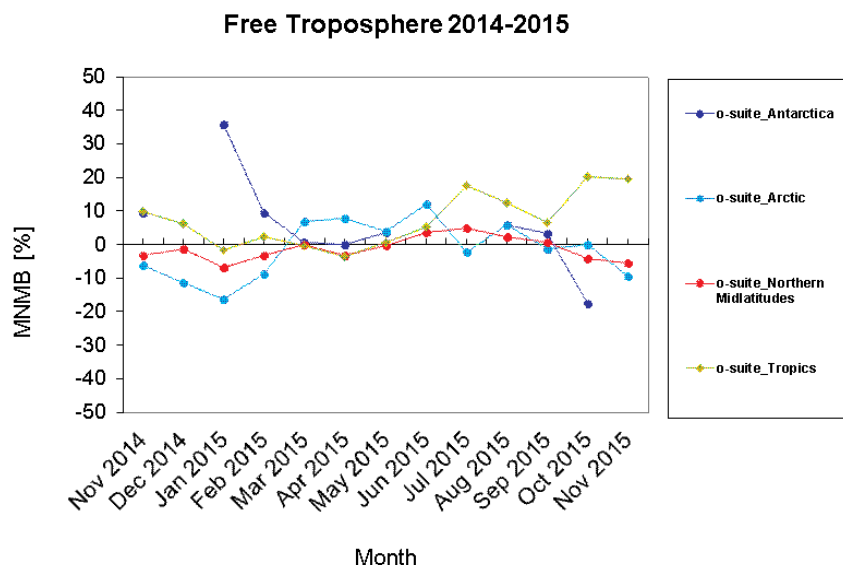


Figure S1: Time series of MNMB of ozone in the o-suite, compared against ozone sondes, averaged over different latitude bands.

Evaluation against IAGOS also shows that the model runs have some difficulty in reproducing the variability of ozone in the tropopause region. The models generally show a positive bias in ozone throughout the troposphere.

At the surface, both GAW and ESRL stations show an overestimation of surface ozone during September and November 2015, except for the high latitude stations. MNMBs range between 4-20% for European stations and MNMBs are larger for stations located in Asia and the Tropics (30%- 40%, respectively). Towards the end of the period (November) MNMBs improve. Free tropospheric ozone is captured by the models over Europe with MNMBs < 5%.

Tropospheric Nitrogen dioxide (NO₂)

Model validation, with respect to SCIAMACHY/Envisat NO₂ data before April 2012 and GOME-2/MetOp-A NO₂ data afterwards, shows that tropospheric NO₂ columns are well reproduced by the NRT model runs, indicating that emission patterns and NO_x photochemistry are generally well represented. Since December 2014, the agreement between satellite retrievals and model results for seasonal maxima over East-Asia and Europe is better than for previous years (Fig. S2), mainly because observed columns of NO₂ decreased recently, likely associated with reduced emissions. Spring and summertime values over East-Asia are overestimated by the o-suite in 2015, a feature which does not occur for previous years. Compared to satellite data, tropospheric background values over Africa and South America are currently underestimated by the models. All model runs overestimate boreal forest fire emissions over Canada and Siberia, which leads to local maxima that do not show up in the satellite retrievals. Evaluation against MAX-DOAS observations illustrates the positive impact of data assimilation for urban sites, leading to an increase in NO₂.

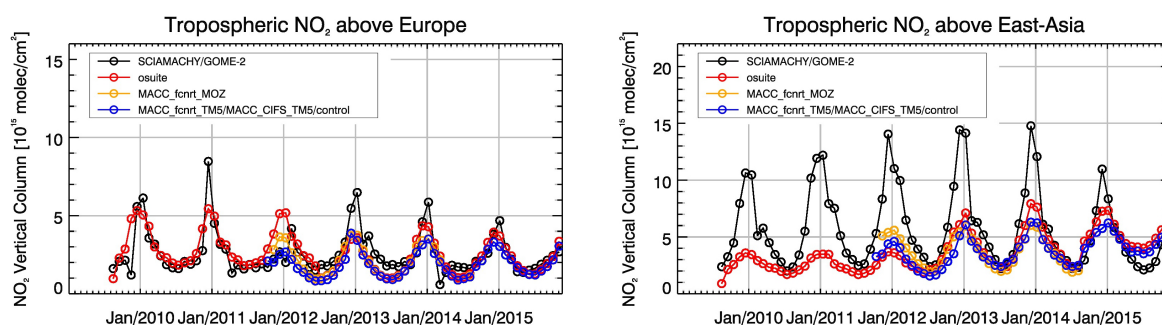


Figure S2: Time series of tropospheric NO₂ columns from SCIAMACHY (up to March 2012), GOME-2 (from April 2012 onwards) compared to model results for Europe and East-Asia. The o-suite is in red, control is in blue (before Sept 2014 blue and yellow represent older model configurations).

Tropospheric Carbon Monoxide (CO)

Model validation with respect to GAW network surface observations, IAGOS airborne data, FTIR observations and MOPITT and IASI satellite retrievals reveals that the seasonality of CO can be reproduced well by all models. In

comparison with satellite retrievals (MOPITT, IASI) for the annual cycle over different regions it is found that modelled CO seasonality is mostly in good agreement with the retrievals, although significant differences between MOPITT and IASI are observed over many parts of the globe. Comparatively small negative biases (-5%) appear in the o-suite during winter and early spring in Europe and the US in 2015, which has improved against previous years. Also during the fire season over Alaska and Siberia negative biases are only up to -5% for this model run. Still the o-suite, as well as the Control, overestimate CO total columns in the tropics and SH. Significant positive biases up to 50% for Control are found over the central part of South America and for Indonesia.

At the surface, in Europe and Asia observed CO mixing ratios are still underestimated by the models. Free tropospheric background CO mixing ratios show a good correspondence to the observed CO concentrations in Europe and Asia. A marked period with enhanced levels of CO as observed by IAGOS over the Frankfurt station, possibly associated with enhanced heating emissions during cold weather conditions, are not captured by the o-suite.

Formaldehyde

Model validation, with respect to SCIAMACHY/Envisat HCHO data before April 2012 and GOME-2/MetOp-A HCHO data afterwards, shows that modelled monthly HCHO columns for September-November 2015 represent well the magnitude of oceanic and continental background values and the overall spatial distribution in comparison with mean satellite HCHO columns. Simulated maxima over South America are generally underestimated compared to GOME-2 satellite retrievals, while there is a strong overestimation of values for Northern Australia and Central Africa. For time series over East-Asia and the

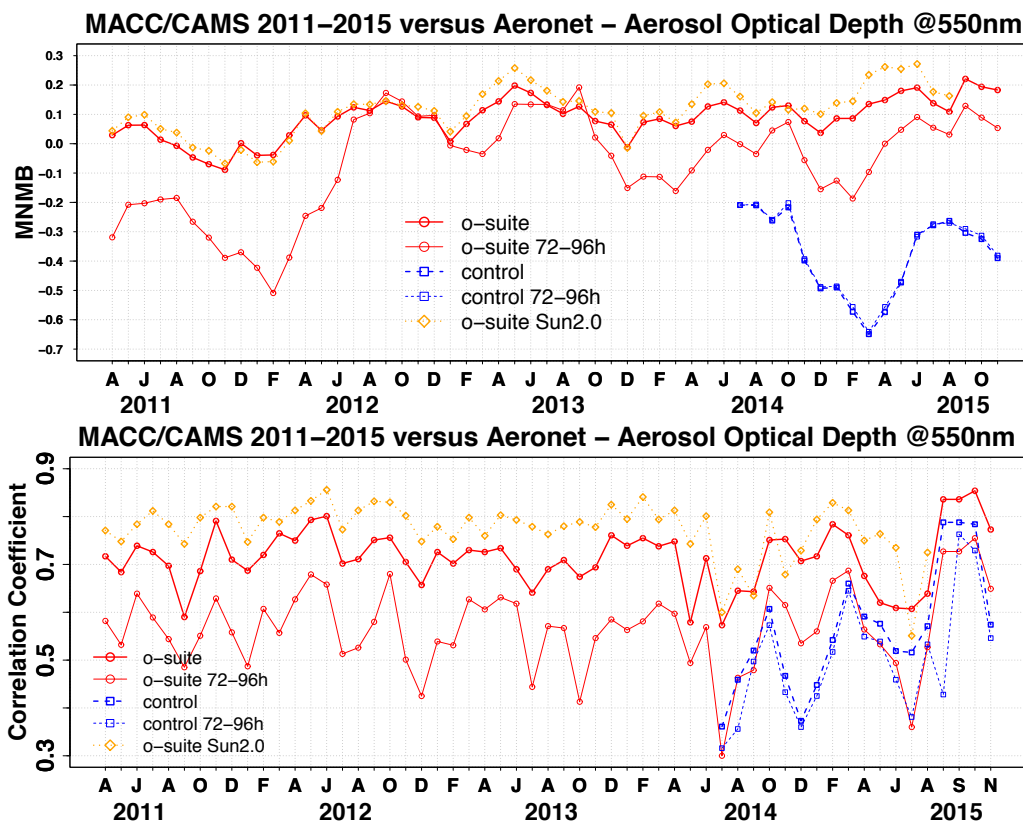


Figure S3. Aerosol optical depth at 550nm in IFS model simulations for April 2011 - November 2015 against daily matching Aeronet NRT level 1.5 and level 2.0 data a) Modified normalized mean bias (MNMB); o-suite (thick red curve); o-suite at last forecast day (light red curve); Control (blue dashed); Control at last forecast day (light blue dashed); o-suite but evaluated against quality assured Aeronet level 2.0 data (orange dashed); b) Corresponding correlation coefficient. Note that quality assured level 2.0 data amount decreases from ca 3000 data points per month (status for mid of 2014) to 500 data points in the last month of the time series.

Eastern US, both regions where HCHO columns are probably dominated by biogenic emissions, models and retrievals agree rather well. However, the yearly cycle over East-Asia is underestimated by the models. For Indonesia simulated values are strongly over-estimated for September and October 2015, associated with errors in fire HCHO emissions over this region.

The validation of model profiles with ground-based UV-VIS DOAS measurements over Xianghe, near Beijing, shows that background column values are underestimated by around 30%. The latter is in agreement with satellite observations, which also show an underestimation for East-Asia. It is also seen that local pollution events are not captured correctly, in part due to the relatively coarse horizontal resolution of the global models, and in part associated with uncertainties in HCHO and precursor emissions. It should be noted that no formaldehyde observations are assimilated, and these results reflect the performance of the unconstrained models.

Aerosol



We estimate that the o-suite aerosol optical depth showed an average positive bias in 2015 of +20%, measured as modified normalized mean bias against daily Aeronet sun photometer data. The latest model version, in place since October 2013, has a smaller positive bias (+10%) in winter, increasing in summer (+25%). The +3 day forecasted aerosol distributions, since July 2012, show 10-30% less aerosol optical depth (AOD) than those from the initial day, as shown all in Figure S3a. Correlation, shown in figure S3b, shows month-to-month variation ranging from 0.65 to 0.8, indicating the simulation reproduces approximately 50% of the day to day AOD variability across all Aeronet stations, with no clear trend. The o-suite forecast at +3 days shows slightly lower correlation, as a consequence of imperfect forecasted meteorology and fading impact of the initial assimilation of MODIS AOD and MODIS fire info on model performance.

The regional AOD performance of the o-suite with respect to the AERONET data exhibits a seasonal cycle depending on region. Variations in correlation, which are larger than 0.1 from month-to-month and region-to-region, can be viewed as significant. A lower correlation in autumn in North America can be noted. A continued negative bias is shown in South-Eastern Asia, and last months show a higher positive bias in North America.

Since October 2013 a revised aerosol model version has led to a shift in modelled aerosol composition. AOD due to sea salt decreased by 50%, while that of sulphate increased by 60%. The aerosol Ångström exponent contains information about the size distribution of the aerosol, and implicitly composition. As a consequence of the aerosol composition shift, the o-suite shows in SON 2015 a positive global bias against Aeronet data of +20% (indicating too fine particles in the model), which is significantly different from the more negative bias before October 2013. Correlation is slightly lower as compared to 2013.

Modelled dust optical depth over different sub-regions of North Africa were compared with AERONET sun photometers observations of coarse and total aerosol optical depths. The o-suite is also compared to a multi-model ensemble established at the WMO-SDS regional center BSC/AEMET. The o-suite reproduces high dust peaks fairly well. The quality of the o-suite is very similar to the multi-model Median but varies from region to region.

An evaluation of the PM10 surface concentration against a climatological average (2000-2009) at 155 remote sites in North America and Europe indicates an overestimation of sea salt concentrations, visible in coastal regions, leading to an overall positive bias of 30%.

System performance in the Arctic



The CAMS model runs are validated using surface ozone measurements from the ESRL-GMD the IASOA networks (2 sites) and ozone concentrations in the free troposphere are evaluated using balloon sonde measurement data. CO total columns are compared to MOPITT V5 and V6 (thermal infrared radiances) and IASI observations. More data sets will be added to the validation in the next report.

For the period from December 2014 to November 2015 the simulations of the surface ozone concentrations are on average in good agreement with the observations apart from ozone depletion events in March – June 2015, which are not captured by the model simulations. These events are related to halogen chemistry reactions that are not represented in the C-IFS model.

For the September – November 2015 period the surface ozone concentrations are underestimated at the two sites by -4% and -10% (o-suite) and -9% and -20% (control). The short term variability is well captured at Barrow, Alaska ($r=0.9$) for both runs, but not in Northern Greenland. In the free troposphere the MNMB of ozone is between 0% and -10% for the o-suite, while it is around +10% for the control run.

Data coverage of total column CO is not complete over the Arctic, but the model runs generally underestimate total column CO in the Arctic, except over most of Greenland where the total column CO is overestimated. The o-suite generally performs better than the control run.

System performance in the Mediterranean

The CAMS model run performance in the Mediterranean is evaluated using AOD observations from 42 AERONET sites. During September to November 2015, CAMS o-suite reproduces better the daily variability of AERONET observations than the control experiment, which tends to underestimate the background levels over Southern European sites (more influenced by urban/industrial aerosol sources). Observations at 12 Airbase background sites show that the CAMS experiments reproduce the daily variability of the most intense aerosol events observed, which are associated with long-range desert dust transport. However, the magnitude predicted by the CAMS simulations (control and o-suite) is overestimated. In general, CAMS o-suite presents better results in terms of mean biases for both PM₁₀ and PM_{2.5}.

The model is further compared to surface O₃ observations from the AirBase network. Our analysis shows that both model runs in general underestimate surface O₃ in a group of stations located in the north-east Spain down to -30%. The model reproduces well the mean surface concentration over stations located in the south and east-south-east Spain Mediterranean shore (MNMBs \approx 0) as well as over Finokalia station in Crete, Greece. Finally, both runs slightly overestimate ozone mixing ratios by 10% at Plan Aups/Ste Baume

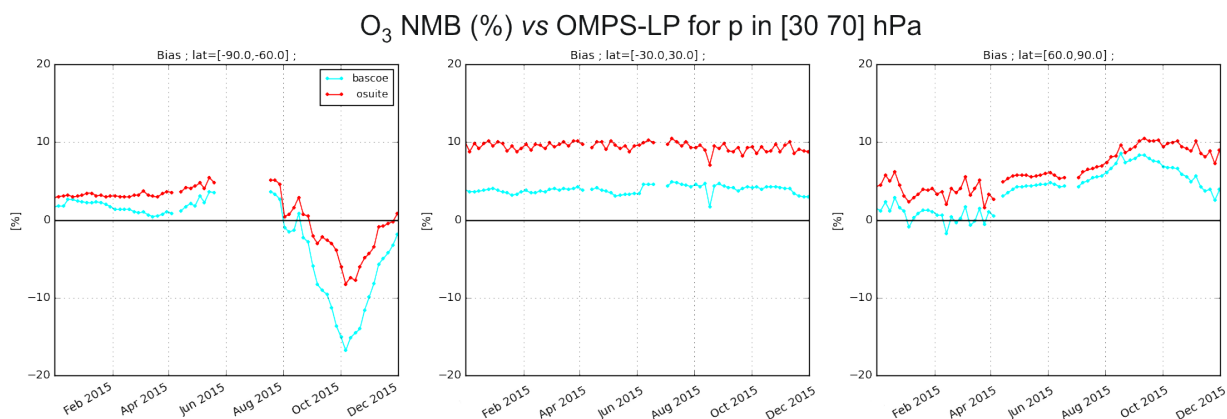


Figure S4. Time evolution of the Normalized Mean bias ((model-obs)/obs in %) for ozone from the o-suite (red) and BASCOE (cyan) using OMPS-LP satellite observations: middle stratosphere (30-70hPa) averages.

station, in South France. Correlations between simulated and observed surface ozone are high for both o-suite and control runs over all stations with few exceptions (r up to 0.8).

Regional air quality

Ozone, CO and aerosol boundary conditions

Free tropospheric ozone concentrations in the o-suite in the northern midlatitudes are generally in good correspondence with ozone sondes, MNMBs in the range of $\pm 10\%$. The o-suite shows a positive bias in surface ozone concentrations in Europe, North America and Asia, with MNMBs for GAW and ESRL stations ranging between 5% and 25% between June 2015 and November 2015. All model runs underestimate CO surface concentrations in Europe and East Asia with MNMBs with respect to GAW up to -15%. This has improved compared to CO biases for previous years. Evaluation of the PM₁₀ surface concentration in North America and Europe indicates an overestimation of sea salt concentrations, likely explaining the overall positive bias in PM₁₀ of 30%.

Ozone layer

Ozone partial columns and vertical profiles

Ozone columns and profiles have been compared with the following observations: vertical profiles from balloon-borne ozonesondes; ground-based remote-sensing observations from the NDACC (Network for the Detection of Atmospheric Composition Change, <http://www.ndacc.org>); and satellite observations by the limb-scanning instruments Aura-MLS (assimilated) and OMPS. Furthermore, the o-suite analyses are compared with those delivered by two independent assimilation systems: BASCOE, and TM3DAM.

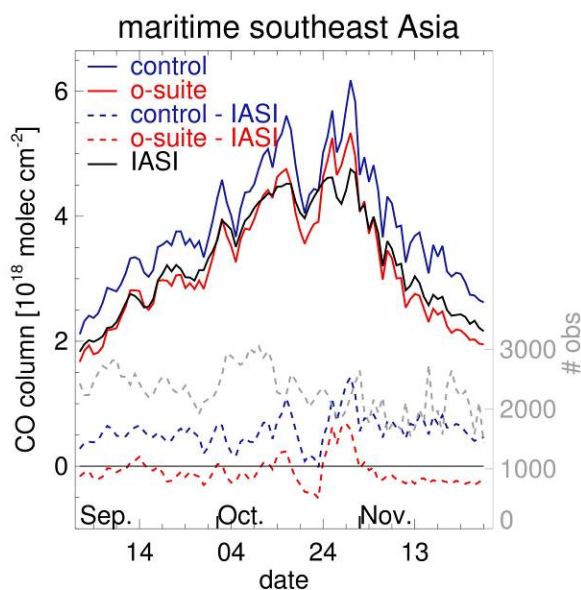


Figure S5. Time series of three-day running mean CO total column from model simulations and IASI satellite observations over a region including Indonesia and its outflow region over the ocean (70°E - 150°E and 11°S - 6°N), and their biases (dashed lines). The scaled daily number of available observations (right axis) is given in grey.

Compared to ozone sondes the model O_3 partial pressures are mostly slightly overestimated in all latitude bands (MNMB between 0 and +10%). For total columns, the dedicated system TM3DAM is used as a reference because it assimilates GOME-2 data which is bias-corrected using surface Brewer-Dobson measurements. In the Arctic and the Tropics, the o-suite gives results nearly identical to TM3DAM (a slight underestimation of 2-3 DU is noted in the Tropics but this is well within the observational uncertainties).

In the Antarctic, the o-suite matches TM3DAM during the whole period except for the months of March-April 2015 (underestimation of 10DU at most) and July 2015 (overestimation reaching 15DU in mid-July).

The comparison with OMPS-LP delivers a good agreement in the middle stratosphere and an overestimation by the o-suite in the lower stratosphere, reaching 10% in the Tropics (70 hPa) and the Antarctic (100 hPa) and 20% in the mid-latitudes and the Arctic (100 hPa). The time evolution of the normalized mean bias in the lower middle stratosphere (figure S4) shows a systematic overestimation by the o-suite (5-10%), except over the Antarctic in September-November (i.e. ozone hole season) where the o-suite underestimates ozone by up to 8%. Hence the polar ozone depletion described by the o-suite analyses is stronger than observed by OMPS-LP.

Comparisons with the NDACC network use microwave observations for Ny Alesund (78.9°N) and Bern (47°N) and LIDAR observations at Hohenpeissenberg (47.8°N) and Lauder (45°S). Among these stations the o-suite performs best at Bern with stratospheric columns evolving since 1 Sept. 2014 with seasonally averaged relative biases smaller than 5%, which is smaller than the reported



measurement uncertainties. At Ny Alesund, the seasonally averaged bias of the stratospheric column has decreased during summer months but since Sept 2015, the o-suite overestimates (>10%) the ozone abundance between 25km and 35km. Compared with the LIDAR at Lauder and Hohenpeissenberg, the o-suite does not show significant biases with the observed ozone between 25km and 35km.

Other stratospheric trace gases

Due to the lack of stratospheric chemistry in the C-IFS-CB05 scheme, the only useful product in the stratosphere is ozone. NO₂ columns have nonetheless be compared with the GOME-2/MetOP-A satellite retrievals, and the unfavourable results confirm that the latest version of o-suite does not provide a useful stratospheric NO₂ product

Events

The year 2015 was marked by a *strong El Niño* event which intensified the dry season over large regions of Indonesia. During September and October 2015 the *largest amount of fire emissions were recorded in Indonesia* since 1997, based on GFAS and GFED emissions time series.

The o-suite CO total columns showed among the highest amounts of CO recorded, in agreement with both IASI and MOPITT CO satellite observations (Figure S5). The control run shows a growing positive bias by 15% to 25%, suggesting a net positive bias in the GFAS CO emissions. Also evaluation against GOME-2 HCHO observations suggests a positive bias in HCHO emissions by about 30%.

Around 13 November a high *layer of dust* moved from north-western Africa covering the area around the Canary Islands. The o-suite is able to timely reproduce the spatial distribution of the dust plume as observed by MODIS over the ocean, although the spatial extent of the dust layer is quite low. Also the model tracks fairly well the changes in the shape and size of the dust layer throughout the episode. The model shows a clear overestimation on the onset of the dust event in both the Santa Cruz de Tenerife and Izana stations. The whole episode is a bit better simulated by CAMS o-suite than control although in Santa Cruz de Tenerife and Izana stations with regard to the ability to capture the peak in AOD.



Table of Contents

1	Introduction	12
2	System summary and model background information.....	15
2.1	System based on the ECMWF IFS model	15
2.2	Evolution of the IFS-based system	18
2.3	Other systems.....	19
2.4	CAMS products.....	20
2.5	Availability and timing of CAMS products.....	20
3	Validation results	22
3.1	Tropospheric Ozone	22
3.2	Tropospheric nitrogen dioxide.....	36
3.3	Carbon monoxide	40
3.4	Formaldehyde	53
3.5	Aerosol.....	57
3.6	Stratospheric ozone	76
3.7	Stratospheric NO ₂	85
4	Events	87
4.1	Fires in Indonesia, September-October 2015	87
4.2	A dust event over Canary Islands in November 2015	90
5	References	94
	Annex 1: Acknowledgements.....	98



1 Introduction

The Copernicus Atmosphere Monitoring Service (CAMS, <http://atmosphere.copernicus.eu/>) is a component of the European Earth Observation programme Copernicus. The CAMS global near-real time (NRT) service provides daily analyses and forecasts of trace gas and aerosol concentrations. The CAMS system was developed by a series of MACC research projects (MACC I-II-III) until 1 December 2015.

The CAMS near-real time services consist of daily analysis and forecasts with the Composition-IFS system with data assimilation of trace gas concentrations and aerosol properties. This document presents the system evolution and the validation statistics of the CAMS NRT global atmospheric composition analyses and forecasts. The validation methodology and measurement datasets are discussed in Eskes et al. (2015).

In this report the performance of the system is assessed in two ways: both the longer-term mean performance (seasonality) as well as its ability to capture recent events are documented. Table 1.1 provides an overview of the trace gas species and aerosol aspects discussed in this CAMS near-real time validation report. This document is updated every 3 months to report the latest status of the near-real time service.

This report covers results for a period of at least one year to document the seasonality of the biases. Sometimes reference is made to other model versions or the reanalysis to highlight aspects of the near-real time products.

Key CAMS NRT products and their users are: Boundary conditions for regional air quality models (e.g. AQMEII, air quality models not participating in CAMS); Long range transport of air pollution (e.g. LRTAP); Stratospheric ozone column and UV (e.g. WMO, DWD); 3D ozone fields (e.g. SPARC).

As outlined in the MACC-II Atmospheric Service Validation Protocol (2013) and MACC O-INT document (2011), relevant user requirements are quick looks of validation scores, and quality flags and uncertainty information along with the actual data. This is further stimulated by QA4EO (Quality Assurance Framework for Earth Observation, <http://www.qa4eo.org>) who write that "all earth observation data and derived products is associated with it a documented and fully traceable quality indicator (QI)". It is our long-term aim to provide such background information. The user is seen as the driver for any specific quality requirements and should assess if any supplied information, as characterised by its associated QI, are "fit for purpose" (QA4EO task team, 2010).



Table 1.1: Overview of the trace gas species and aerosol aspects discussed in this CAMS near-real time validation report. Shown are the datasets assimilated in the CAMS analysis (second column) and the datasets used for validation, as shown in this report (third column). Green colors indicate that substantial data is available to either constrain the species in the analysis, or substantial data is available to assess the quality of the analysis. Yellow boxes indicate that measurements are available, but that the impact on the analysis is not very strong or indirect (second column), or that only certain aspects are validated (third column).

Species, vertical range	Assimilation	Validation
Aerosol, optical properties	MODIS Aqua/Terra AOD	AOD, Ångström: AERONET, GAW, Skynet, MISR, OMI, lidar
Aerosol mass (PM10, PM2.5)	-	European AirBase stations
O ₃ , stratosphere	MLS, GOME-2A, GOME-2B, OMI, SBUV-2	Sonde, lidar, MWR, FTIR, OMPS, BASCOE and MSR analyses
O ₃ , UT/LS	Indirectly constrained by limb and nadir sounders	IAGOS, sonde
O ₃ , free troposphere	Indirectly constrained by limb and nadir sounders	IAGOS, sonde
O ₃ , PBL / surface	-	Surface ozone: WMO/GAW, NOAA/ESRL
CO, UT/LS	-	IAGOS
CO, free troposphere	IASI, MOPITT	IAGOS, MOPITT, IASI
CO, PBL / surface	Indirectly constrained by satellite IR sounders	Surface CO: WMO/GAW, NOAA/ESRL
NO ₂ , troposphere	OMI, partially constrained due to short lifetime	SCIAMACHY, GOME-2, UV-Vis DOAS
HCHO	-	GOME-2, UV-Vis DOAS
SO ₂	GOME-2A, GOME-2B (Volcanic eruptions)	-
Stratosphere, other than O ₃	-	NO ₂ column only: SCIAMACHY, GOME-2

CAMS data are made available to users as data products (grib or netcdf files) and graphical products from ECMWF, <http://atmosphere.copernicus.eu/global-near-real-time-data-access>. Also dedicated netcdf files for use as boundary conditions in regional AQ models world-wide can be downloaded from Forschungszentrum Jülich, <http://join.iek.fz-juelich.de/macc>. The stratospheric ozone service is provided by BIRA-IASB at <http://copernicus-stratosphere.eu>.

A summary of the system and its recent changes is given in section 2. Section 3 gives an overview of the performance of the system from a seasonal (climatological) perspective, for various species. Section 4 describes the performance of the system during recent events. Extended validation can be found online via regularly updated verification pages, <http://atmosphere.copernicus.eu/user-support/validation/verification-global-services>. Table 1.2 lists all specific validation websites that can also be found through this link.



Table 1.2: Overview of quick-look validation websites of the CAMS system.

Reactive gases – Troposphere
GAW surface ozone and carbon monoxide: http://macc.copernicus-atmosphere.eu/d/services/gac/verif/grg/gaw/gaw_station_ts/ IAGOS tropospheric ozone and carbon monoxide: http://www.iagos.fr/cams/ Surface ozone from EMEP (Europe) and NOAA-ESRL (USA): http://www.academyofathens.gr/kefak/macc Tropospheric nitrogen dioxide and formaldehyde columns against satellite retrievals: http://www.doas-bremen.de/macc/macc_veri_iup_home.html Tropospheric CO columns against satellite retrievals: http://cams.mpimet.mpg.de
Reactive gases - Stratosphere
Stratospheric composition: http://www.copernicus-stratosphere.eu NDACC evaluation in stratosphere and troposphere (the NORS server) http://nors-server.aeronomie.be
Aerosol
Evaluation against selection of Aeronet stations: http://www.copernicus-atmosphere.eu/d/services/gac/verif/aer/nrt/ Aerocom evaluation: http://aerocom.met.no/cgi-bin/aerocom/surfobs_annualrs.pl?PROJECT=MACC&MODELLIST=MACC-VALreports& WMO Sand and Dust Storm Warning Advisory and Assessment System (SDS-WAS) model intercomparison and evaluation: http://sds-was.aemet.es/forecast-products/models
Satellite data monitoring
Monitoring of satellite data usage in the Reanalysis and Near-Real-Time production: http://copernicus-atmosphere.eu/d/services/gac/monitor/

This validation report is accompanied by the "Observations characterisation document" CAMS84_1_D8.1_201512.pdf, which describes the observations used in the comparisons, and the validation methodology (this document will become available in March/April 2016).



2 System summary and model background information

The specifics of the different CAMS model versions are given (section 2.1) with a focus on the model changes (section 2.2). An overview of products derived from this system is given in section 2.3. Several external products used for validation and intercomparison are listed in section 2.4. Timeliness and availability of the CAMS products is given in section 2.5.

2.1 System based on the ECMWF IFS model

Key model information is given on the CAMS data-assimilation and forecast run o-suite and its control experiment, used to assess the sensitivity to assimilation. The forecast products are listed in Table 2.1. Table 2.2 provides information on the satellite data used in the o-suite. Further details on the different model runs and their data usage can be found at

<http://atmosphere.copernicus.eu/documentation-global-systems>

Table 2.1: Overview of model runs assessed in this validation report.

Forecast system	Exp. ID	Brief description	Status
o-suite	0001	Operational CAMS DA/FC run	20150903-present (g9rr) 20140918-20150902 (g4e2) 20120705-20140917 (fnyp)
Control	geuh g4o2	control FC run for g9rr / g4e2, without DA	20150901-present (geuh) 20140701-20150902 (g4o2)

2.1.1 o-suite

Starting from 18 September 2014 the o-suite consists of the C-IFS-CB05 chemistry combined with the MACC aerosol model. The chemistry is described in Flemming et al. (2015), aerosol is described by the bulk aerosol scheme (Morcrette et al., 2009). Dissemination of o-suite forecasts is at 22:00UTC. The forecast length is 120 h. The o-suite data is stored under expver '0001' of class 'MC'. On 3 September 2015 an update has been taken place, where the meteorological model has changed significantly, moving from cy40r2 to cy41r1. Here a summary of the main specifications of this version of the o-suite is given.

- The meteorological model is based on IFS version cy41r1, see also <http://www.ecmwf.int/en/forecasts/documentation-and-support/changes-ecmwf-model/cy41r1-summary-changes>; the model resolution is T255L60
- The CB05 tropospheric chemistry is used (Williams et al., 2013), originally taken from the TM5 chemistry transport model (Huijnen et al., 2010)



- Stratospheric ozone during the forecast is computed from the Cariolle scheme (Cariolle and Teyssère, 2007) as already available in IFS, while stratospheric NO_x is constrained through a climatological ratio of HNO₃/O₃ at 10 hPa.
- Monthly mean dry deposition velocities are based on the SUMO model provided by the MOCAGE team.
- Data assimilation is described in Inness et al. (2015) and Benedetti et al. (2009) for chemical trace gases and aerosol, respectively. Satellite data assimilated is listed in Table 2.2.
- Anthropogenic and biogenic emissions are based on the MACCity (Granier et al., 2011) and a climatology of the MEGAN-MACC emission inventories (Sindelarova et al., 2014)
- NRT fire emissions are taken from GFASv1.2 (Kaiser et al. 2012).

The aerosol model includes 12 prognostic variables, which are 3 bins for sea salt and desert dust, hydrophobic and hydrophilic organic matter and black carbon, sulphate aerosols and its precursor trace gas SO₂ (Morcrette et al., 2009). Aerosol total mass is constrained by the assimilation of MODIS AOD

Table 2.2: Satellite retrievals of reactive gases and aerosol optical depth that are actively assimilated in the o-suite.

Instrument	Satellite	Provider	Version	Type	Status
MLS	AURA	NASA	V02 V3.4	O3 Profiles	20090901 – 20130107 20130107 -
OMI	AURA	NASA	V883	O3 Total column	20090901 -
GOME-2A	Metop-A	Eumetsat	GDP 4.7	O3 Total column	20131007 -
GOME-2B	Metop-B	Eumetsat	GDP 4.7	O3 Total column	20140512 -
SBUV-2	NOAA	NOAA	V8	O3 6 layer profiles O3 21 layer profiles	20090901 - 20121006 20121007 -
IASI	MetOp-A	LATMOS/ULB	-	CO Total column	20090901 -
IASI	MetOp-B	LATMOS/ULB	-	CO Total column	20140918 -
MOPITT	TERRA	NCAR	V4 V5-TIR	CO Total column	20120705-20130128 20130129-
OMI	AURA	KNMI	DOMINO V2.0	NO2 Tropospheric column	20120705 -
OMI	AURA	NASA	v003	SO2 Tropospheric column	20120705-20150901
GOME-2A/2B	METOP A/B	Eumetsat	GDP 4.7	SO2 Tropospheric column	20150902-
MODIS	AQUA / TERRA	NASA	Col. 5 Deep Blue	Aerosol total optical depth	20090901 - 20150902 -



(Benedetti et al. 2009). A variational bias correction for the MODIS AOD is in place based on the approach used also elsewhere in the IFS (Dee and Uppala, 2009).

A brief history of updates of the o-suite is given in Table 2.4, and is documented in earlier MACC-VAL reports: http://www.gmes-atmosphere.eu/services/aqac/global_verification/validation_reports/

2.1.2 Control

The control run (expver=geuh/g4o2) applies the same settings as the respective o-suites, based on the coupled C-IFS-CB05 system with MACC aerosol for cy41r1/cy40r2, except that data assimilation is not switched on. The only two exceptions with regard to this setup are:

- at the start of every forecast the ECMWF operational system is used to initialise *stratospheric* ozone, considering that stratospheric ozone, as well as other stratospheric species are not a useful product of this run. As a consequence, the behavior of this control run will not be discussed in the stratospheric contribution of this report. The reason for doing so is that this ensures reasonable stratospheric ozone as boundary conditions necessary for the tropospheric chemistry.
- The full meteorology in control is also initialized from the ECMWF operational NWP analyses. Note that this is different from the o-suite, which uses its own data assimilation setup for meteorology. This can cause slight differences in meteorological fields between o-suite and control, e.g. as seen in evaluations of upper stratospheric temperatures.

2.1.3 MACC_fcprt_MOZ

The MACC_fcprt_MOZ run (expver=fkya) applied the same settings as the old o-suite (expver=fnyp) based on the coupled IFS-MOZART system, except that data assimilation is not switched on and the spatial resolution is lower: T159L60 for IFS and $1.875^\circ \times 1.875^\circ$ for the CTM. This model version did not contain aerosol. Anthropogenic CO emissions were also scaled up.

2.1.4 MACC_CIFS_TM5

MACC_CIFS_TM5 referred to the first NRT data stream based on C-IFS-CB05 (expver=fsd7) and ran from December 2012 to September 2014. The model resolution was T159L60 using the meteorological cycle cy38r2. The tropospheric chemistry is based on the modified CB05 chemical mechanism (Williams et al., 2013). This run did not contain aerosol. Compared to the current control and o-suite, there are a number of additional differences as documented in earlier VAL reports.



Table 2.3: Recent key changes in the CAMS NRT model runs.

Date	Change
2014.09.01-2014.09.04	Temporary mis-interpretation of lava on Iceland as wildfire emissions by the GFAS emission analysis system. Fixed on 4 September 2014.
2014.09.18	Update of o-suite to CY40R2 C-IFS-CB05 with experiment id g4e2
2014.10.07-2014.12.02	Temporarily blacklist IASI CO from METOP A and B to assess the change in the retrieval from V5 to V6. V6 agrees better to MOPITT, except some very high IASI CO values, which are currently rejected.
2014.11.01-2014.11.10	Temporarily the CO retrievals were essentially overly-constrained by the a priori.
2015.03.23-2014.04.14	Temporarily no assimilation of MOPITT CO
2015.04.15	Only allow OMI - SO2 assimilation for rows 1-20.
2015.09.03	Update of o-suite to CY41R1 C-IFS-CB05 with experiment id g9rr

Table 2.4: Long-term o-suite system updates.

Date	o-suite update
2009.08.01	Start of first NRT experiment f7kn with coupled MOZART chemistry, without aerosol. Also without data assimilation.
2009.09.01	Start of first MACC NRT experiment f93i, based on meteo cy36r1, MOZART v3.0 chemistry, MACC aerosol model, RETRO/REAS and GFEDv2 climatological emissions, T159L60 (IFS) and 1.875°×1.875° (MOZART) resolution.
2012.07.05	Update to experiment fnyp: based on meteo cy37r3, MOZART v3.5 chemistry, where changes mostly affect the stratosphere, MACCity (gas-phase), GFASv1 emissions (gas phase and aerosol), T255L60 (IFS) and 1.125°×1.125° (MOZART) resolution. Rebalancing aerosol model, affecting dust.
2013.10.07	Update of experiment fnyp from e-suite experiment fwu0: based on meteo cy38r2, no changes to chemistry, but significant rebalancing aerosol model. Assimilation of 21 layer SBUV/2 ozone product
2014.02.24	Update of experiment fnyp from e-suite experiment fzpr: based on meteo cy40r1. No significant changes to chemistry and aerosol models.
2014.09.18	Update to experiment g4e2: based on meteo cy40r2. In this model version C-IFS-CB05 is introduced to model atmospheric chemistry.
2015.09.03	Update to experiment g9rr: based on meteo cy41r1.

2.2 Evolution of the IFS-based system

A list with system changes from September 2014 until December 2015 are given in Table 2.3. A full list with all changes concerning the assimilation system can be found via <http://www.copernicus-atmosphere.eu/operational-info>. The CAMS o-suite system is upgraded regularly, following updates to the ECMWF meteorological model as well as CAMS-specific updates such as changes in chemical data assimilation. These changes are documented in e-suite validation reports, as can be found from the link above. Essential model upgrades are also documented in Table 2.4.



2.3 Other systems

2.3.1 BASCOE

The NRT analyses and forecasts of ozone and related species for the stratosphere, as delivered by the Belgian Assimilation System for Chemical Observations (BASCOE) of BIRA-IASB (Lefever et al., 2014; Errera et al., 2008), are used as an independent model evaluation of the CAMS products.

The NRT BASCOE product is the ozone analysis of Aura/MLS-SCI level 2 standard products, run in the following configuration (version 04.03):

- The following species are assimilated: O₃, H₂O, HNO₃, HCl, HOCl, N₂O. ClO has been added on 20130819.
- It lags by typically 4 days, due to latency time of 4 days for arrival of non-ozone data from Aura/MLS-SCI (i.e. the scientific offline Aura/MLS dataset).
- Global horizontal grid with a 3.75° longitude by 2.5° latitude resolution.
- Vertical grid is hybrid-pressure and consists in 137 levels extending from 0.01 hPa to the surface.
- Winds, temperature and surface pressure are interpolated in the ECMWF operational 6-hourly analyses.
- Timesteps of 20 minutes, output every 3 hours

See the stratospheric ozone service at <http://www.copernicus-stratosphere.eu/>. It delivers graphical products dedicated to stratospheric composition and allows easy comparison between the results of o-suite, BASCOE, SACADA and TM3DAM. The BASCOE data products (HDF4 files) are also distributed from this webpage. Other details and bibliographic references on BASCOE can be found at <http://bascoe.oma.be/>. A detailed change log for BASCOE can be found at http://www.copernicus-stratosphere.eu/4_NRT_products/3_Models_changelogs/BASCOE.php.

2.3.2 TM3DAM and the multi-sensor reanalysis

One of the MACC products was a 30-year reanalysis, near-real time analysis and 10-day forecast of ozone column amounts performed with the KNMI TM3DAM data assimilation system, the Multi-Sensor Reanalysis (MSR) system (van der A et al., 2010, 2013),

http://www.temis.nl/macc/index.php?link=o3_msr_intro.html. The corresponding validation report can be found at http://www.copernicus-atmosphere.eu/services/gac/global_verification/validation_reports/.

The NRT TM3DAM product used for the validation of the CAMS NRT streams is the ozone analysis of Envisat/SCIAMACHY (until April 2012), AURA/OMI, and MetOp-A/GOME-2, run in the following configuration:

- total O₃ columns are assimilated
- Global horizontal grid with a 3° longitude by 2° latitude resolution.



- Vertical grid is hybrid-pressure and consists in 44 levels extending from 0.1 hPa to 100 hPa.
- Dynamical fields from ECMWF operational 6-hourly analysis.

2.3.3 SDS-WAS multimodel ensemble

The World Meteorological Organization's Sand and Dust Storm Warning Advisory and Assessment System (WMO SDS-WAS) for Northern Africa, Middle East and Europe (NAMEE) Regional Center (<http://sds-was.aemet.es/>) has established a protocol to routinely exchange products from dust forecast models as the basis for both near-real-time and delayed common model evaluation. Currently, nine (BSC-DREAM8b, MACC-ECMWF, DREAM-NMME-MACC, NMMB/BSC-Dust, NASE GEOS-5, NCEP NGAC, EMA_RegCM, DREAMABOL and NOA) provides daily operational dust forecasts (i.e. dust optical depth, DOD, and dust surface concentration).

Different multi-model products are generated from the different prediction models. Two products describing centrality (multi-model median and mean) and two products describing spread (standard deviation and range of variation) are daily computed. In order to generate them, the model outputs are bi-linearly interpolated to a common grid mesh of $0.5^\circ \times 0.5^\circ$. The multimodel DOD (at 550 nm) Median from nine dust prediction models participating in the SDS-WAS Regional Center is used for the validation of the CAMS NRT streams.

2.4 CAMS products

An extended list of output products from the NRT stream o-suite are available as 3-hourly instantaneous values up to five forecast days. These are available from ECMWF (through ftp in grib2 and netcdf format, <http://atmosphere.copernicus.eu/global-near-real-time-data-access>) and on the Jülich server (<http://join.iek.fz-juelich.de/macc>, in netcdf format).

2.5 Availability and timing of CAMS products

The availability statistics provided in Table 2.6 are computed for the end of the 5-day forecast run, and are obtained from July 2012 onwards. A forecast is labeled "on time", if everything is archived on MARS before 22UTC. This is based on requirements from the regional models. We note that at present most regional models can still provide their forecasts even if the global forecast is available a bit later.

Between December 2012 and February 2015 on average about 97% of the forecasts were delivered on time. For the period September November 2015, 95% of the forecasts were delivered before 21.14.



Table 2.6: Timeliness of the o-suite from July 2012 – to August 2015

Months	On time, 22 utc	80th perc	90th perc	95th perc
March-May 2013	97%	D+0, 17:54	D+0, 18:36	D+0, 18:49
June-August 2013	97%	D+0, 18:34	D+0, 18:46	D+0, 19:23
Sept-Nov 2013	99%	D+0, 19:14	D+0, 19:22	D+0, 19:29
Dec-Feb '13-'14	94%	D+0, 19:45	D+0, 20:40	D+0, 21:55
Mar-May 2014	98%	D+0, 19:44	D+0, 19:57	D+0, 20:03
Jun-Aug 2014	95%	D+0, 20:03	D+0, 20:57	D+0, 22:43
Sept-Nov 2014	96%	D+0, 19:24	D+0, 20:31	D+0, 21:14
Dec-Feb '14-'15	97%	D+0, 19:43	D+0, 20:28	D+0, 21:13
Mar-May 2015	96%	D+0, 19:38	D+0, 21:03	D+0, 21:40
Jun-Aug 2015	95%	D+0, 20:24	D+0, 20:53	D+0, 21:54
Sept-Nov 2015	95%	D+0, 19:44	D+0, 20:55	D+0, 21:51



3 Validation results

This section describes the validation results of the CAMS NRT global system up to November 2015. The validation focuses on the results from the NRT analysis (or D+0 FC) stream. For a selection of instances 1-3 day forecasts issued from them have been explicitly considered. Naming and color-coding conventions predominantly follow the scheme as given in Table 3.1.

Table 3.1 Naming and color conventions as adopted in this report.

Name in figs	experiment	Color
{obs name}	{obs}	black
o-suite	0001	red
Control	g4o2 / geuh	blue

3.1 Tropospheric Ozone

3.1.1 Validation with sonde data in the free troposphere

Model profiles of the CAMS runs were compared to free tropospheric balloon sonde measurement data of 38 stations taken from the NDACC, WOUDC, NILU and SHADOZ databases for November 2014 to November 2015 (see Fig. 3.1.1 - 3.1.3). Towards the end of the period, the number of available soundings decreases, which implies that the evaluation results may become less representative. The figures contain the number of profiles in each month that are available for the evaluation. The observations, and the methodology for model comparison against the observations is described in a separate document which will become available in March 2016. The free troposphere is defined as the altitude range between 750 and 200 hPa in the tropics and between 750 and 300 hPa elsewhere.

In all zonal bands the MNMB is within the range -25 to +30%, for all months, see Fig. 3.1.1-3.1.3. Over the Arctic, the o-suite shows slightly positive MNMBs from spring 2015 onwards (MNMBs up to 10%), while during the winter season the MNMB gets negative by up to -16%, Fig. 3.6.1. Over the NH mid-latitudes MNMBs for the o-suite are on average close to zero all year round (-7% to +5%), which is a clear improvement compared to the control run, which shows larger positive MNMBs (up to 20%). MNMBs are larger over the Tropics and Antarctica where tropospheric O₃ values are comparatively lower than over the polluted NH.

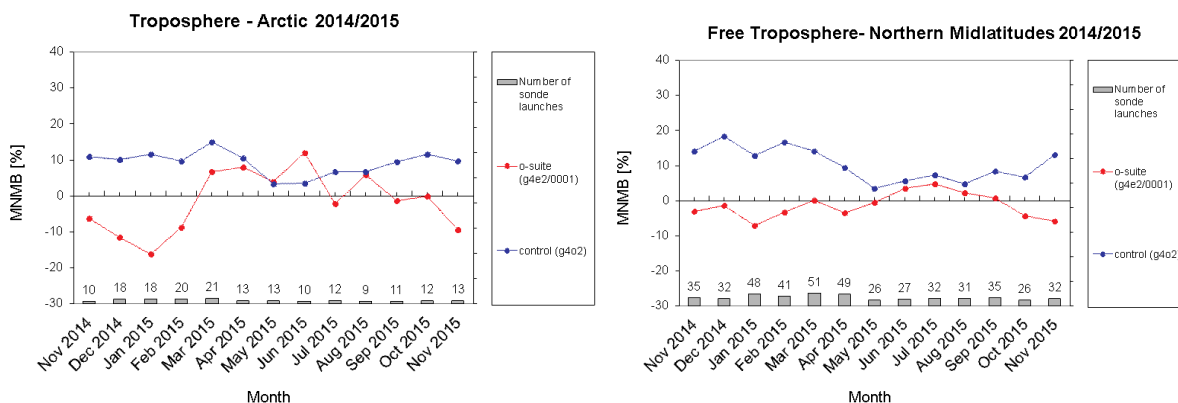


Figure 3.1.1: MNMBs (%) of ozone in the free troposphere (between 750 and 300 hPa) from the IFS model runs against aggregated sonde data over the Arctic (left) and the Northern midlatitudes (right). The numbers indicate the amount of individual number of sondes.

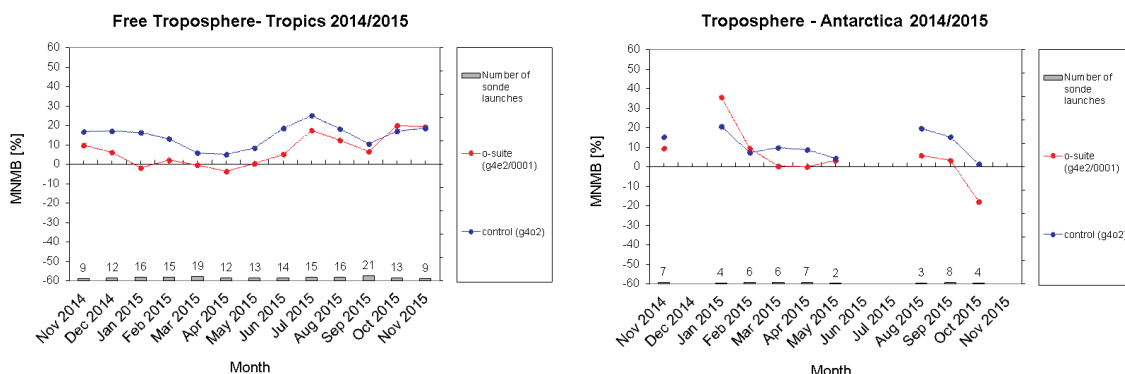


Figure 3.1.2: MNMBs (%) of ozone in the free troposphere (between 750 and 200 hPa (Tropics) / 300 hPa) from the IFS model runs against aggregated sonde data over the Tropics (left) and Antarctica (right). The numbers indicate the amount of individual number of sondes.

3.1.2 Ozone validation with IAGOS data

The daily profiles of ozone measured at airports around the world, are shown on the website at http://www.iagos.fr/macc/nrt_day_profiles.php. For the period from September to November 2015, the data displayed on the web pages and in this report include only the data as validated by the instrument PI. The available flights and available airports are shown in figure 3.1.3 top and bottom respectively. Performance indicators have been calculated for different parts of the IAGOS operations.

With the whole fleet of 6 aircraft, operating fully over the three month period, we can expect a total of 1260 flights. The actual number of flights within the period was 598 giving a performance of 47%. The actual number of flights with usable data is 326 (26% of the total possible). Eighty four percent (84%) of the operational flights had usable measurements of ozone or CO.

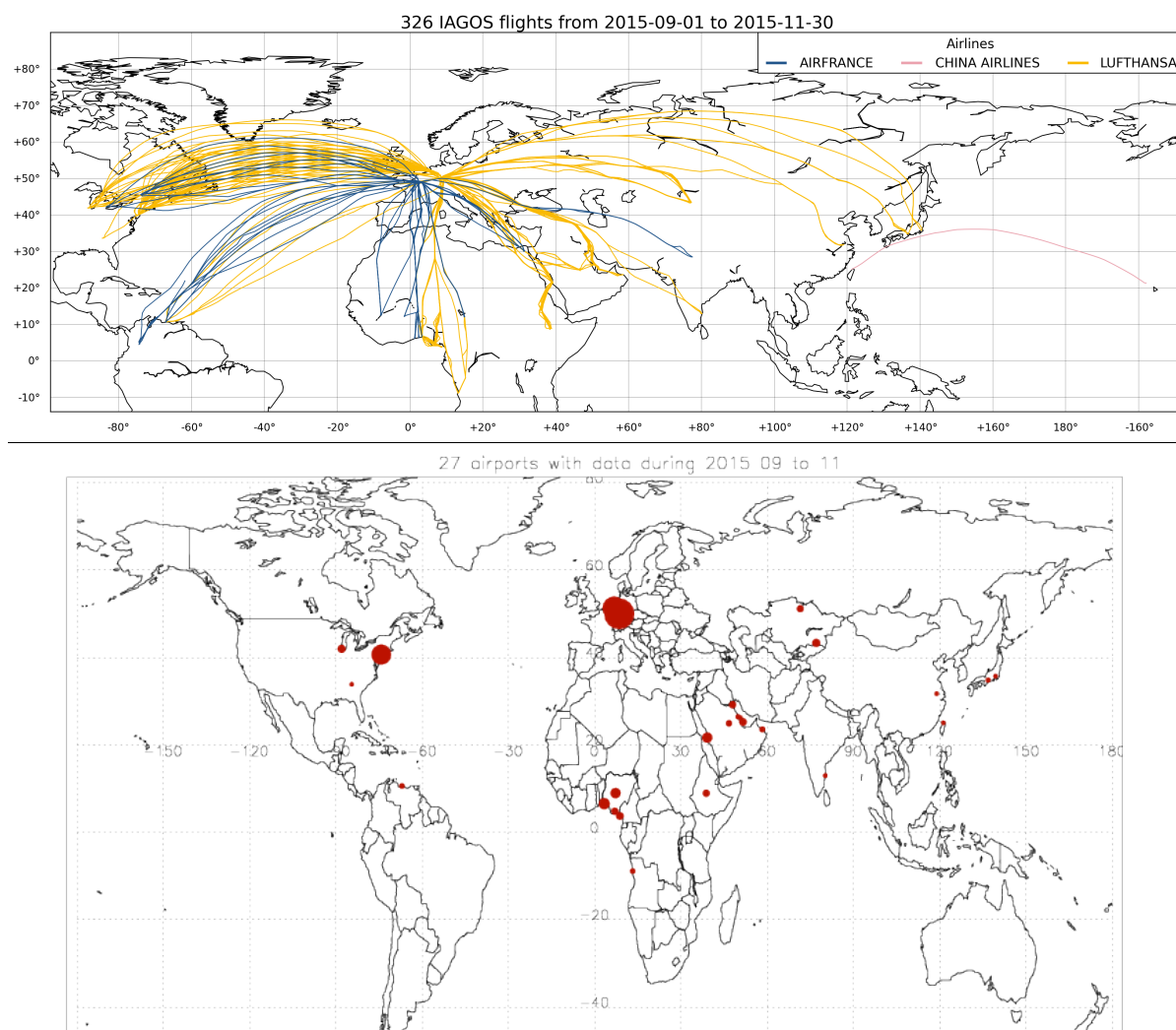


Figure 3.1.3 : Map of the flights (top) and the visited airports (bottom) during the period September-November 2015, by the IAGOS equipped aircraft. The size of the plotting circle represents the number of profiles available.

Delivering these O_3 and CO data are the two aircraft from Lufthansa (one of which is based in Frankfurt and the other based in Dusseldorf), and the aircraft from China Airlines based in Taipei. The Airfrance aircraft has no valid O_3 or CO measurements. This report therefore displays profiles recorded by these aircraft, covering mainly the North-East of the USA (New York and Chicago) the Arabian Peninsula (Jeddah, Doha, Kuwait, Riyadh, Muscat), and Equatorial West Africa (Lagos, Port Harcourt), as shown on the map in Figure 1 (with a plotting circle scaled to the highest number of flights at an airport). Apart from the home-base airports of Frankfurt and Dusseldorf most of the airports are only visited at low frequency. Frankfurt, Dusseldorf and New York are the three most frequently and regularly visited airports during this period.

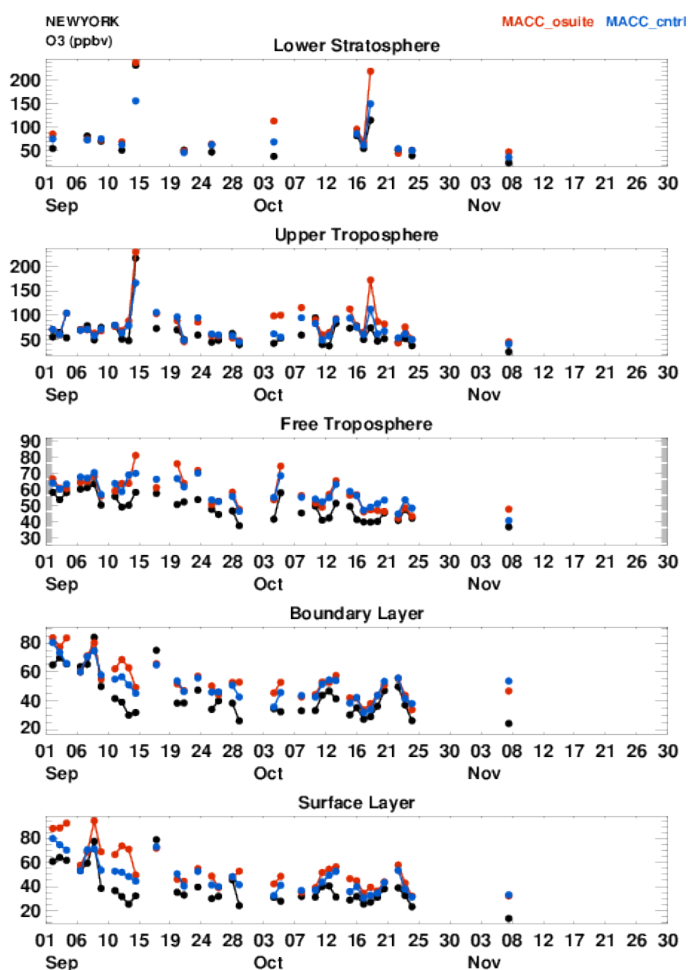


Figure 3.1.4: Time series of daily mean ozone over New York from Sept. to Nov. 2015 for 5 layers, Surface, Boundary layer, Free Troposphere, Upper Troposphere and Lower Stratosphere.

Figure 3.1.4 takes advantage of the regular flight between Dusseldorf and New York over the period, while Figure 3.1.5 takes advantage of the quasi daily operations from Dusseldorf and Frankfurt and present the time series of ozone for different levels in the troposphere. As in the summer months, ozone in the model is generally slightly overestimated, especially in the surface and boundary layer. The assimilation shows an improvement over the control run the free troposphere.

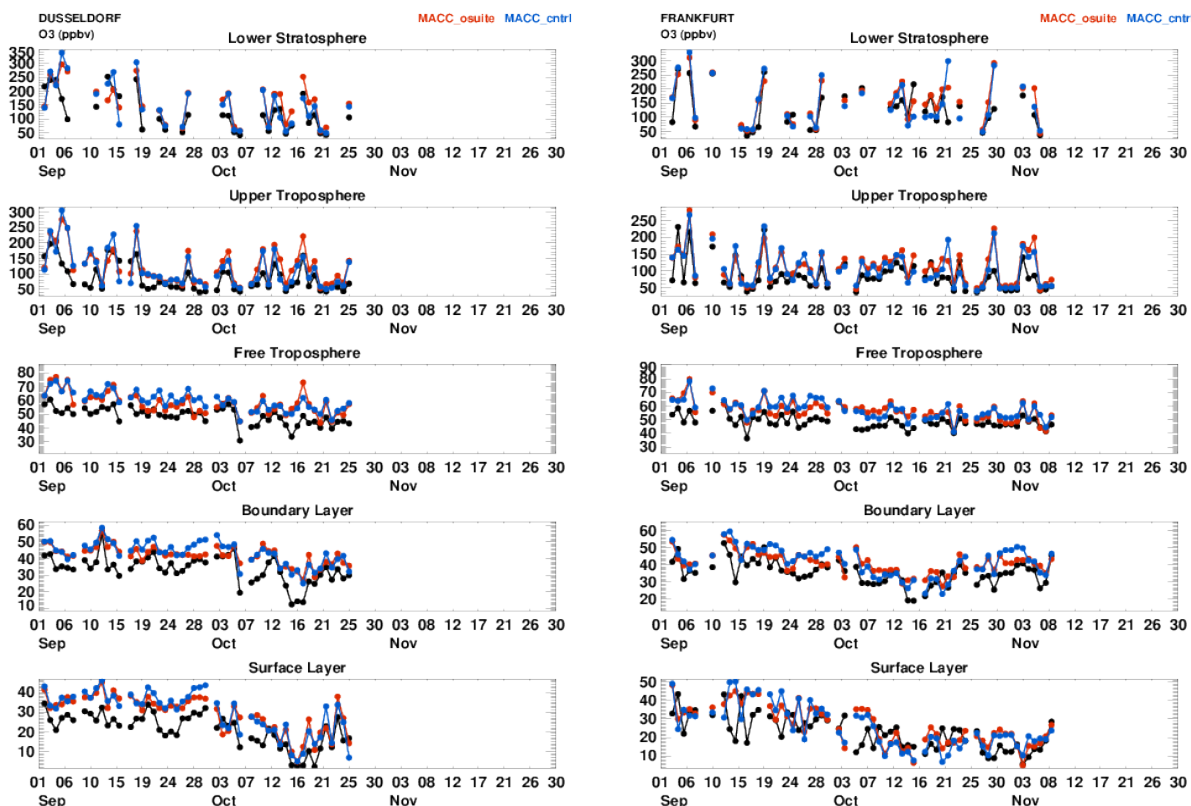


Figure 3.1.5: Time series of daily mean ozone over Dusseldorf (left) and Frankfurt (right) from September to November 2015 for 5 layers, Surface, Boundary layer, Free Troposphere, Upper Troposphere and Lower Stratosphere.

Europe and USA

Examples in Figure 3.1.6 have been chosen to show the variety of behaviours in the UTLS, with some examples showing a good representation of ozone around the tropopause and others being much poorer. On 22nd September, profiles were available at Dusseldorf and Frankfurt. For this day, there is a large difference between Dusseldorf and Frankfurt for the measured tropopause but the model runs are similar. Therefore the UTLS is poorly captured at Frankfurt. As noted in the previous NRT report covering JJA, the models have difficulty in capturing the variability in altitude of the tropopause and in representing the strong gradients in ozone. Some of the previous reports have noted that the control run does better job at representing ozone in the UTLS and this is generally the case in this season, with the profile on 5th October at New York being a good example. The o-suite shows generally better agreement throughout the troposphere than the control run.

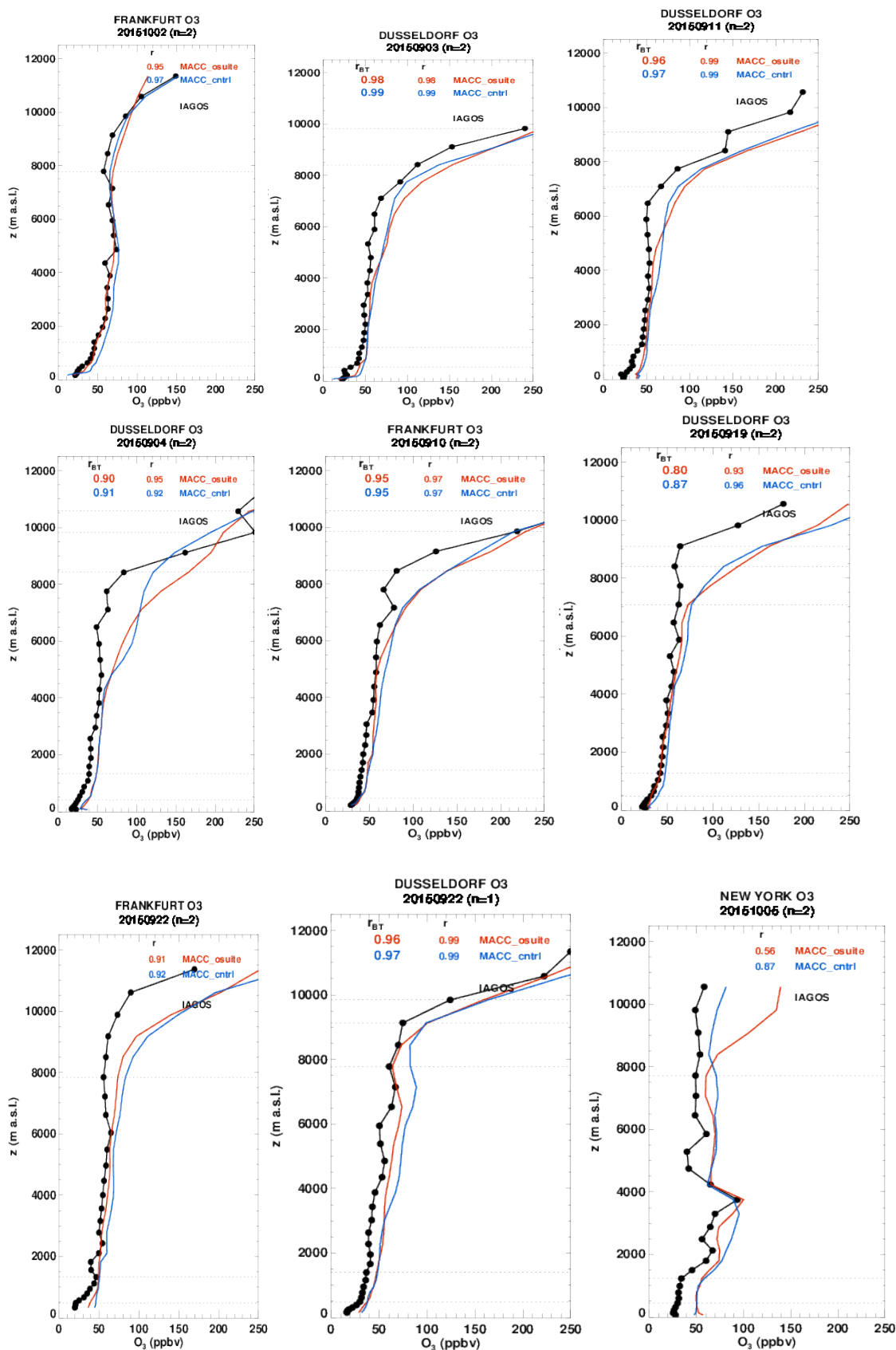


Figure 3.1.6: Selection of daily profiles of ozone from IAGOS (black) and the two NRT runs over Europe and USA (Frankfurt, Dusseldorf, and New-York) over the period September-November 2015.

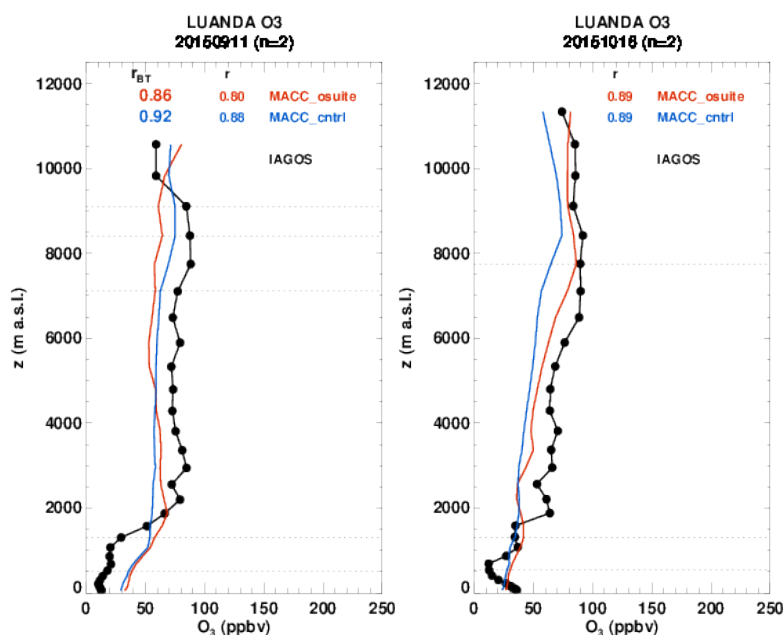


Figure 3.1.7: Profiles of ozone from IAGOS (black) and the two NRT runs over Luanda in September-November 2015.

Africa

Thanks to the second Lufthansa aircraft equipped with IAGOS we have now regular data over Equatorial and West Africa, especially over Nigeria (Lagos and Port-Harcourt). This region is characterized by an intense pollution from oil industries all year long, also under the influence of biomass burning over north-equatorial Africa from December to April, approximately, and the influence of the West African monsoon in June-August. In September-October, the region may see biomass burning plumes originating from the southern hemisphere which is experiencing biomass burning at this time, but by November most of the biomass burning has moved north of the equator and has a more pronounced influence on the Equatorial West African region. The influence of biomass burning is easily seen at Luanda in CO profiles (see Sec 3.3.2). The corresponding ozone (Figure 3.1.7) is elevated at altitudes above 2000m and underestimated by both control and o-suite.

Middle-East

The same second Lufthansa aircraft in the IAGOS fleet is also visiting the Middle-East region regularly (Kuwait City, Jeddah and Doha, Dubai and Muscat). Over this region, in JJA, the ozone profiles are characterised by a maximum in the mid to upper troposphere which models have difficulty in reproducing. In SON, this feature is still present but less marked. Usually we note a quasi-systematic overestimation by the model throughout the troposphere. We see this behaviour in figure 3.1.8 for Muscat whereas for Doha, the models do a better job. Assimilation tends to improve the agreement between model and observations, the profile at Kuwait being a good example.

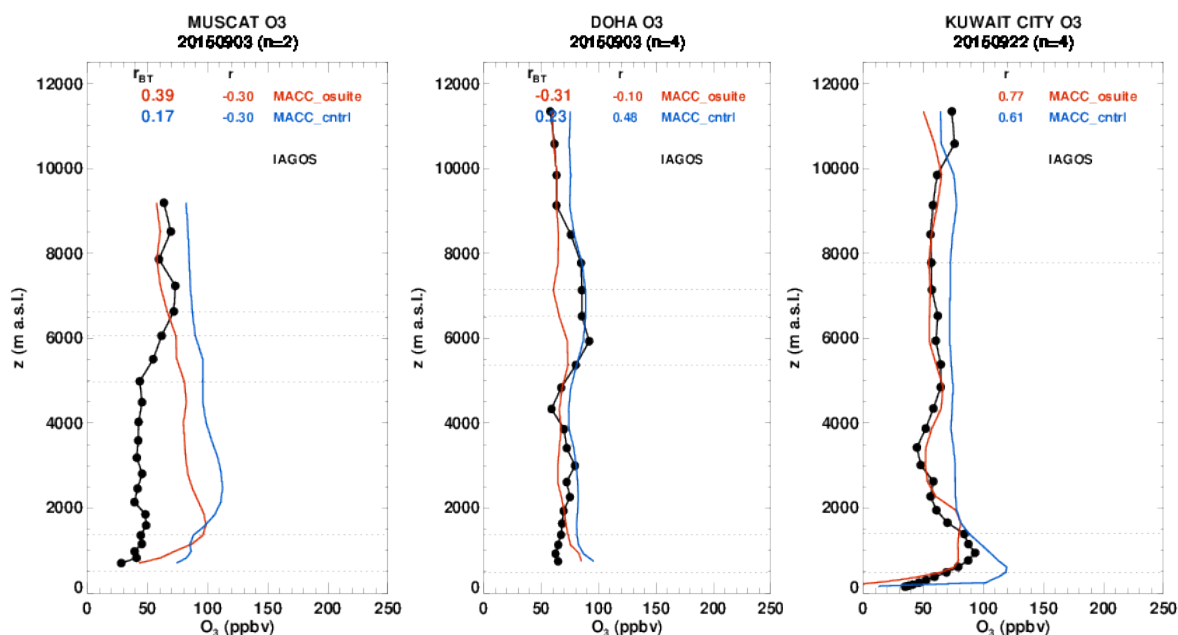


Figure 3.1.8: Profiles of ozone from IAGOS (black) and the two NRT runs over Doha, Dubai, Almaty, Kuwait City, Jeddah, and Muscat, over the period September-November 2015.

3.1.3 Validation with GAW and ESRL-GMD surface observations

For the Near Real Time (NRT) validation, 13 GAW stations and 11 ESRL stations are currently delivering O_3 surface concentrations in NRT, and the data are compared to model results. In addition validation results for Finokalia Station in the Mediterranean are presented. In the following, a seasonal evaluation of model performance for the 2 NRT runs (o-suite and control) has been carried out for the period from September 2015 to November 2015. The latest validation results based on GAW stations can be found on the CAMS website, <http://www.copernicus-atmosphere.eu/d/services/gac/verif/grg/gaw/>, and based on ESRL on <http://www.academyofathens.gr/kefak/macc/index.html>. Results are summarized in Fig. 3.1.9. Between September and November 2015, both the o-suite and the control run show an overestimation of O_3 surface mixing ratios for all GAW stations.

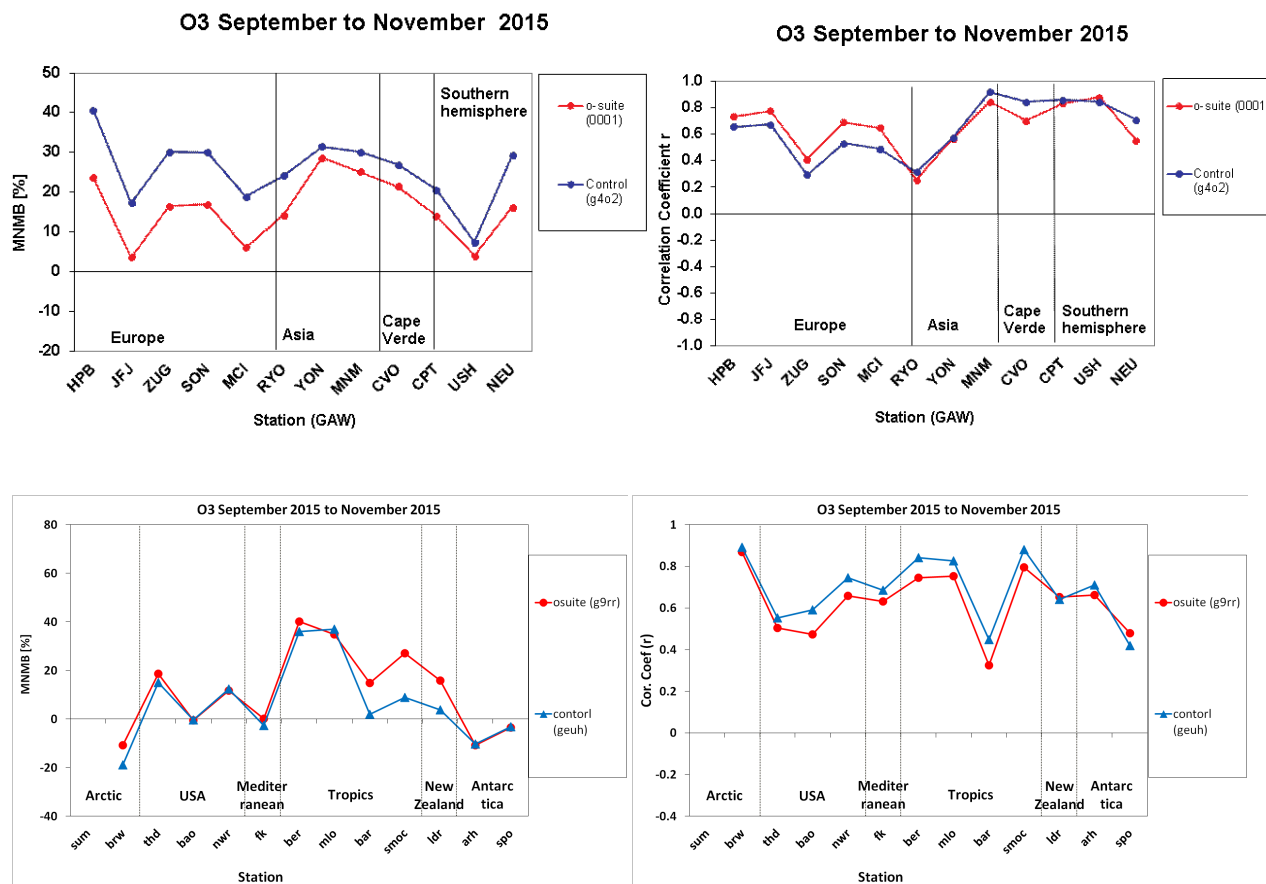


Figure 3.1.9: Modified normalized mean bias in % (left) and correlation coefficient (right) of the NRT model runs compared to observational GAW (top) and ESRL (bottom) data in the period September to November 2015.

For European stations (HPB, JFJ, ZUG, SON, MCI), observed O₃ surface mixing ratios are overestimated with MNMBs between 4 to 24% for the o-suite. The control run shows larger MNMBs between 17 and 40%. The o-suite provides slightly better correlation coefficients for the European stations (o-suite: between 0.4 and 0.8, control: between 0.3 and 0.7). o-suite and control reproduce very well surface ozone mean concentrations and variability at Finokalia Station in the Mediterranean (MNMBs≈0%, r>0.6).

Over Point Barrow, Alaska Station (BRW) both o-suite and control underestimate surface ozone values by -10% (o-suite) to -20% (control). Correlations between simulated and observed surface ozone at Point Barrow station are high for both models (r>0.8).

Over USA stations both models reproduce well surface ozone mean concentrations at BAO (MNMBs≈0%) and slightly overestimate it at NWR and at THD (both runs MNMBs≈10% and 15% respectively). Correlations between simulated and observed surface ozone are high at BAO and at THD stations (o-suite r ≈0.5 and control r ≈0.6) and even higher at NWR (o-suite r ≈0.65 and control r ≈0.75). It should be noted that data assimilation seems to reduce slightly correlation between simulated and observed surface ozone Over USA stations.

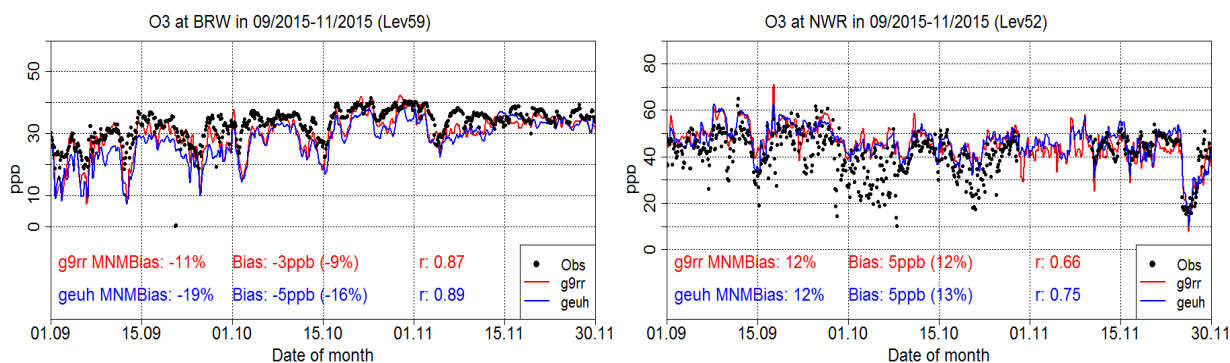


Fig. 3.1.10: Time series for the o-suite (red) and Control (blue) compared to ESRL observations at Point Barrow station (71.32°N, 156.61°W, left) and Niwot Ridge, Colorado station (40.04°N, 105.54°W, right).

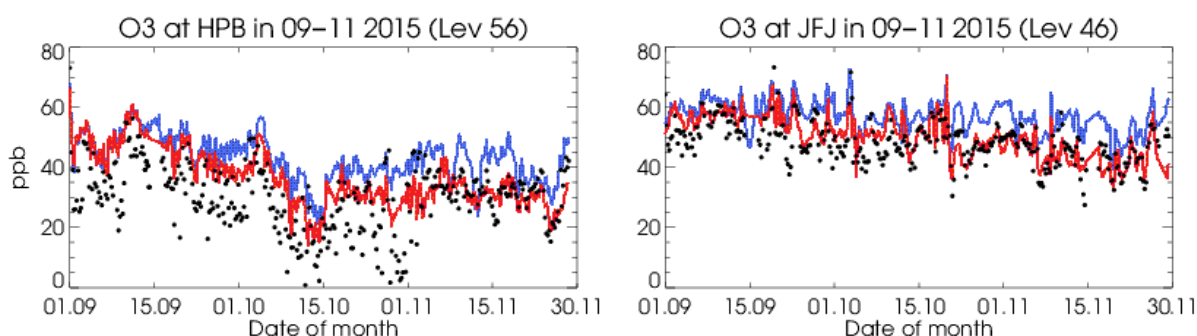


Fig. 3.1.11: Time series for the o-suite (red) and Control (blue) compared to GAW observations at Hohenpeissenberg (47.8°N, 11.0°E) and Jungfrauoch (46.5°N, 7.9°E).

Over the tropical stations (BER, MLO, BAR, SMOC) both model versions overestimate ozone mixing ratios, the o-suite by 40% at BER and MLO, 30% at SMOC and 20% at BAR. Correlations are high at BER, MLO and SMOC ($r > 0.6$) and lower at BAR ($r > 0.3$). Over the tropical stations data assimilation seems to reduce slightly the model performance in terms of both correlation and biases.

For Asian stations (RYO, YON, MNM), the control run again shows a positive offset in surface O_3 mixing ratios with MNMBs between 24 and 31%, which is partly corrected by the assimilation of satellite data for the o-suite (MNMBs between 14 and 30%). The overestimation mostly concerns the minimum concentrations in the model. Concentration peaks are reproduced well, as can be seen in Fig.3.1.12. Correlation coefficients are similar for both runs and amount between 0.3 and 0.9.

For the two stations in the Southern Hemisphere, the o-suite realistically reproduces the background concentrations. For Ushuaia station, decreasing O_3 mixing ratios between September and November are well reproduced by both runs, see Fig.3.1.13. Correlation coefficients are fair for both runs (between 0.6 and 0.9).

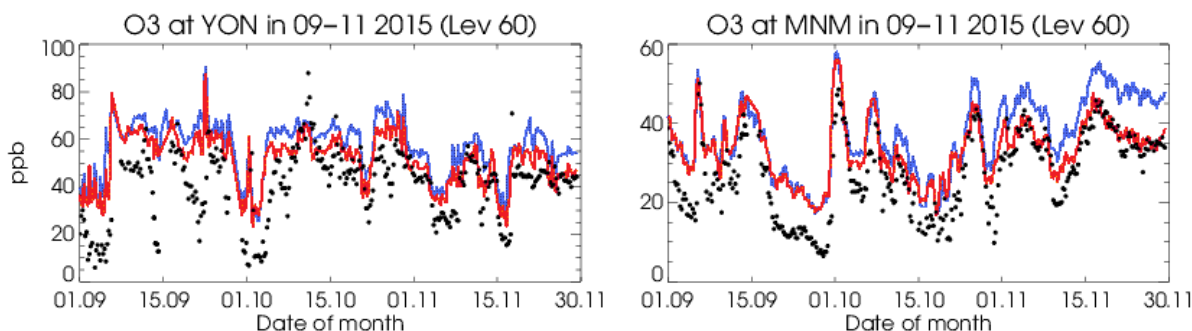


Fig. 3.1.12: Time series for the o-suite (red) and Control (blue) compared to GAW observations at Yonaguijima (24.5°N, 1°123.0°E) and Minamitorishima (24.3°N, 123.9°E).

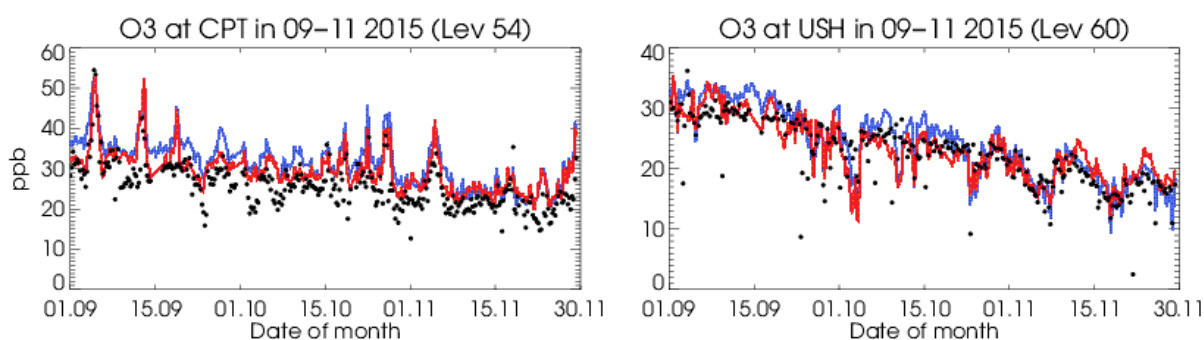


Fig. 3.1.13: Time series for the o-suite (red) and control (blue) compared to GAW observations at Cape Point (34.35°S, 18.5°E) and Ushuaia (54.9°S, 68.2°W).

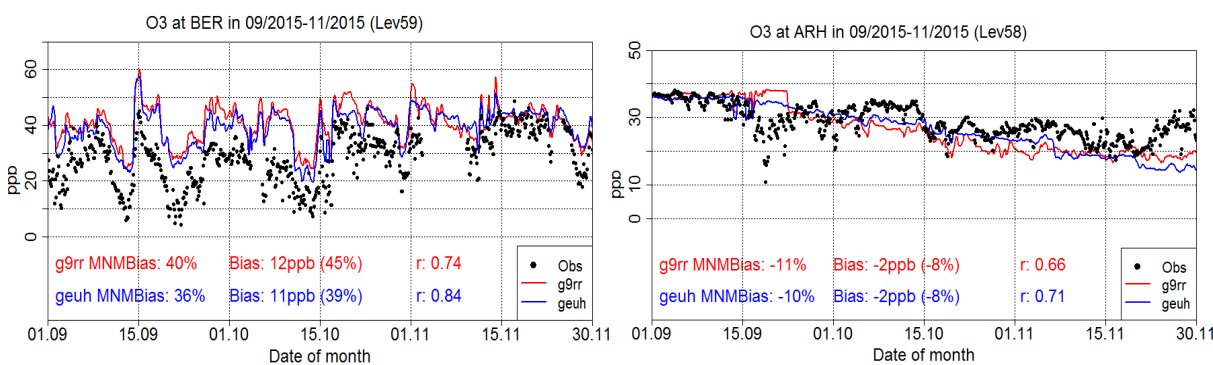


Figure 3.1.14: Time series compared to ESRL observations (black dots) at Tudor Hill, Bermuda station (32.27°N, 64.48°W) and at Arrival Heights, Antarctica (-77.80°N, 166.78°W).

The o-suite and control overestimate surface ozone mean values at Lauder in New Zealand by 15% (o-suite) and 5% (control). Correlations between simulated and observed values are high for both versions ($r=0.65$).

Finally at SPO both models reproduce well surface ozone mean concentrations (MNMBs \approx 0%) and underestimate it by 10% at ARH Antarctica Station. Correlations between simulated and observed surface ozone values are high for both o-suite and control ($r>0.65$) at ARH and lower ($r\approx 0.4$) at SPO. To summarize, control performs equal or even better than o-suite in both biases and correlations of surface ozone.

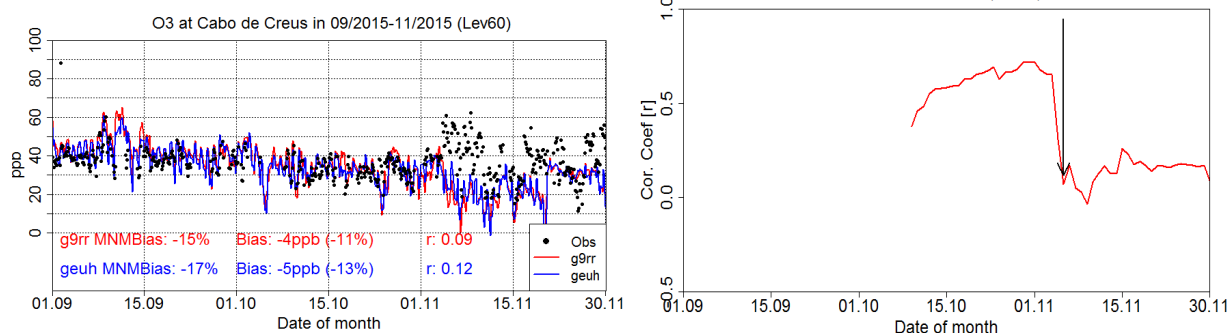


Figure 3.1.15: a) Time series of control run (blue) and o-suite run (red) compared to observations (black dots) at Cabo de Creus, Spain stations (42.32°N, 3.32°E). Correlations progress in time between observations and o-suite run (red). The black arrow denote the day when correlation became statistically insignificant at 0.95 c.l

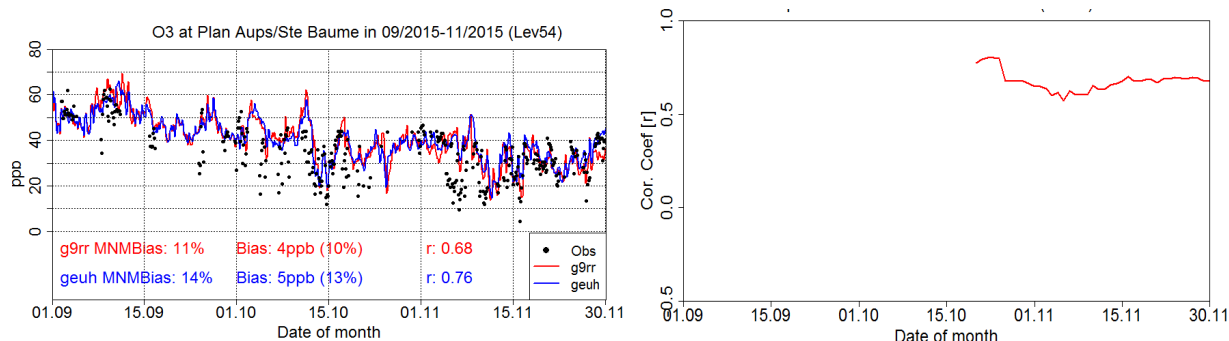


Figure 3.1.16: a) Time series of control run (blue) and o-suite run (red) compared to observations (black dots) at Plan Aups/Ste Baume, France station (43.34°N, 5.73°E) b) Correlations progress in time between observations and o-suite run (red)

3.1.4 Validation with AirBase observations in Mediterranean

The validation analysis over the Mediterranean is based on station observations from the Airbase (NRT) Network. The model performance for the 2 forecast runs (o-suite and control) has been carried out for the period from 1 September 2015 to 30 November 2015. We started with stations located within about 100 km from the shoreline of the Mediterranean, selected to fall in the classes 1 and 2 in the O₃ Joly-Peuch classification. Furthermore, stations were selected according to data availability, warning flags, diurnal amplitude, statistically significant correlations, and differences in topography between the model and station not exceeding 500m. Table 3.1.1 shows the names, coordinates, elevation and the MNMBs and correlations obtained with the 2 forecast runs (o-suite and control).

As we can see from table 3.1.1 with the exception of stations Cabo de Creus (see also Figure 3.1.15) and Zarra the variance explained by each station of both the Control and o-suite runs is high and correlations highly significant. At the bottom of table 3.1.1 the correlations have been repeated by taken the daily average of all (9) stations as well as averaging over the best 7 stations.



Table 3.1.1: Coordinates, elevation as well as validation scores (MNMBs and correlations) obtained with the 2 forecast runs (o-suite and control), for each one of the selected Mediterranean stations.

Station Name	Station ID	Longitude	Latitude	Elevation (m)	Distance from the Shore	MNMB (%)		Cor. Coef. (r)	
						O-suite	Control	O-suite	Control
Al Cornocales	ES1648A	-5.66	36.23	189	0.16	4.40	2.90	0.43	0.41
Zarra	ES0012R	-1.1	39.08	885	0.70	-2.70	-1.90	0.06	0.16
Gandesa	ES1379A	0.44	41.06	368	0.15	-31.60	-33.30	0.82	0.80
Els Torms	ES0014R	0.74	41.39	470	0.27	-35.00	-39.50	0.71	0.72
Al Agullana	ES1201A	2.84	42.39	214	0.25	-17.20	-26.00	0.72	0.72
Begur	ES1311A	3.21	41.96	200	0.09	-6.10	-5.00	0.55	0.59
Cabo de Creus	ES0010R	3.32	42.32	23	0.08	-14.60	-16.60	0.09	0.12
Plan Aups/Ste Baume	FR03027	5.73	43.34	675	0.21	10.80	14.10	0.68	0.76
Finokalia	GR0002R	25.67	35.32	250	0.10	0.20	-2.60	0.64	0.68
All 9 Stations mean						-9.03	-10.69	0.72	0.75
7 Stations mean (Zarra and Cabo de Creus excluded)						-9.33	-11.34	0.82	0.84

Concerning biases our analysis shows that both model runs reproduces well surface ozone mean concentrations at Al Cornocales (near Gibraltar) and Zarra (east Spain) stations (MNMBs \approx 0). In Table 3.1.1 we can see also that both model runs underestimate surface ozone values down to 30% in a group of stations located in the north east shore of Spain. On the contrary at the Plan Aups/Ste Baume station, in South France (see Figure 3.1.16), both runs slightly overestimate ozone mixing ratios by 10%. Finally, both o-suite and control runs reproduce very well surface ozone mean concentrations at Finokalia station in Crete, Greece (MNMBs \approx 0%)

Observed and simulated surface ozone values at Cabo de Creus station in Spain are shown in Figure 3.1.15 (a). It is evident that model and observed ozone values deviates significantly from 3 November on. Figure 3.1.15 (b) provides an example of an independent test that shows the instability of the correlations between the models and the observations. These is clearly seen as the correlations progress in time (right axis shows the correlation coefficient) drop significantly in the beginning of November and became statistically insignificant at 0.95 c.l (black arrow). If this test is robust we will be proven in the few months to come but at present it looks quite promising to use the correlation to identify instabilities either in the data and/or in the models.

Same validation results for Plan Aups/Ste Baume, south France station are shown in Figure 3.1.16. From figure 3.1.16 (b) it is evident that correlation coefficient remains stable during the study period.

In addition to the above 7 Mediterranean stations (still we are missing Malta, Italy, Cyprus and North shore of Africa) we have done our validation expanding the Mediterranean longitudes towards to the Atlantic shore west of Gibraltar as seen in figure 3.1.17 which shows the spatial distribution of MNMBs and correlations.

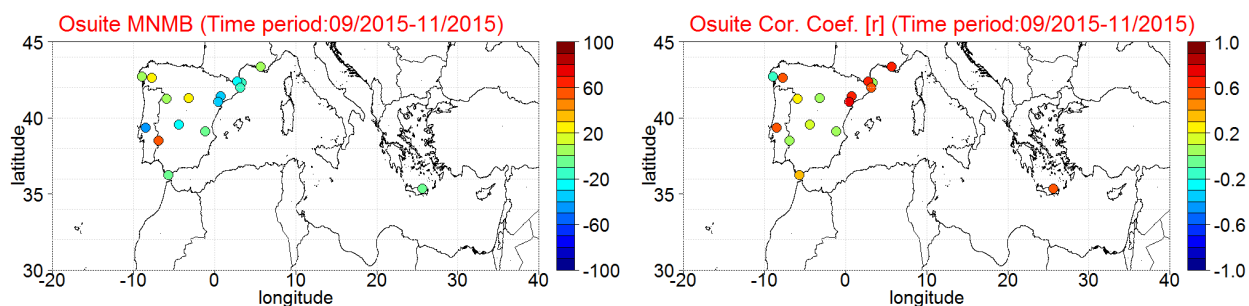


Figure 3.1.17: Spatial distribution of MNMB in % (left) and correlation coefficient (right) of osuite run compared to observational data during the period from 1 September 2015 to 30 November 2015.

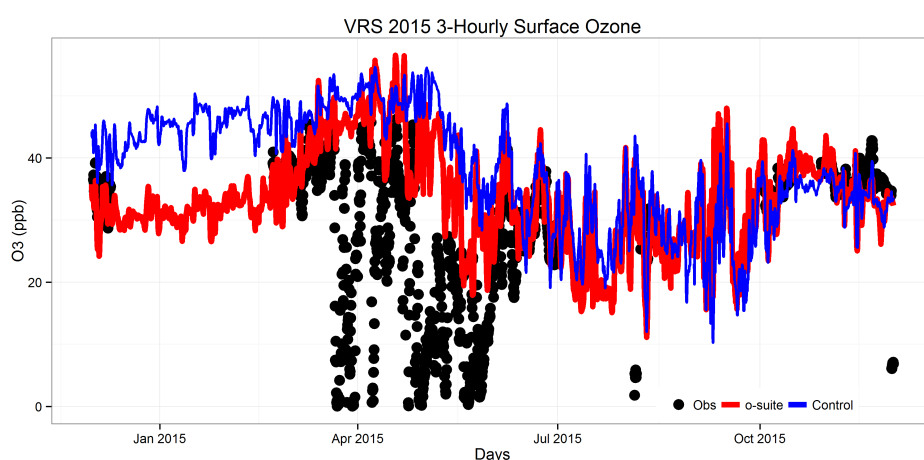


Figure 3.1.18: Time series for o-suite (red) and Control (blue) compared to observations (black dots) at the Villum Research Station, Station Nord, Greenland.

The above analysis has been restricted to only 7 stations providing surface ozone in NRT. In the next report we shall include additional stations and most of the relevant reactive gases (ozone, NO_x , CO), as well as the altitude effect in the validation of the modeled reactive gases.

3.1.5 Validation with IASOA surface observations

To expand the NRT validation for the Arctic area, O_3 observations from the Villum Research Station, Station Nord in north Greenland from the IASOA network were compared to model results, Fig. 3.1.18. There are large gaps in the measurement time series covering the period from December 2014 to November 2015. Ozone depletion events in March – June 2015 are not captured by the model simulations during spring. These events are related to halogen chemistry reactions that are not represented in the model simulations. The simulations are on average in good agreement with the observations apart from the spring depletion events. The normalized mean bias for the full period is offset by the depletion events and is therefore high (31% for the o-suite and 46% for the control run). The correlation coefficient is low for the o-suite ($r = 0.14$) but it performs better than the control run ($r = -0.05$), especially in winter and spring 2015.

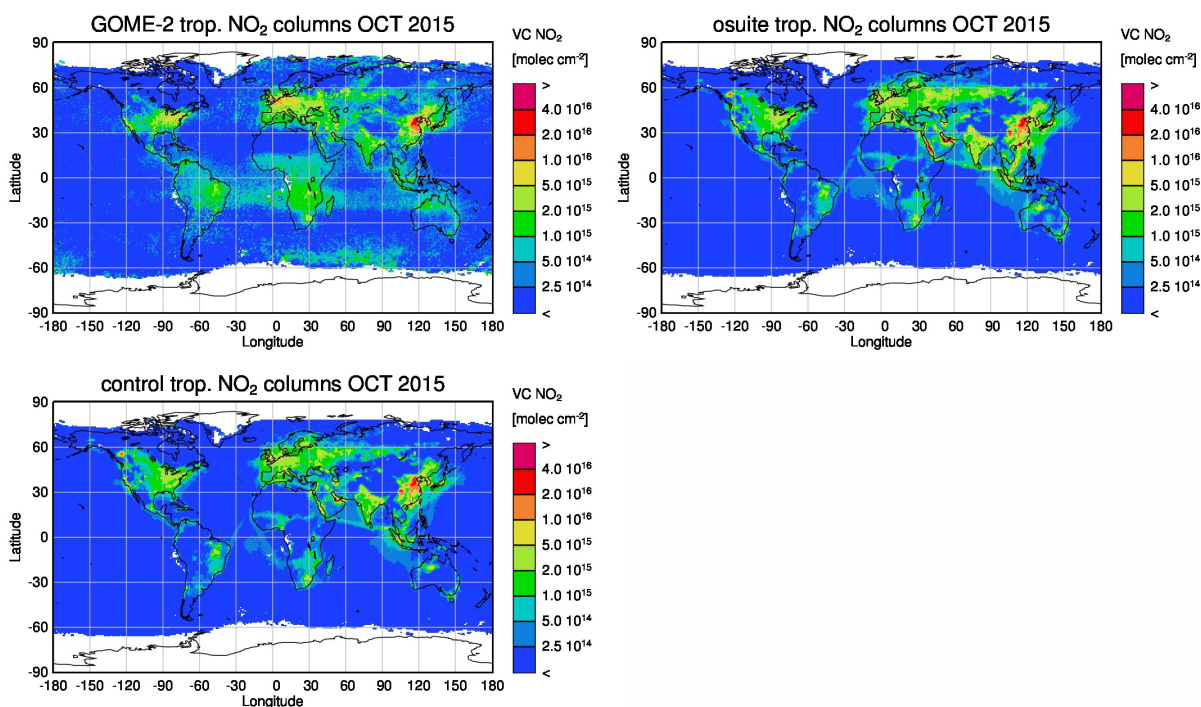


Figure 3.2.1: Monthly mean tropospheric NO₂ columns [molec cm⁻²] from GOME-2 compared to model runs for October 2015. GOME-2 data were gridded to model resolution (i.e. 0.75° deg x 0.75° deg). Model data were treated with the same reference sector subtraction approach as the satellite data.

For the period September – November 2015 the measurements are not quality controlled. The model simulations are on average in good agreement with the observations although they underestimate the observed concentrations at the end of the period, resulting in a normalized mean bias of -4% and -9% for the o-suite and control run, respectively, for the period. The short-term variability is not well captured with a low correlation coefficient for both simulations: $r = 0.08$ for the o-suite and $r = -0.03$ for the control run for September – November 2015.

3.2 Tropospheric nitrogen dioxide

3.2.1 Evaluation against GOME-2 retrievals

In this section, model columns of tropospheric NO₂ are compared to SCIAMACHY/Envisat NO₂ satellite retrievals (IUP-UB v0.7, Richter et al., 2005) for model data before April 2012, and to GOME-2/MetOp-A NO₂ satellite retrievals (IUP-UB v1.0, Richter et al., 2011) for more recent simulations. This satellite data provides excellent coverage in space and time and very good statistics. However, only integrated tropospheric columns are available and the satellite data is always taken at the same local time, roughly 10:00 LT for SCIAMACHY and 09:30 LT for GOME-2, and at clear sky only. Therefore, model data are vertically integrated, interpolated in time and then sampled to match the satellite data. Uncertainties in NO₂ satellite retrievals are large and depend

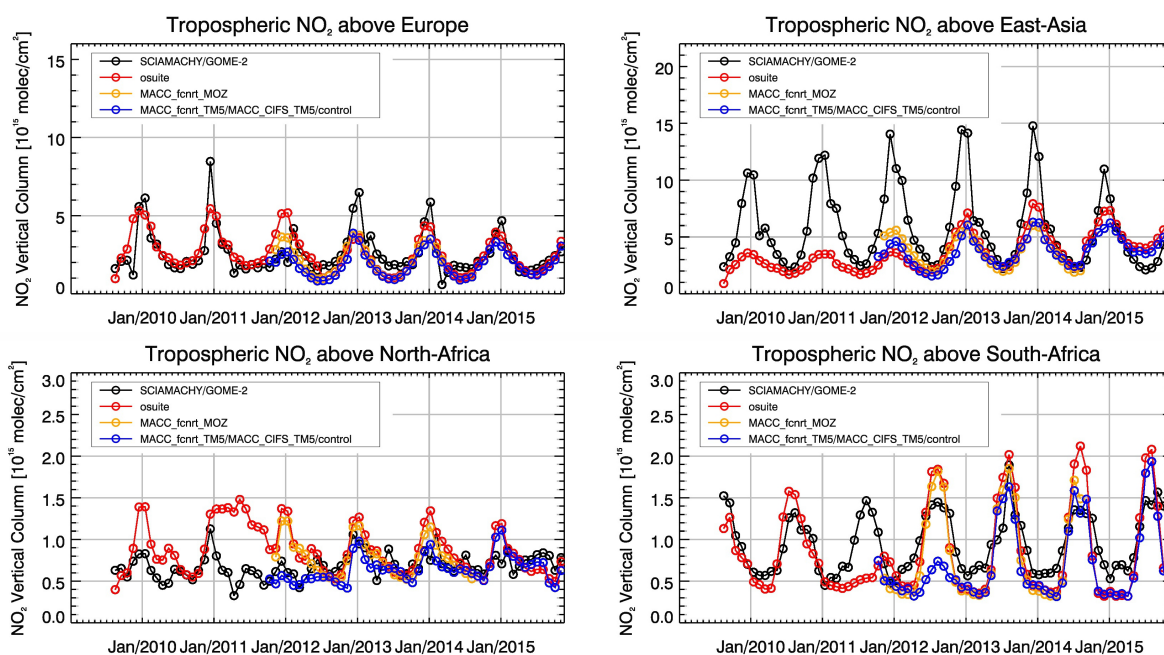


Figure 3.2.2: Time series of average tropospheric NO₂ columns [10^{15} molec cm^{-2}] from SCIAMACHY (up to March 2012) and GOME-2 (from April 2012 onwards) compared to model results for different regions (see Annex 2 for definition of regions). Upper panels represent regions dominated by anthropogenic emissions, lower panels represent those dominated by biomass burning. The blue line shows MACC_fcirt_TM5 from November 2011 to November 2012, MACC_CIFS_TM5 results from December 2012 to August 2014 and control results from September 2014 onwards.

on the region and season. Winter values in mid and high latitudes are usually associated with larger error margins. As a rough estimate, systematic uncertainties in regions with significant pollution are of the order of 20% – 30%.

Fig. 3.2.1 shows monthly mean tropospheric NO₂ columns for October 2015. The overall spatial distribution and magnitude of tropospheric NO₂ is well reproduced by both model runs, indicating that emission patterns and NO_x photochemistry are reasonably represented. Some differences are apparent between observations and simulations, with generally larger shipping signals simulated by the models. For example, shipping signals are largely overestimated to the south of India. Moreover, the o-suite simulates NO₂ column values almost as large as those over East-Asian emission hotspots over the Red Sea and the Persian Gulf which is unrealistic, but the reasons for this require further investigation. The control run performs a bit better here, indicating that data assimilation may add up to the overestimation of values in these regions. Compared to satellite data, all model runs underestimate tropospheric background values over Africa and South America. Local maxima of values observed over emission hotspots in Central Europe are underestimated by the models, while they are overestimated over the heavily populated Sichuan Basin in East Asia (30°N, 105°E). Moreover, both runs show a local maximum over Canada (around 125° W, 55° N), which does not show up in the satellite retrievals. A reasonable explanation is an overestimation of NO_x fire emissions in this area (the presence of fires in October 2015 is confirmed by global fire maps, <http://rapidfire.sci.gsfc.nasa.gov/firemaps/>).



Note that this issue has occurred over biomass burning regions before and as such was already reported in previous MACC/CAMS near real time reports.

Closer inspection of the seasonal variation of tropospheric NO₂ in some selected regions (Fig. 3.2.2) reveals significant differences between the models and points to some simulation problems. Over regions where anthropogenic emissions are major contributors to NO_x emissions, models catch the shape of the satellite time series rather well. However, over East-Asia absolute values and seasonality are in general strongly underestimated by all model runs (most likely due to an underestimation of anthropogenic emissions), with the o-suite showing the best results since the o-suite model change in July 2012. As the December peak in tropospheric NO₂ column retrievals decreased for 2014, model simulated values are since then in better agreement with the satellite retrieved ones. However, the decrease in peak values from 2013 to 2014 is not reproduced by the simulations. Springtime and summertime model values increased in 2015 compared to previous years which is not confirmed by the satellite retrievals, so that the simulated values for spring/summer 2015 are by more than 50% larger than satellite retrieved ones. As for East-Asia, a decrease in wintertime satellite retrieved values also occurs for Europe where the peak is usually found around January, which is, as a result, only slightly underestimated by the models for January 2015. The underestimation of tropospheric NO₂ columns over Europe may be caused to some extent by a change of emission inventories in 2012.

Over regions where biomass burning is the major contributor to NO_x emissions, seasonality and amplitude of model columns are determined by fire emissions. The seasonality for the two regions in Africa is simulated reasonably well for 2010 and after October 2011. In the time period in between, a bug in reading fire emissions lead to simulation errors for all MOZART runs. Over North-Africa, the o-suite shows improved results since the update in July 2012 and the change to CIFS-CB05 in September 2014. However, tropospheric NO₂ columns around December are still overestimated by the models. Summertime NO₂ columns in 2015 over North-Africa are underestimated compared to the satellite data. Compared to MACC_fcirt_TM5, the magnitude of tropospheric NO₂ columns over South-Africa is much better simulated by MACC_CIFS_TM5 and the control run. However, the latter runs and especially the o-suite overestimate the seasonal cycle for South-Africa for the years 2014/2015. All runs overestimate the seasonal maximum over South-Africa in 2014 and 2015 which usually occurs around August of each year. This overestimation is most pronounced for the o-suite which shows a value of about a factor of 1.6 larger than GOME-2 retrievals in August 2014. In this case, for 2014 (and in contrast to 2015) model runs without data assimilation agree much better with satellite observations. For November 2015, satellite retrieved values over South-Africa do not decrease below 1×10^{15} molec/cm², a feature which did not show up in the timeseries before. While wintertime values over South-Africa were also

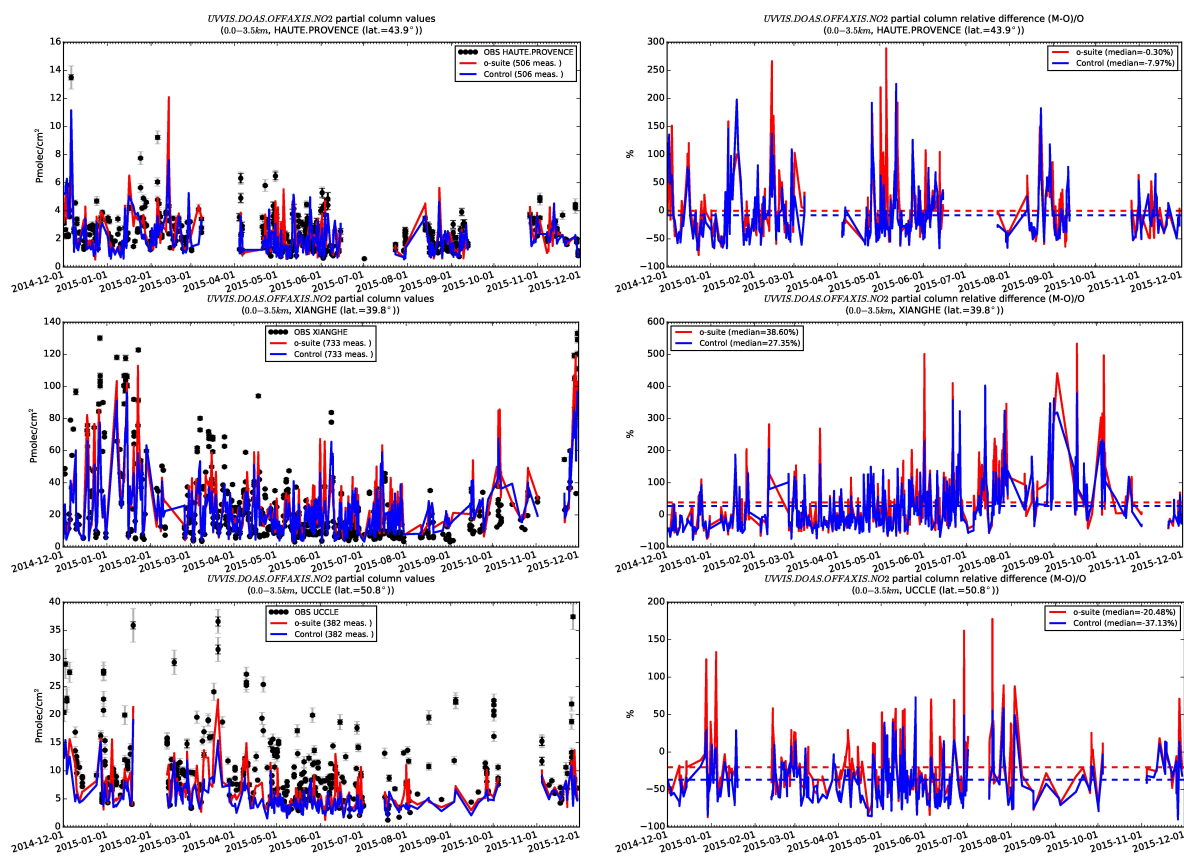


Figure 3.2.3: Daily mean relative differences of tropospheric NO₂ columns (till 3.5km) by the o-suite (red) and control run (blue) compared to NDACC UVVIS DOAS data at Haute Provence (43.9°N, 5.71°E, top), Xianghe (39.8°N, 117°E, middle) and Uccle (50.8°N, 4.36°E, bottom) for the period Dec 2014 -Dec 2015. The number of measurement days and seasonal bias is indicated in the legend (the overall measurement uncertainty is 8%).

underestimated by the models for previous years, the underestimation is now even stronger given the comparatively large satellite retrieved NO₂ column for November 2015.

3.2.2 Evaluation against ground-based DOAS observations

In this section, we compare the NO₂ profiles of the CAMS models with UVVIS DOAS measurements at Xianghe (39.8°N, 117°E, station near Beijing, altitude 92m), Haute Provence (43.9°N, 5.71°E, rural station, altitude 650m) and Uccle (50.8°N, 4.36°E, urban). This ground-based, remote-sensing instrument is sensitive to the NO₂ abundance in the lower troposphere, up to 1km altitude with an estimated uncertainty of 8%. Tropospheric NO₂ profiles and columns are validated (up to 3.5km). A description of the instruments and applied methodologies is the same all DOAS OFFAXIS measurements, see <http://nors.aeronomie.be>. It is important to mention here that the model partial column values between the surface and 3.5 km are calculated for the smoothed model profiles (see Fig. 3.2.3). This guarantees that the model levels where the measurement is not sensitive do not contribute to the observed bias. We should mention that the measurement data is still catalogued as rapid delivery and not in the consolidated NDACC database.

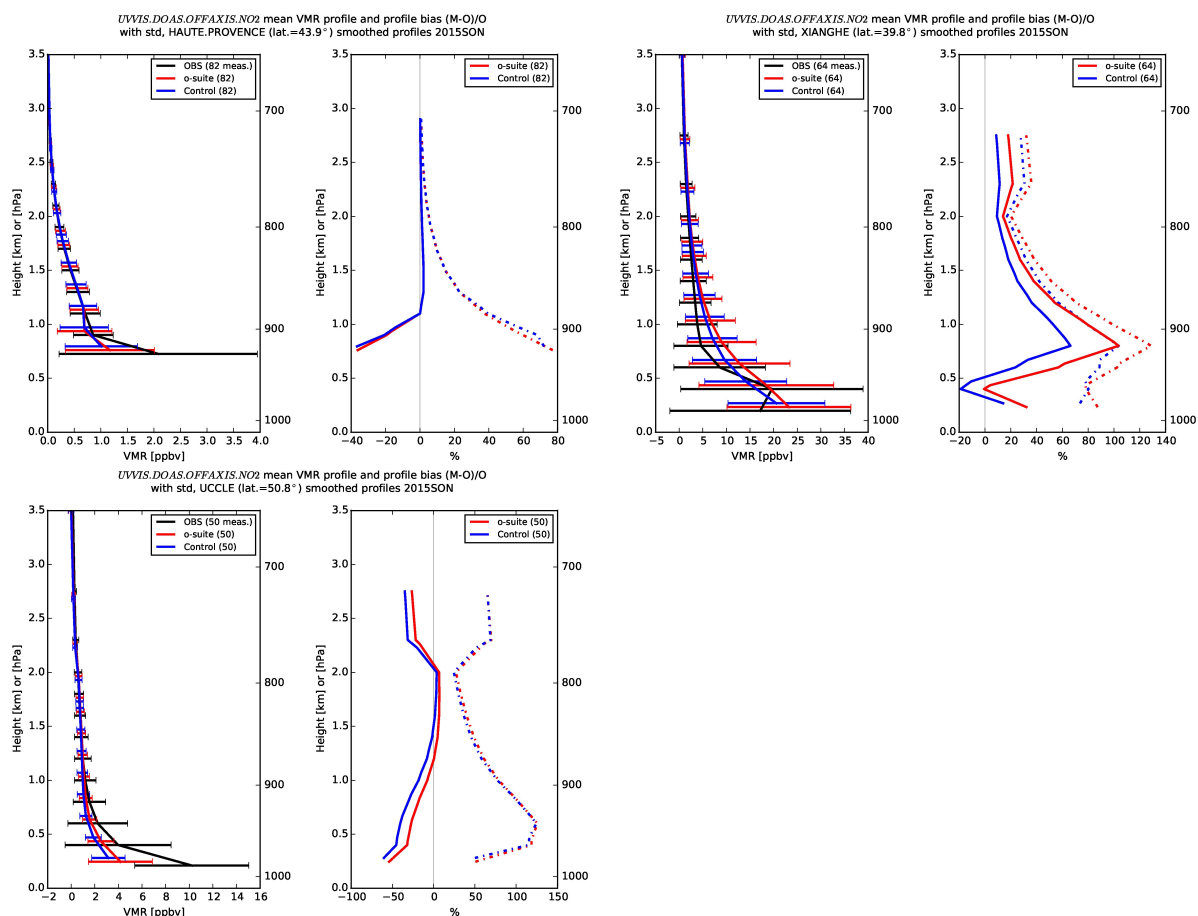


Figure 3.2.4: Seasonal mean tropospheric NO₂ profiles by o-suite (red) and Control (blue) compared to NDACC UVVIS DOAS data at Haute Provence (43.9°N, 5.71°E, left top), Xianghe (39.8°N, 117°E, right) and Uccle (50.8°N, 4.36°E, bottom) for Sept-Oct-Nov 2015.

From Figs. 3.2.4 we see the assimilation has a positive effect on the observed profile biases all three stations. In JJA the o-suite overestimates the NO₂ abundance in Xianghe.

3.3 Carbon monoxide

3.3.1 Validation with Global Atmosphere Watch (GAW) Surface Observations

For the Near-Real-Time (NRT) validation, 7 GAW stations have delivered CO surface mixing ratios in NRT and data is compared to model results as described in Annex 2 of CAMS-VAL report #1. In the following, a seasonal evaluation of model performance for the production runs (o-suite and Control) has been carried out for September - November 2015. The latest validation results can be found on the CAMS website:

<http://www.copernicus-atmosphere.eu/d/services/gac/verif/grg/gaw/>

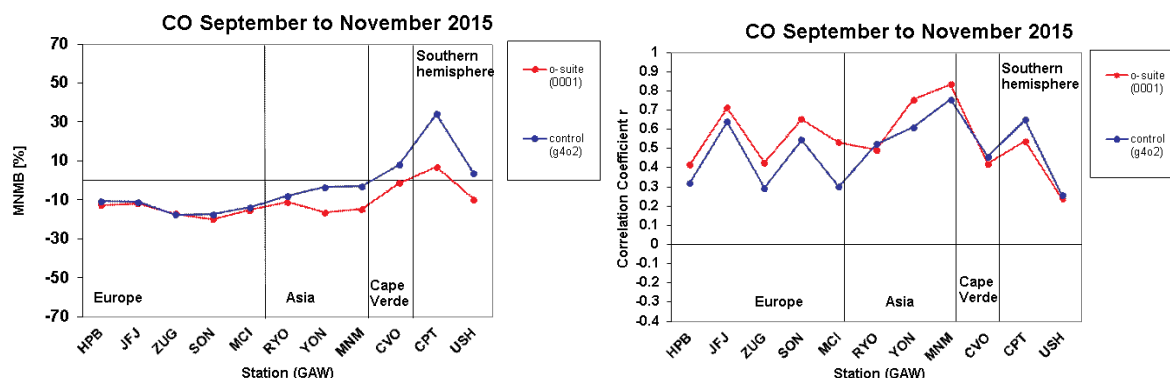


Figure 3.3.1: Modified normalized mean bias in % (left) and correlation coefficient (bottom right) of the NRT model runs compared to observational GAW data in the period September to November 2015.

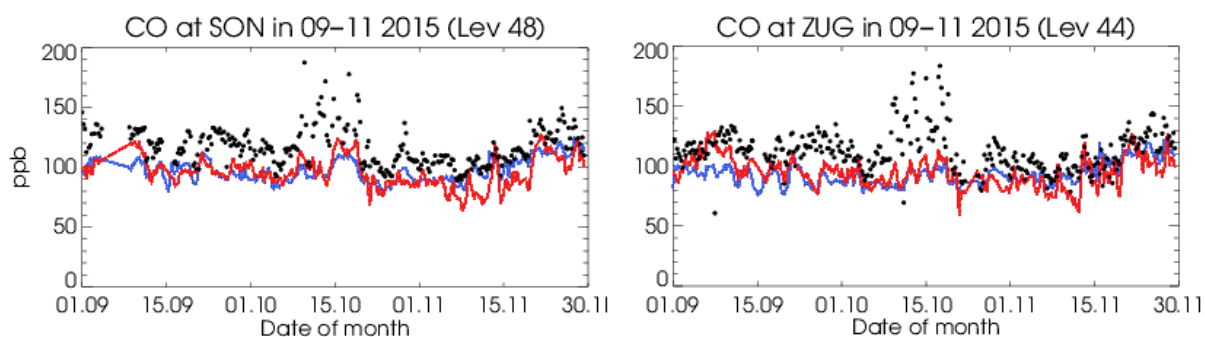


Figure 3.3.2: Time series for the o-suite (red) and Control (blue) compared to GAW observations at Sonnblick (47.0°N, 12.9°E) and Zugspitze (47.1°N, 12.9°E).

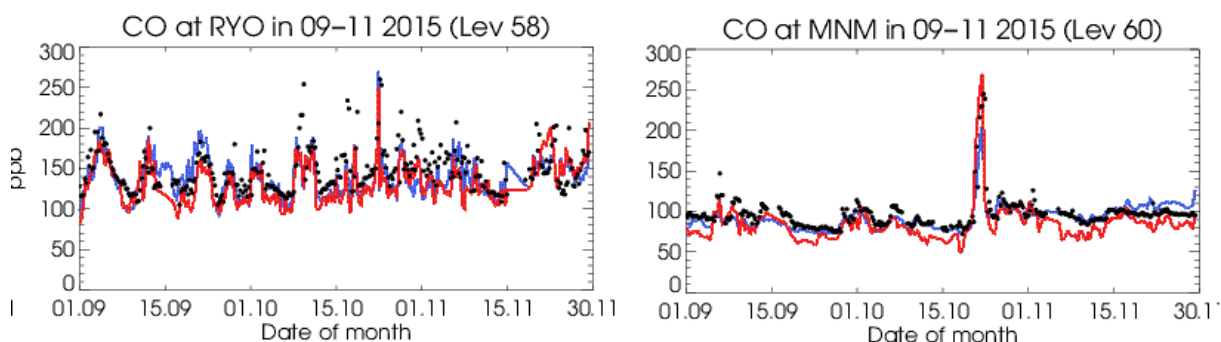


Figure 3.3.3: Time series for the o-suite (red) and Control (blue) compared to GAW observations at Ryori (39.0°N, 141.8°E) and Minamitorishima (24.3°N, 123.9°E).

For European and Asian stations, both model runs slightly underestimate measured CO surface mixing ratios, see Fig. 3.3.1. For Europe, MNMBs are between -10 and -20% for both runs, for stations in Asia between -11 and -17% for the o-suite and between -3 and -8% for the control run. Correlation coefficients are slightly higher for the o-suite and lie between 0.4 and 0.7. For Asian stations, both runs correspond well to the observations. However, the o-suite shows a slight negative offset, see also Fig 3.3.3. Concentration peaks are resolved well by both runs. For the two stations in the Southern Hemisphere,

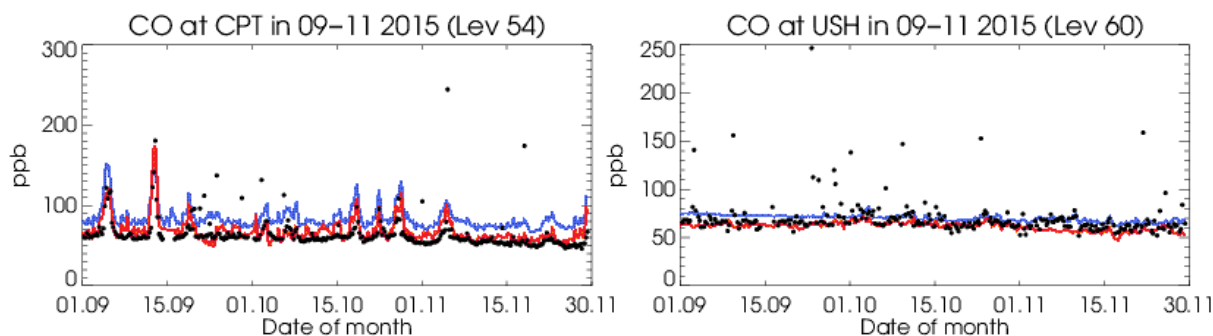


Fig. 3.3.4: Time series for the o-suite (red) and Control (blue) compared to GAW observations at Cape Point (34.35°S, 18.5°E) and Ushuaia (54.9°S, 68.2°W).

especially the o-suite shows a very good correspondence with the observations, see Fig.3.3.4.

3.3.2 Validation with IAGOS Data

The daily profiles of ozone and CO measured at airports around the world, are shown on the website at http://www.iagos.fr/macc/nrt_day_profiles.php. For the period June-August 2015, data from two aircrafts have been validated, as discussed in Sec. 3.1.2.

Figure 3.3.5 shows the time series of CO over New York for the 5 different layers throughout the troposphere. Figure 3.3.6 shows the time series of CO over Dusseldorf and Frankfurt. For these two regions (Europe and North-East of the USA) the model is quasi systematically underestimating the observations especially in the lower troposphere (surface and boundary layer), and to a lesser extent in the free troposphere. The assimilation shows a slight improvement over the control run in free troposphere. The model has failed to capture a striking period of enhanced CO which peaks on 16th October at Frankfurt and at Dusseldorf in the surface and boundary layers and in the free troposphere. This period coincides with “cold pool” meteorological conditions which brought cold weather and early snowfall to Germany. The descent of this polar airmass also led to elevated ozone levels at altitudes above 5km. In the days prior to this event, ozone at Frankfurt did not exceed 50ppbv throughout the troposphere, increasing up to 200ppbv in the UTLS (around 10000m). On 14th October, ozone increases above 50ppbv at altitudes above 5000m and

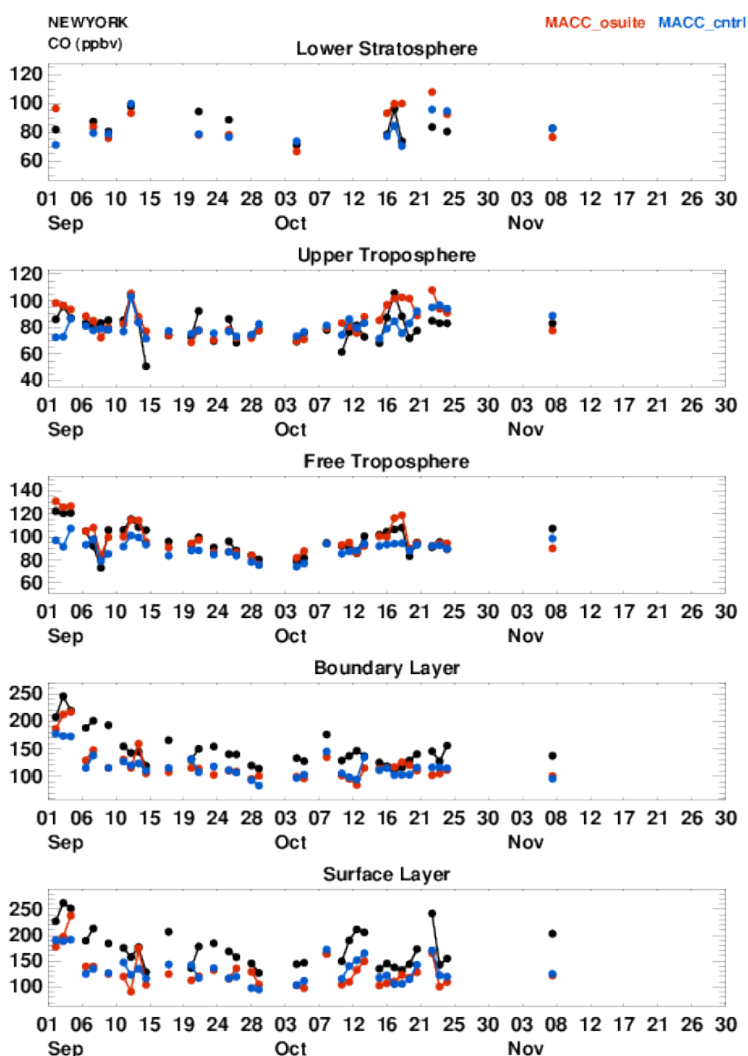


Figure 3.3.5: Time series of daily mean CO over New York from September to November 2015 for 5 layers, Surface, Boundary layer, Free Troposphere, Upper Troposphere and Lower Stratosphere.

150ppbv is recorded at 8000m. The peak in CO seen at this time may therefore be due to the emissions created by a sudden increase in domestic heating, being trapped in the lower troposphere by the cold stable air of the cold pool aloft. The ozone profile over Frankfurt on 14 October suggests a particularly low tropopause or stratospheric intrusion whereas in the boundary layer, the sudden excess in pollution is marked by a reduction in ozone through titration (noted at Frankfurt and Dusseldorf).

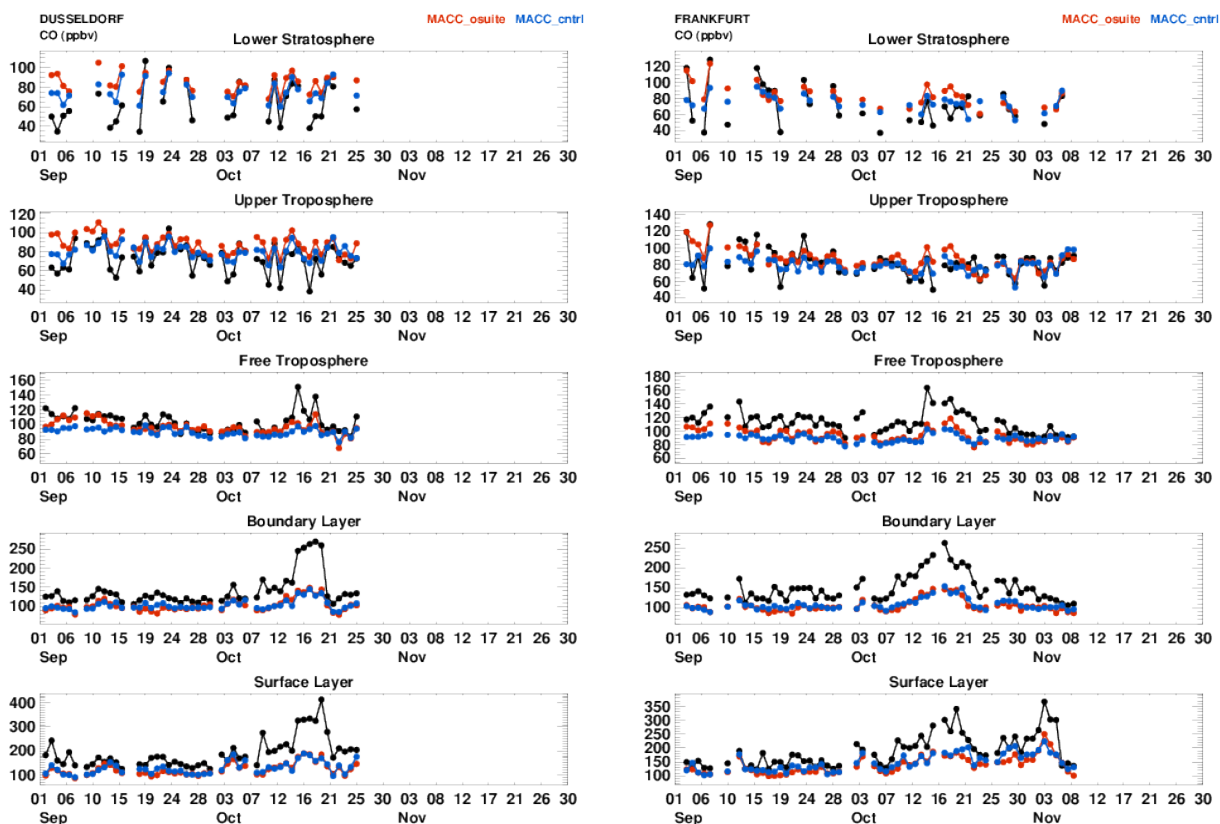


Figure 3.3.6: Time series of daily mean CO over Dusseldorf (left) and Frankfurt (right) from September to November 2015 for 5 layers, Surface, Boundary layer, Free Troposphere, Upper Troposphere and Lower Stratosphere.

For northern hemisphere mid-latitudes, JJA is usually the season of minimum CO due to reduced anthropogenic and increased photochemistry. However, we may observe significant CO enhanced layers because of boreal fires emissions from Siberia, Canada, and Alaska at this time of year. Such CO plumes may be observed thousands of km away as far as over Europe. By September-October-November we no longer expect to find plumes from boreal fires, and anthropogenic emissions are yet to increase. The season can be considered to be 'quiet'.

Europe and USA

Figure 3.3.7 gives examples of the CO profiles over Frankfurt, Dusseldorf and New York. In general we find that CO in the mid-troposphere is well estimated by the models. However there is a systematic underestimation of CO in the boundary and surface layers which was particularly prominent during 14-17 October at altitudes below 4000m (see also the timeseries in Fig. 3.3.6). This coincided with a 'cold pool' meteorological event with snow and cold

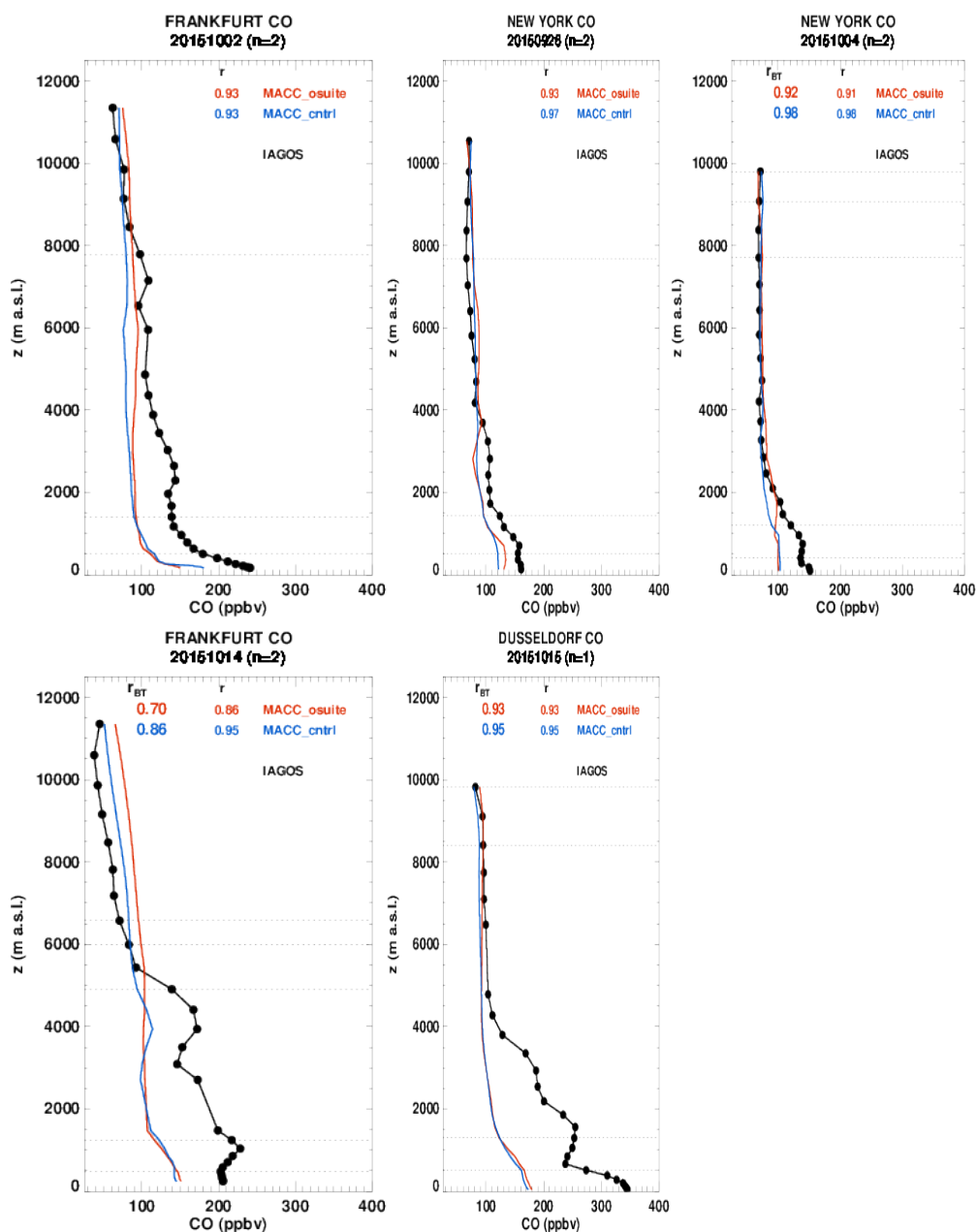


Figure 3.3.7: Selection of profiles of CO from IAGOS (black) and the two NRT runs over Europe and USA in September –November2015.

temperatures centered over Germany. This sudden and early-season cold-snap probably increased emissions from the domestic sector leading to the sudden spike in CO.

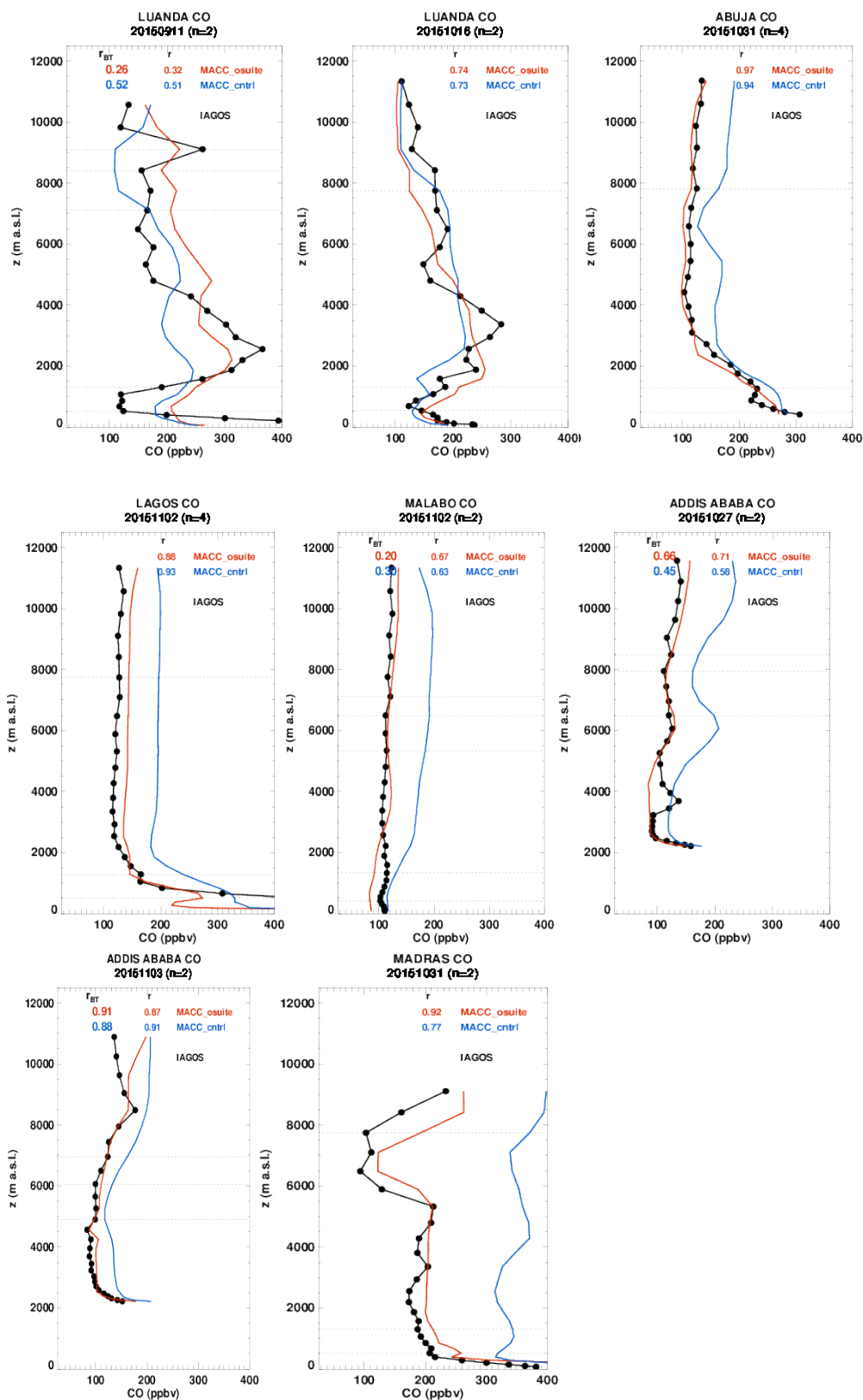


Figure 3.3.8: Profiles of CO from IAGOS (black) and the two NRT runs over Luanda, Abuja, Malabo, Addis Ababa and Madras during the period September to October 2015.

Africa



Figure 3.3.8 highlights some examples of CO profiles over Equatorial Africa as regularly sampled by the second Lufthansa IAGOS equipped aircraft since March 2015. In September-October, CO profiles over Luanda are characterized by CO enhanced layers in the lower troposphere (up to 500 ppb) because of the biomass burning which usually occurs in this dry season in the southern part of Equatorial Africa. The profile on the 11th September and 16th October over Luanda (Angola) highlights such behaviour. Both model runs show a CO enhanced layer in the lower troposphere with the assimilation capturing the altitude of the peak on the 11 September but underestimating its magnitude, whereas on the 15th October the magnitude of the peak is well captured, but it is found at the wrong altitude.

At Abuja, Lagos and Malabo, we see a striking overestimation of CO by the control run. Sometimes CO is overestimated by 100%. The assimilation makes a significant improvement over the control run. This is further illustrated by the profiles Addis Ababa and most strikingly at Madras which serve to show that this overestimation by the control run and improvement following the assimilation is a widespread feature of the modelling system.

3.3.3 Validation against FTIR observations from the NDACC network

In this section, we compare the CO profiles of the CAMS models with FTIR measurements at Maido (21°S, 55°E, i.e. southern tropics, altitude 2.2km), Alzomoni (19°N, 261°E altitude 3.9km) and Lauder (46°S, 169.7°E, altitude 370m). These ground-based, remote-sensing instruments are sensitive to the CO abundance in the troposphere and lower stratosphere, i.e. between the surface and up to 20 km altitude. Tropospheric CO profiles and columns are validated (up to 10km). A description of the instruments and applied methodologies can be found at <http://nors.aeronomie.be>.

Table 3.3.1: Seasonal relative mean bias (MB, %), standard deviation (STD, %) for the considered period and number of observations used (NOBS), compared to NDACC FTIR observations at Lauder, Alzomoni and Maido (mean bias and stddev in %). The overall uncertainty for the CO measurements at Lauder and Alzomoni is approximately 9% and at Maido 5%.

		DJF			MAM			JJA			SON		
		MB	stddev	nobs	MB	stddev	nobs	MB	stddev	nobs	MB	stddev	nobs
o-suite	Lauder	-9.00	4.09	70	-8.44	5.07	92	-1.51	4.57	120	-2.36	5.01	148
	Altzo	-10.39	6.42	158	-9.39	7.59	138	-4.83	10.35	170	-8.41	5.89	104
	Maido	-8.48	4.77	45	-	-	4	-7.37	4.06	125	-6.92	4.04	304
control	Lauder	45.56	5.01	70	41.04	5.35	92	28.24	10.45	120	14.13	7.92	148
	Altzo	10.01	8.87	137	5.13	9.94	170	1.63	5.60	104	4.13	7.45	49
	Maido	35.15	6.74	45	--	--	4	13.51	6.46	125	9.68	10.09	304

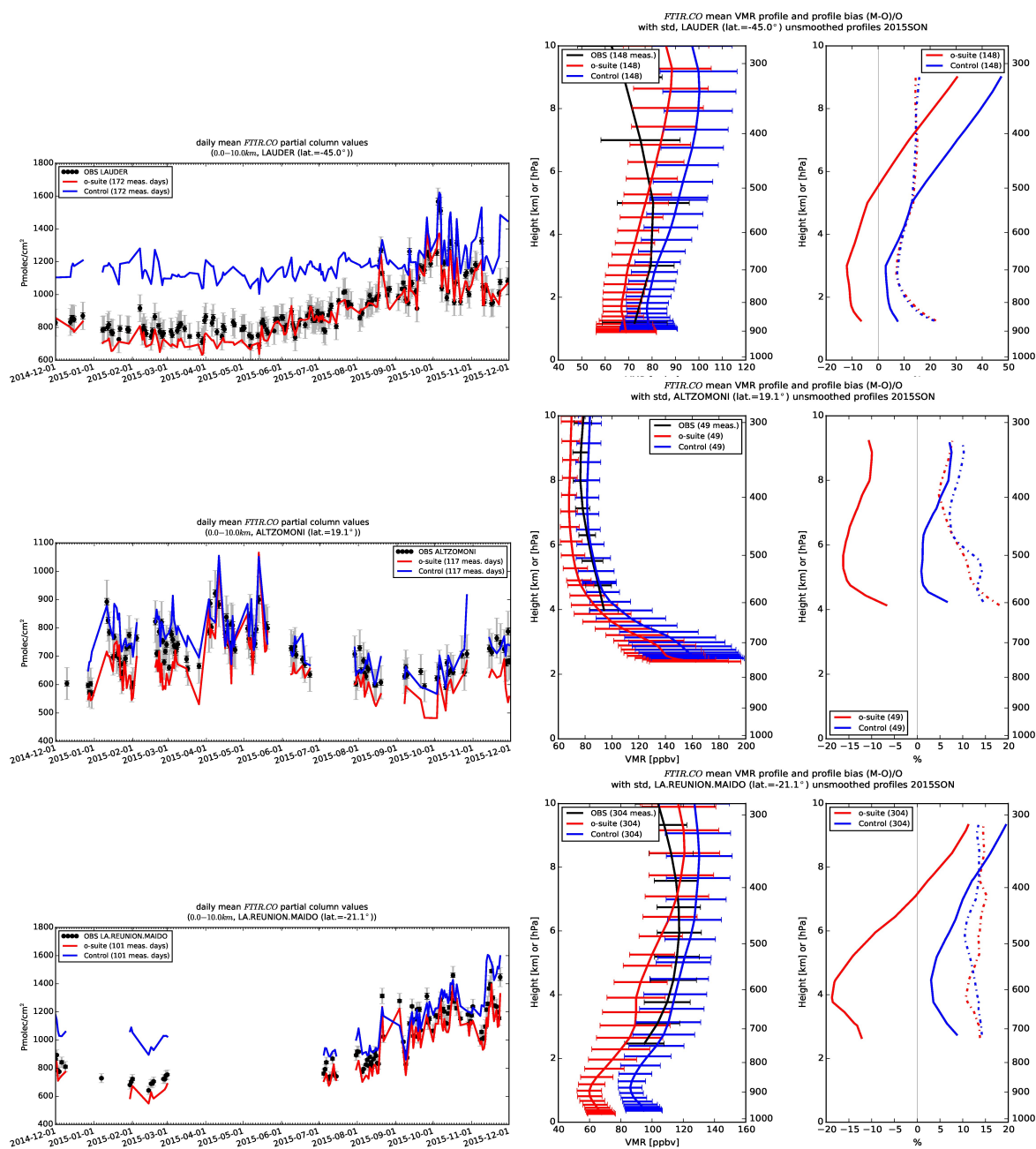


Figure 3.3.9: Daily mean values of tropospheric CO columns (till 10km) by the o-suite (red) and the Control run (blue) compared to NDACC FTIR data at Lauder, New Zealand (45°S, 169.7°E) (top), Altzomoni, Mexico City (19°N, 261°E) (middle) and Maido (21°S, 55°E) (bottom) for the period Dec 2014- Dec 2015. The unsmoothed profile are averaged over Sep-Oct-Nov 2015. The number of measurement days is indicated in the legend.

Table 3.3.1 and Figure 3.3.9 shows that the tropospheric columns of CO agree well. Since the beginning of 2015, the o-suite underestimates at Lauder with values around 9%, reducing to approx. 2% in JJA and SON 2015. At Altzomoni and Maido the o-suite underestimates the CO abundance (approx. 8%). The mean uncertainty on these measurements is 9%, so the observed o-suite biases fall within the measurement’s uncertainty range.

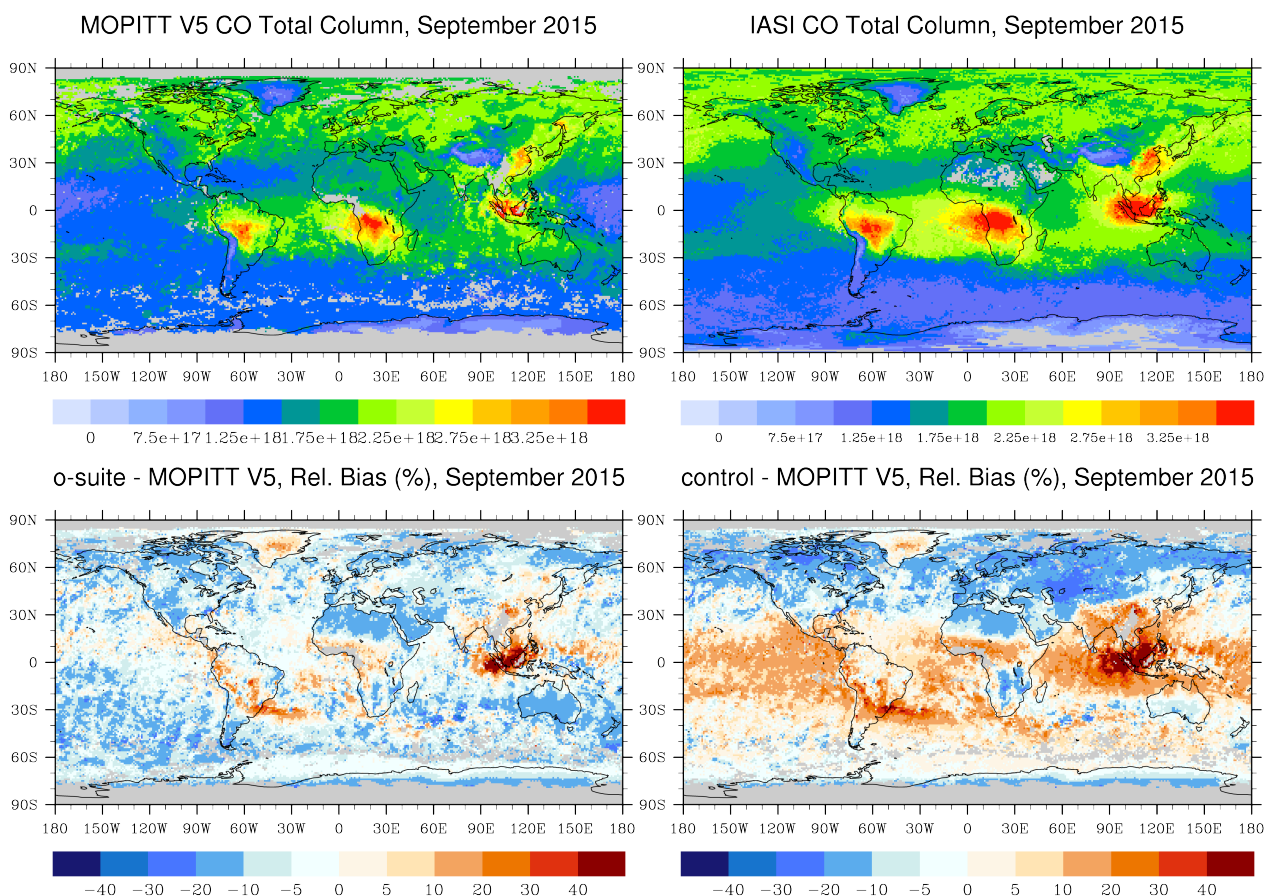
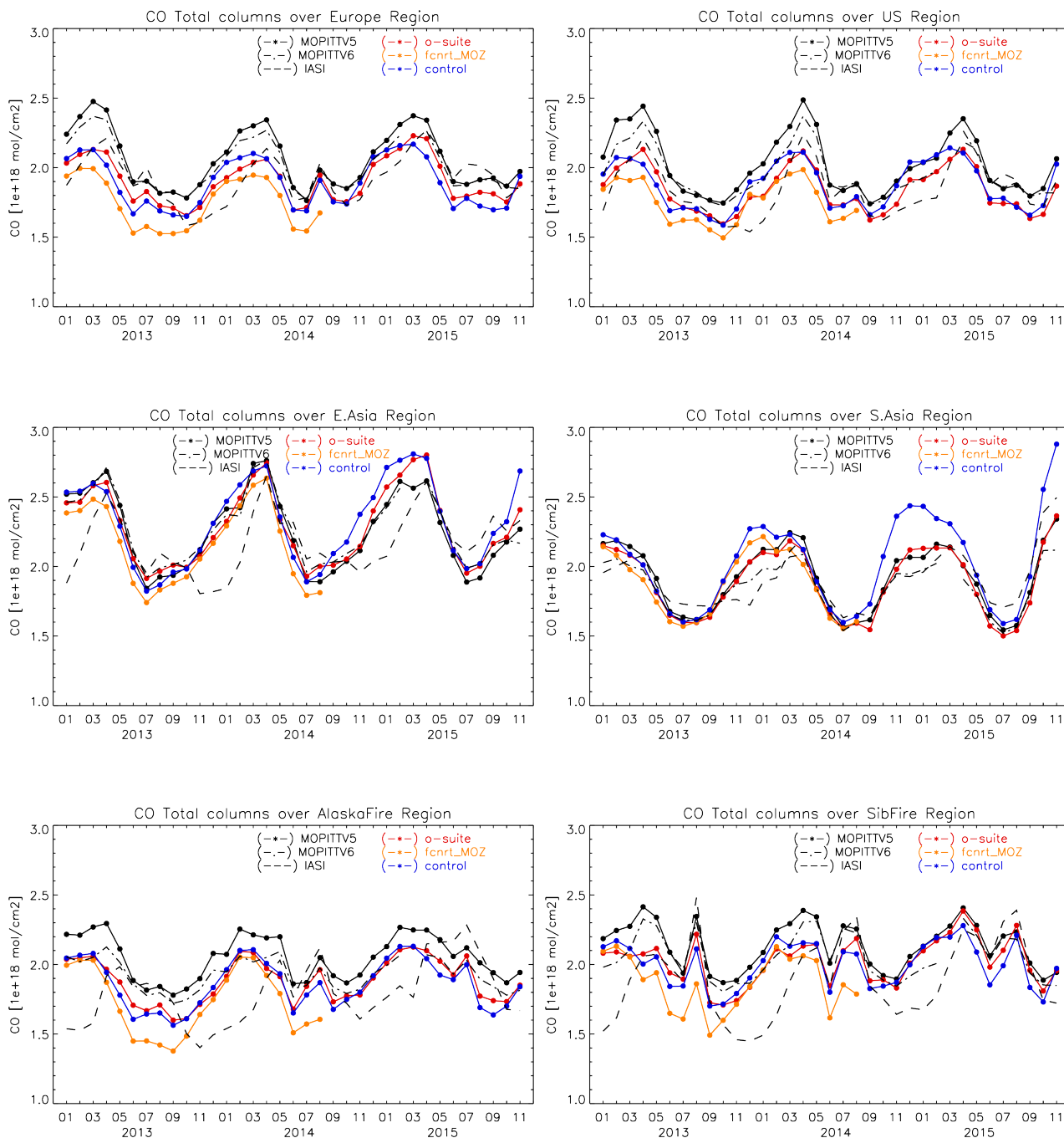


Fig. 3.3.10: CO total column for MOPITT (top left) and IASI (top right) and relative difference between the model runs and MOPITT V5 for September 2015. Left: o-suite, right: control run. Grey colour indicates missing values.

3.3.4 Evaluation with MOPITT and IASI data

In this section, CO total columns from the model forecasts are compared to MOPITT V5 (thermal infrared radiances) and V6 (Emmons et al., 2009, Deeter et al., 2010) and IASI observations. Figure 3.3.10 shows CO total column retrieved from MOPITT (top left) and IASI (top right) and relative bias of modeled values with respect to MOPITT, averaged for September 2015. Autumn 2015 was a notable season in terms of numerous and strong fire events in Indonesia. MOPITT and IASI show similar CO geographical distribution with high values located over Indonesia, South Africa and central part of South America.

The relative difference between the model runs and MOPITT shows that both model runs overestimate CO total column over Indonesia (more than 40 %) and also over the central part of South America (up to 30 %). In general, o-suite overestimates CO total column in the tropics over the land by 10 % to 20 % and underestimates it in the mid- and high-latitudes by 10 % to 20 %. Control simulation shows overestimation over the tropics by 20% to 30%, while negative biases are found in the northern mid- and high-latitudes (up to 30 %).



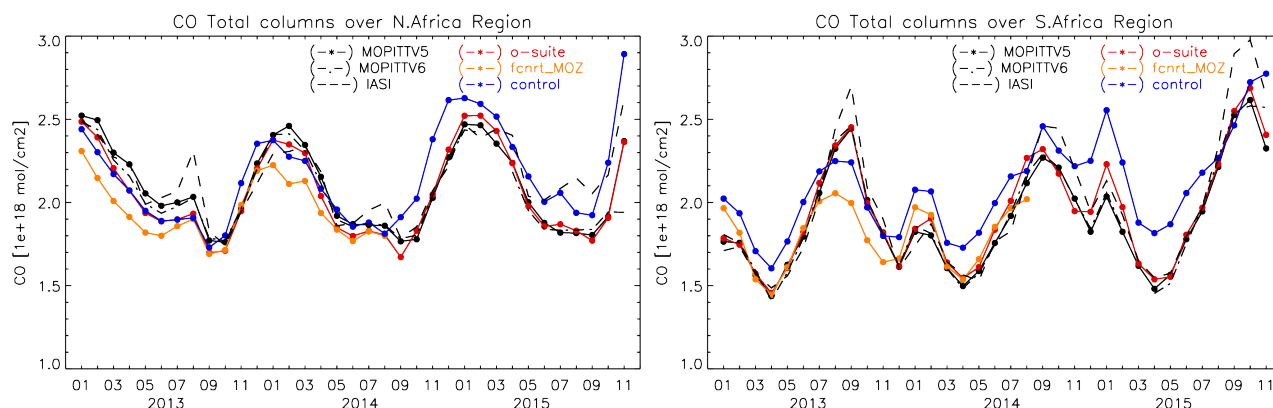


Fig. 3.3.11: Time series of CO total column for MOPITT V5 and V6, IASI and the model runs over the selected regions.

Figure 3.3.11 shows time series of CO total column for MOPITT V5 and V6, IASI and the model runs over different regions. For the comparison with MOPITT, the modelled CO concentrations were transformed using MOPITT V5 averaging kernels (Deeter, 2004). Both MOPITT (V5) and IASI CO total column are assimilated in o-suite run, while a bias correction scheme is applied to IASI data to bring it in line with MOPITT. MOPITT and IASI CO total columns show a relatively similar variability over different regions. In general, IASI CO values are lower compared to MOPITT over most regions, with some seasonal exceptions. Significant differences between MOPITT and IASI are observed over East Asia, Alaskan and Siberian fire regions in winter times, with IASI CO total column values lower by up to 30 %. The differences up to 20 % are also found over Europe and US. Modelled CO seasonality is in relatively good agreement with the retrievals. In general, the comparison between o-suite and control runs shows that assimilation of satellite CO has more positive impact on model results over South Asia and Africa and smaller impact over other regions, like Europe, US, fire regions. It is worth to notice that IASI autumn values are systematically higher compared to MOPITT in South Africa.

The relative bias of the model runs compared to MOPITT V5 (fig. 3.3.12) allows quantifying the impact of assimilation on the model performance. All model forecasts show negative biases over Europe, US and Alaskan fire region. In autumn 2015, o-suite shows good results with bias just about +/- 5 % in Europe, Asia, Africa and Siberian fire region. The control run shows systematic positive bias compared to o-suite in South Asia and North Africa in autumns and winters. In November 2015 the control run shows largest bias in above mentioned regions showing 25 %, which is about 5 % more compared to November 2014.

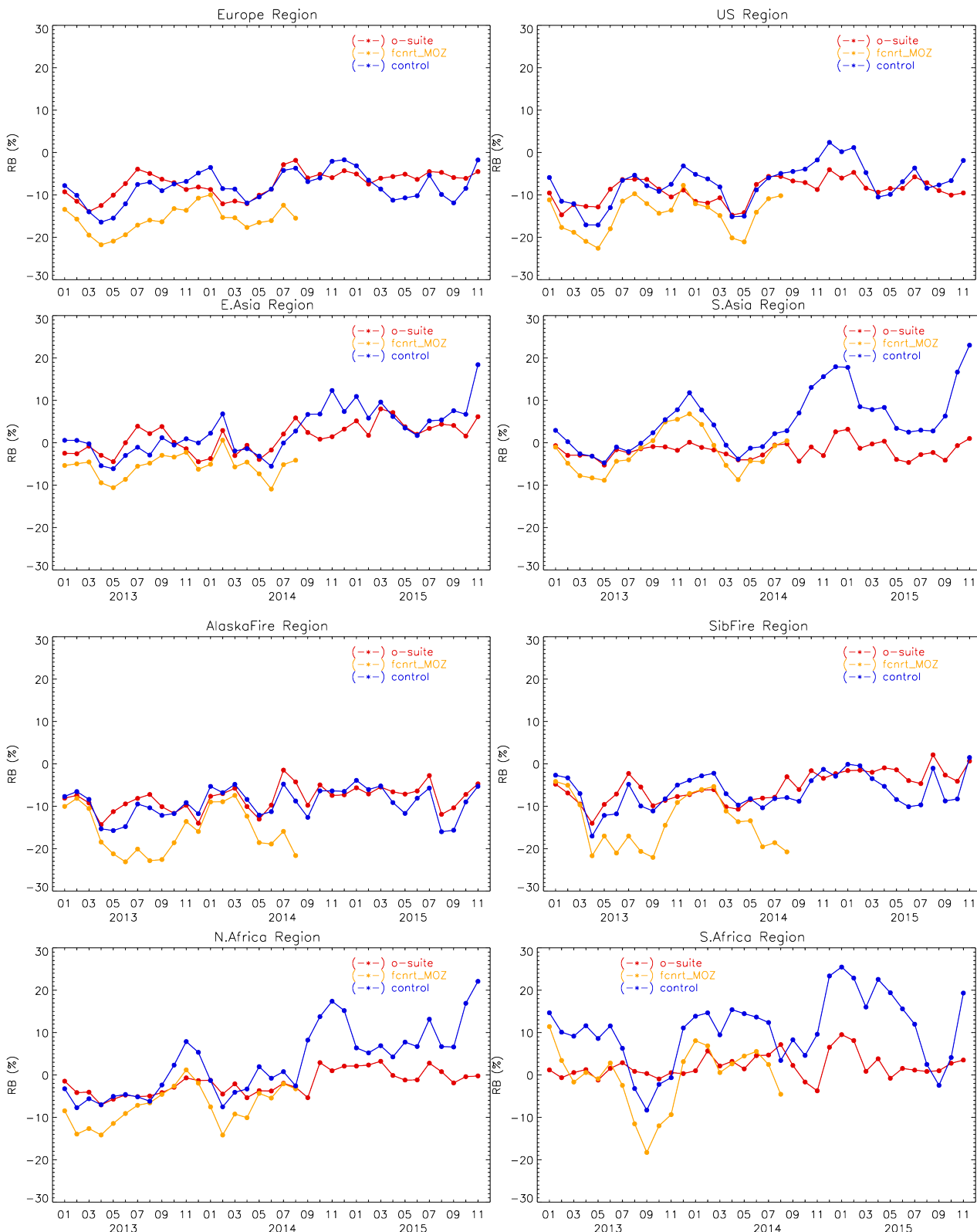


Fig. 3.3.12: Relative biases (%) of CO total columns from the model simulations vs MOPITT V5 retrievals over the selected regions.

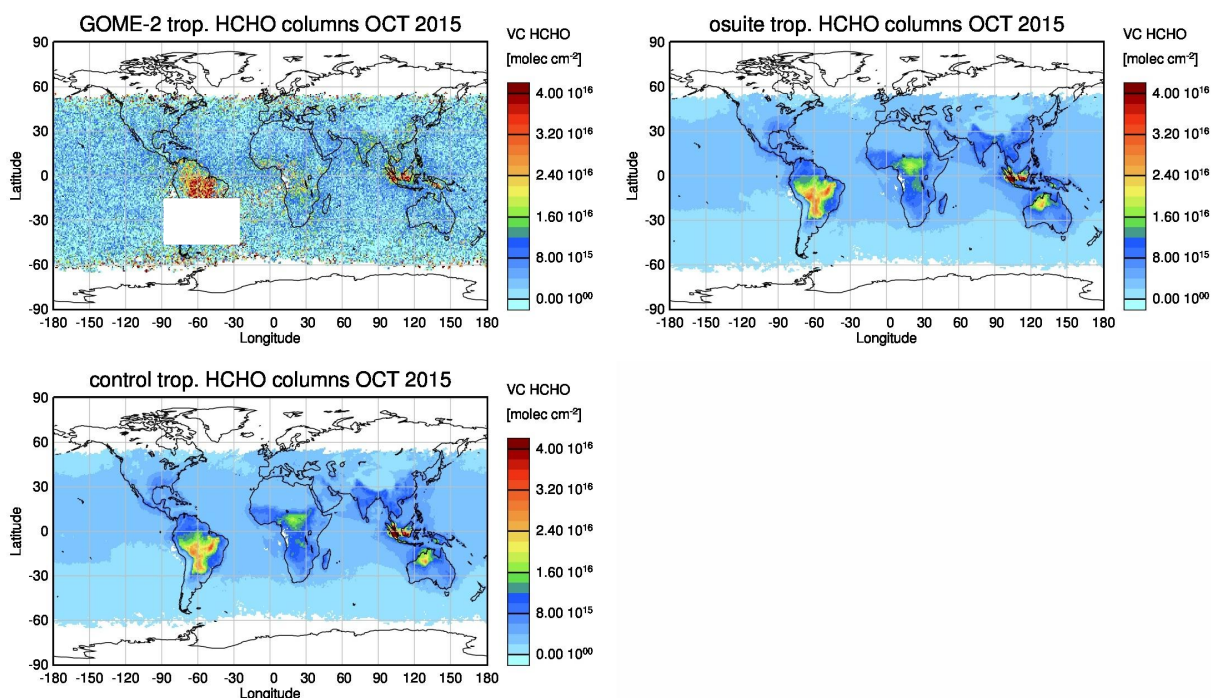


Figure 3.4.1: Monthly mean tropospheric HCHO columns [molec cm⁻²] from GOME-2 compared to model runs for October 2015. GOME-2 data were gridded to model resolution (i.e. 0.75° deg x 0.75° deg). Values in the region of the South Atlantic Anomaly are not valid and therefore masked out (white box in upper left panel).

3.4 Formaldehyde

In this section, simulations of tropospheric formaldehyde are compared to SCIAMACHY/Envisat HCHO satellite retrievals (IUP-UB v1.0, Wittrock et al., 2006) for model data before April 2012 and to GOME-2/MetOp-A HCHO data (IUP-UB v1.0, Vrekoussis et al., 2010) afterwards. As the retrieval is performed in the UV part of the spectrum where less light is available and the HCHO absorption signal is smaller than that of NO₂, the uncertainty of monthly mean HCHO columns is relatively large (20% – 40%) and both noise and systematic offsets have an influence on the results. However, absolute values and seasonality are retrieved more accurately over HCHO hotspots.

In Fig. 3.4.1, monthly mean satellite HCHO columns are compared to model results for October 2015. The magnitude of oceanic and continental background values and the overall spatial distribution are well represented by o-suite and control. Simulated maxima over South America are generally underestimated compared to GOME-2 satellite retrievals, while there is a strong overestimation of values for Northern Australia and Central Africa.

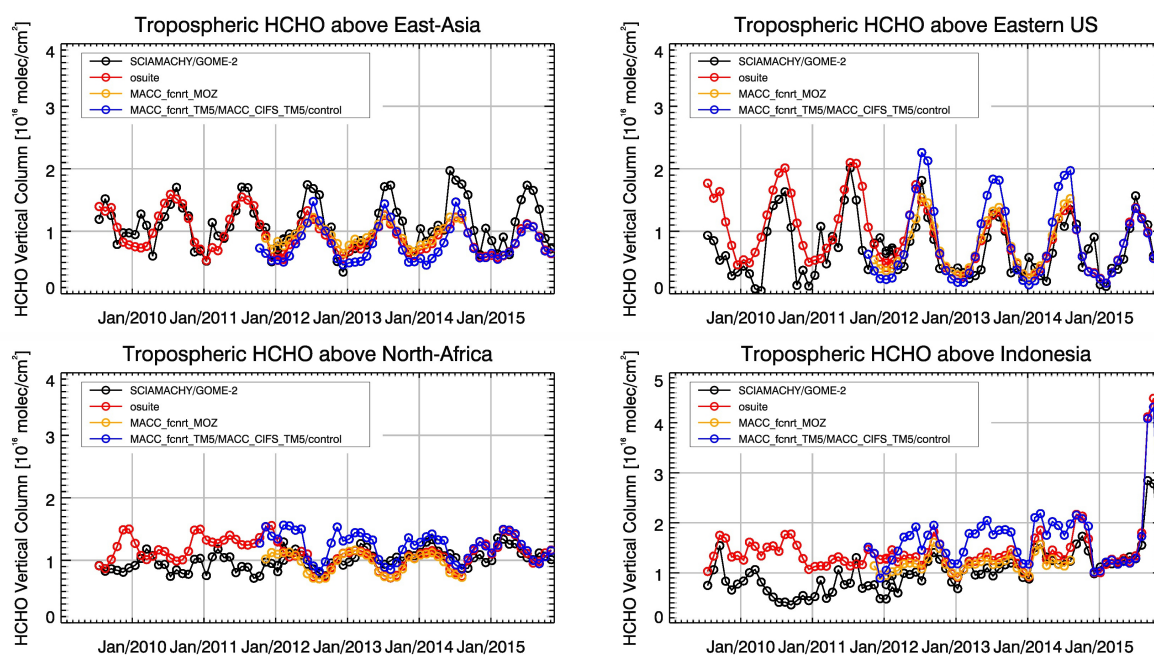


Figure 3.4.2: Time series of average tropospheric HCHO columns [10^{16} molec cm⁻²] from SCIAMACHY (up to March 2012) and GOME-2 (from April 2012 onwards) compared to model results for different regions. The blue line shows MACC_fcprt_TM5 from November 2011 to November 2012, MACC_CIFS_TM5 results from December 2012 to August 2014 and control results from September 2014 onwards. The regions differ from those used for NO₂ (see Annex 2) to better focus on HCHO hotspots: East-Asia (25-40°N, 110-125°E), Eastern US (30-40°N, 75-90°W), Northern Africa (0-15°N, 15°W-25°E) and Indonesia (5°S-5°N, 100-120°E). See text for details.

Time series in Fig. 3.4.2 highlight three cases:

- East-Asia and the Eastern US, where HCHO is dominated by biogenic emissions. Model results and measurements generally agree rather well. However, all model runs tend to underestimate the yearly cycle over East-Asia since 2012. In contrast to MOZART runs, MACC_CIFS_TM5 overestimated satellite values for Eastern US since the middle of 2013. However, the newer CIFS-CB05 runs perform well for Eastern US since 2015. Looking at the whole time period investigated, MOZART chemistry runs simulated a decrease in maximum values which occur around August over East-Asia for each year, which is not observed from satellite. However, satellite values and those simulated by both MOZART chemistry runs agree well since 2012. There is virtually no difference between the new o-suite runs with CIFS-CB05 chemistry and the corresponding control runs without data assimilation. The variability or “ups and downs” in HCHO columns observed by GOME-2 since December 2014 is not reproduced by the models. It is not clear if this variability in satellite data could also point to problems regarding the satellite retrieval.

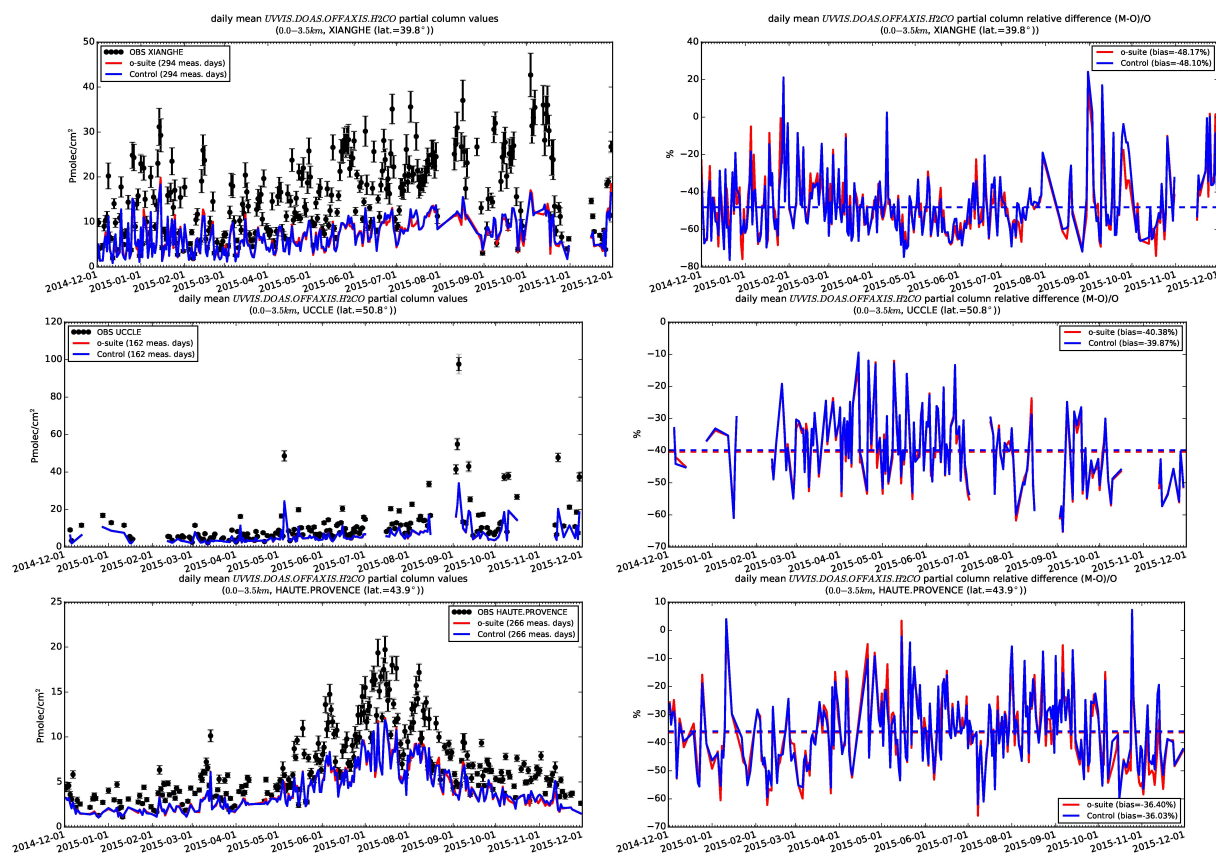


Figure 3.4.3: Daily mean relative differences of tropospheric HCHO columns (till 3.5km) by the o-suite (red) and the control run (blue) compared to NDACC UVVIS DOAS data at Xianghe (39.8°N, 117°E, top), Uccle (50.8°N, 4.36°E, middle) and Haute Provence (43.9°N, 5.71°E, rural station, altitude 650m, bottom) for the period Dec. 2014 –Dec. 2015. The number of measurements and median of differences is indicated in the legend (the overall measurement uncertainty is 10%).

- North-Africa, where biomass burning as well as biogenic sources largely contribute to HCHO and its precursors. Satellite observations over North-Africa are generally overestimated by CIFS-CB05 chemistry runs in the latest o-suite. MOZART-based simulations and observations agree reasonable since 2012.
- Indonesia, where HCHO is also dominated by biogenic sources and biomass burning. The new CIFS-CB05 runs agree very well with satellite retrieved ones for December 2014 to August 2015. For September and October 2015, satellite retrieved HCHO columns show a pronounced maximum.

Earlier model forecasts generally overestimated satellite values here (by a factor of 3 – 4 in the second half of 2010) and failed to reproduce the observed seasonality. This may be due to the use of fire emissions including El Nino years which experience much larger fire activities. MOZART simulations and observations agree much better since late 2012. A closer look at HCHO over Indonesia is given in Sec. 4.1.

Details on the HCHO evaluation can be found at:

http://www.doas-bremen.de/macc/macc_veri_iup_home.html.

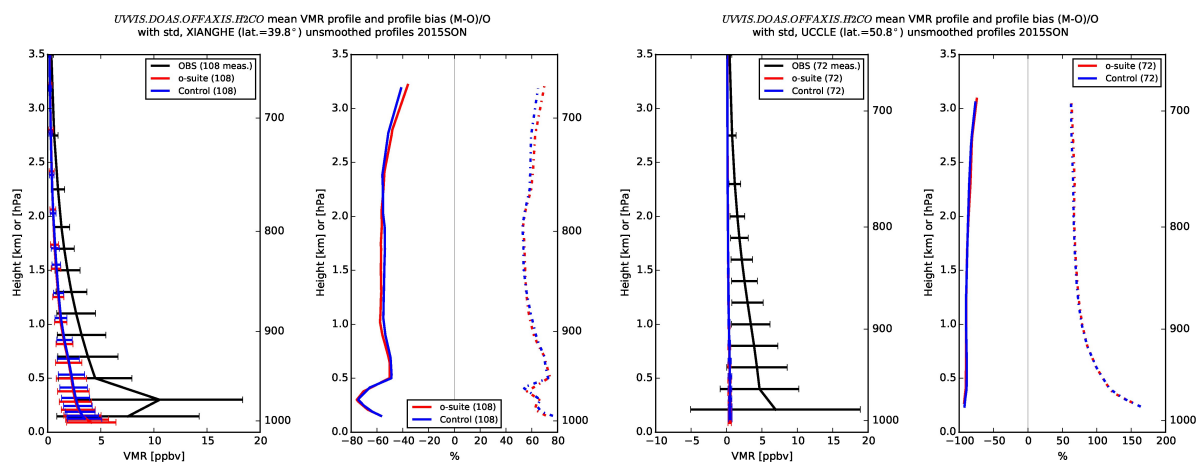


Figure 3.4.4: Mean tropospheric HCHO profiles by the o-suite (red) and the control run (blue) compared to NDACC UVVIS DOAS data at Xianghe (39.8°N, 117°E, left) and Uccle (50.8°N, 4.36°E, right) for the period June-July-August 2015.

3.4.1 Validation against UVVIS DOAS observations from the NDACC network

In this section, we compare the HCHO profiles of the CAMS models with UVVIS DOAS measurements at Xianghe (39.8°N, 117°E, station near Beijing, altitude 92m), Haute Provence (43.9°N, 5.71°E, rural station, altitude 650m) and Uccle (50.8°N, 4.36°E, urban). This ground-based, remote-sensing instrument is sensitive to the HCHO abundance in the lower troposphere, up to 1km altitude. Tropospheric HCHO profiles and columns are validated (up to 3.5km). A description of the instruments and applied methodologies is the same as for the MWR O₃ and FTIR O₃ and CO validations see <http://nors.aeronomie.be>. It is important to mention here that the model partial column values between the surface and 3.5 km are calculated for the smoothed model profiles (see Fig. 3.4.4, left). This guarantees that the model levels where the measurement is not sensitive do not contribute to the observed bias. In this specific situation the smoothing of the model profiles implies a strong increase of the model column data by the MAXDOAS apriori. We should mention that the measurement data is still catalogued as rapid delivery and not in the consolidated NDACC database. The measurements have been quality filtered on cloud conditions: only measurements under “clear sky” and “thin clouds” are used (see Gielen et al., 2014).

From Figs. 3.4.3 and 3.4.4 we see little difference between the o-suite and the control run. Both models underestimate the observations below 1km. Although the background column values are well captured by the models, most of the high emission events are not. Sensitivity tests using the tropospheric 3D-CTM model IMAGES (Stavrakou et al., 2013) showed that this underestimation could be related to the underestimation of aromatics (benzene, toluene, xylene) in current anthropogenic emission inventories over China (see Liu et al., 2012). This might be also due to the model’s horizontal resolution which is not high enough to capture the local emission events in the highly polluted area of Beijing. Regarding OHP, which is a mostly remote site, the strong underestimation by the model in summer seem to indicate an underestimation



of H₂CO source gases in biogenic emission inventories. A possible underestimation of regional anthropogenic sources transported to the station should be also investigated (Franco et al., 2015).

3.5 Aerosol

3.5.1 Global comparisons with Aeronet

Standard scores, maps, scatterplots, bias maps, time series comparison and histograms illustrating the performance of the aerosol simulation in the IFS system are made available through the AeroCom web interface:

http://aerocom.met.no/cgi-bin/aerocom/surfobs_annualrs.pl?PROJECT=MACC&MODELLIST=MACC-VALreports . The model run can be compared to the MACC reanalysis (available until Dec 2012) and the AeroCom Median model. A daily updated comparison against 30 selected Aeronet stations is available via the ECMWF CAMS service website, <http://www.copernicus-atmosphere.eu/d/services/gac/verif/aer/nrt/>.

The MACC/CAMS o-suite has undergone some changes in October 2013 as described in the model changes section. Correlation, based on daily aerosol optical depth and NRT Aeronet observations, is rather stable since 2011, but exhibits significant variation. The o-suite forecast at +3 days shows slightly lower correlation, as expected. See figure S3.

Part of the month-to-month variation in correlation is due to the limited quality of the NRT Aeronet data, which have a preliminary nature. Retrospective analysis of the year 2011 shows that this level 1.5 NRT AOD Aeronet data, due to undetected cloud contamination and any uncorrected drift, are on global average 20% higher than quality assured level 2.0 data. See our comparison for summer 2011 in Fig. 3.5.1. Note that the number of observations available decreases considerably by the quality check procedure effectuated by NASA Goddard (summer 2011: level 1.5 NRT # of observations: 728; as compared to level 2.0 # of obs.: 625). At the time of retrieving Aeronet NRT data it is not possible to know which data will be excluded by the quality check. Further analysis, eg. using “the same stations”, will not help much understanding the bias in the level 1.5 NRT data. The analysis from 2011 suggests that the o-suite bias in AOD, which we establish against AOD NRT data has to be corrected for the likely bias in observations.

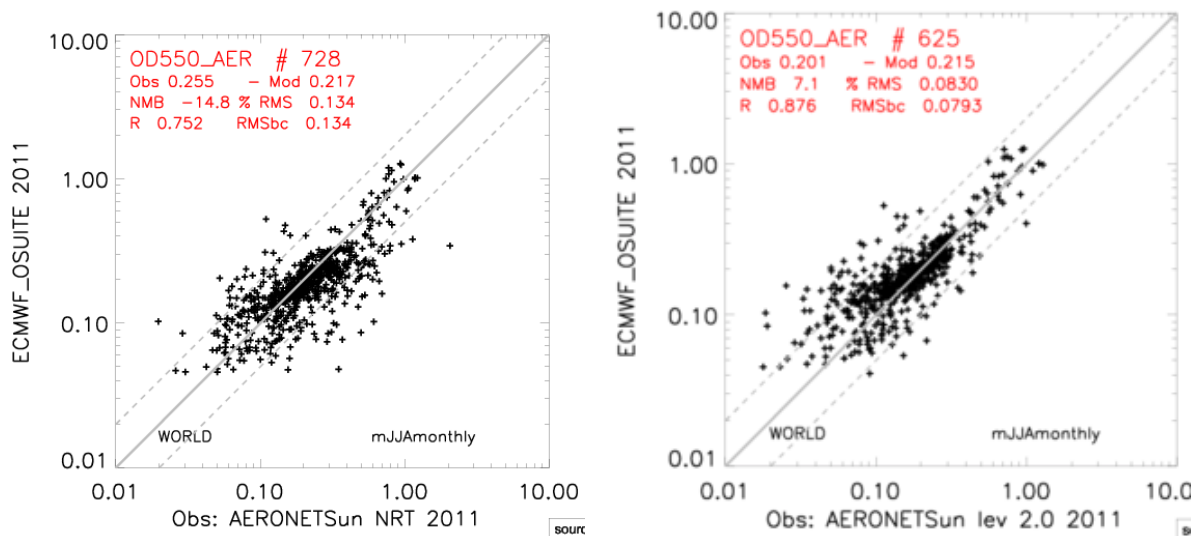


Figure 3.5.1: Retrospective evaluation of the o-suite for the summer months 2011, using NRT Aeronet level 1.5 data (left) and quality assured Aeronet level 2.0 data (right).

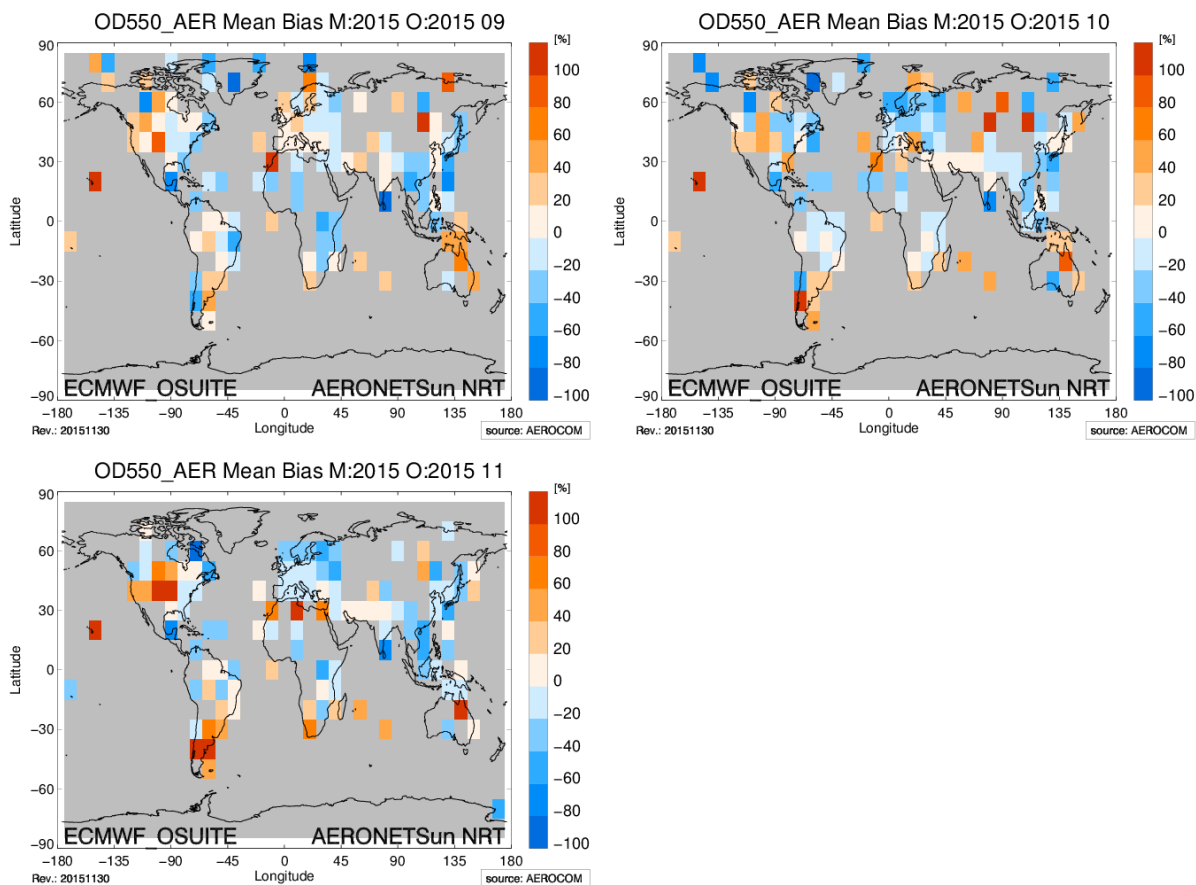


Figure 3.5.2 Aerosol optical depth bias of o-suite in %, against aggregated (10°x10°) NRT Aeronet level 1.5 data for the months of September, October and November 2015.

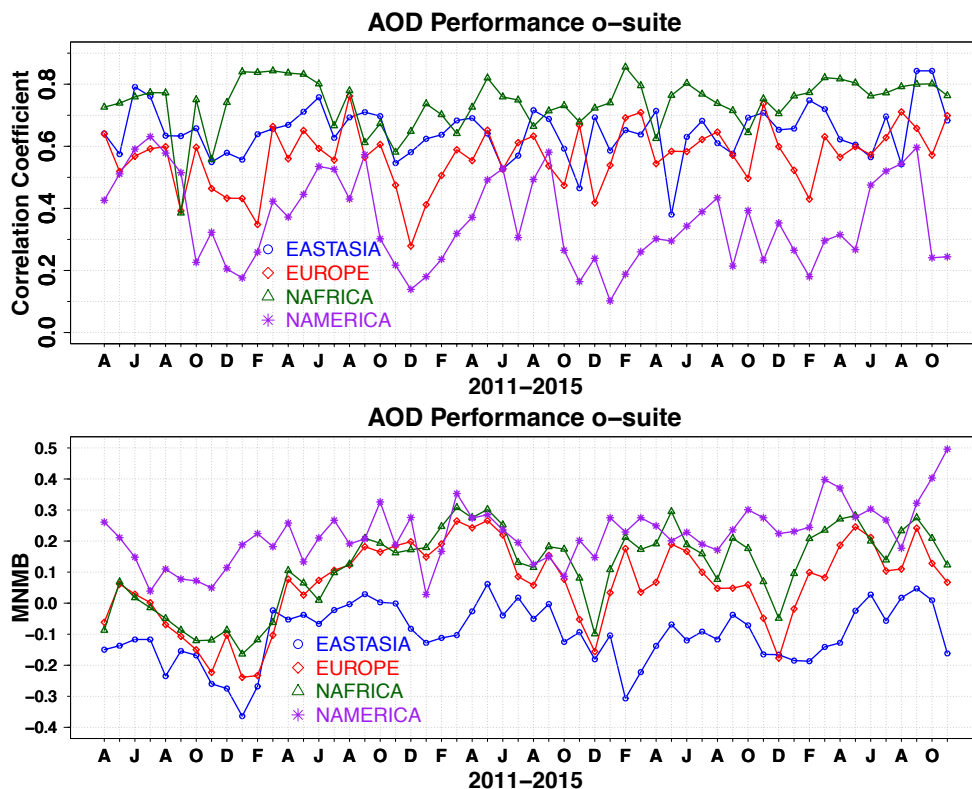


Figure 3.5.3: a) Correlation coefficient and b) modified normalized mean bias (MNMB) in AOD, 2011-2015, based on daily AOD comparison in four world regions [Eastasia(blue); Europe(red); NAfrica(green); NAmerica(purple)] for the o-suite.

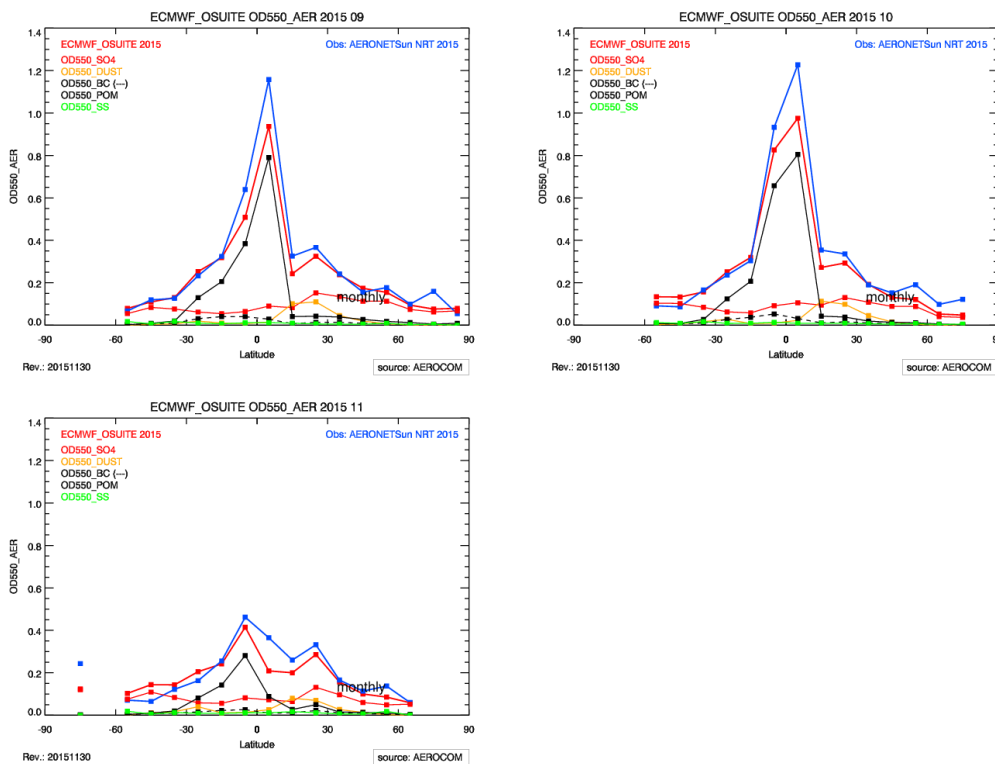


Figure 3.5.4: Aerosol optical depth of o-suite (red) compared to latitudinally aggregated NRT Aeronet level 1.5 data (blue) for the months September, October and November 2015.

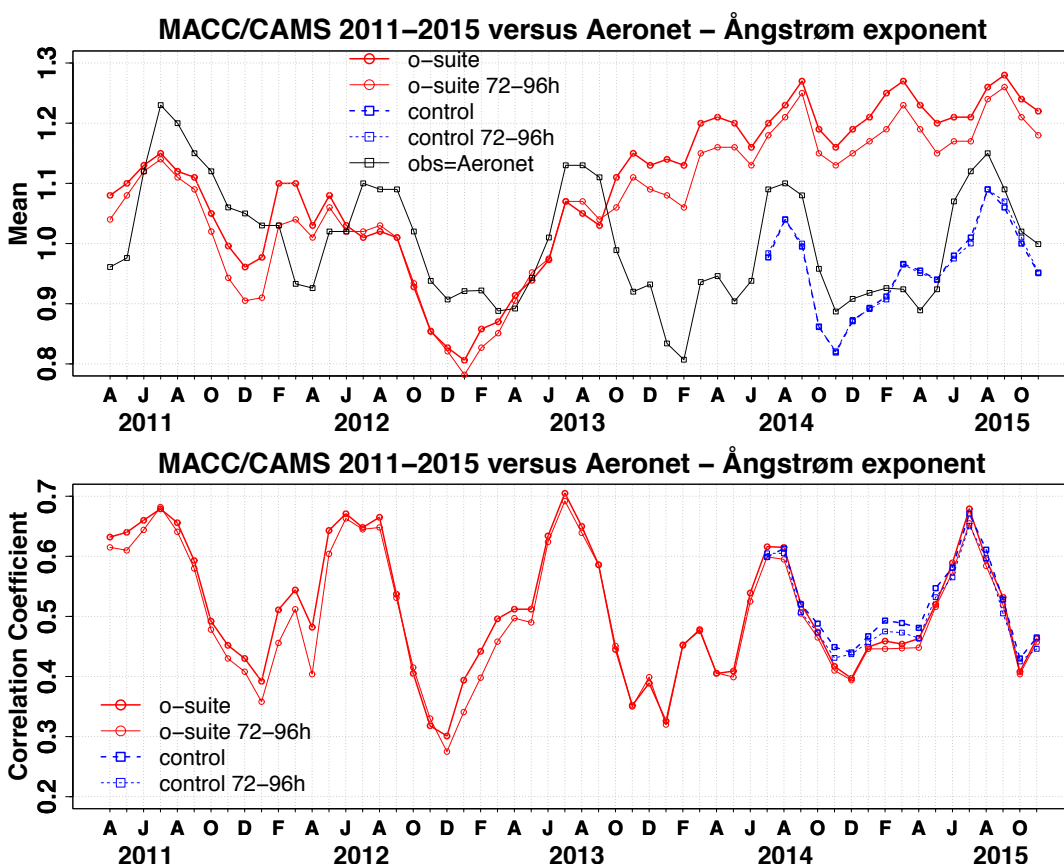


Fig. 3.5.5: a) Evolution of mean Ångström exponent in o-suite and control at Aeronet sites, based on matching monthly mean values. o-suite (thick red curve); o-suite at last forecast day (light red curve); control (blue dashed curve); control at last forecast day (light blue dashed curve). b) Correlation using daily matching Angström exponent.

From daily data we find a bias of +2% in AOD in SON 2015, which, when corrected, corresponds to a likely positive bias of ca +22%, assuming a 20 % bias of NRT data against better quality level 2 data.

The spatial distributions of the AOD bias from September to November are shown in Fig. 3.5.2. The bias pattern is spatially correlated in between months, with some high simulated aerosol optical depth in North and South America in September and November. Note low bias in tropical regions and especially South East Asia in October (missing fire plumes?).

The regional performance of the o-suite model exhibits some seasonal cycle in AOD depending on region (Fig. 3.5.3). Month-to-month variability in correlation in each region may reach 0.1. Larger variations in correlation are probably significant and point to seasonal differences in performance. For instance, the model performance in the North American winter season with respect to correlation seems to be worst, but with some improvement for JJA 2015. In North America the low correlation in winter increasing into spring may be due to large uncertainties in satellite observations over bright land targets, which may not provide enough guidance to the IFS assimilation system, or missing model components such as nitrate. Noteworthy is also the persistent AOD

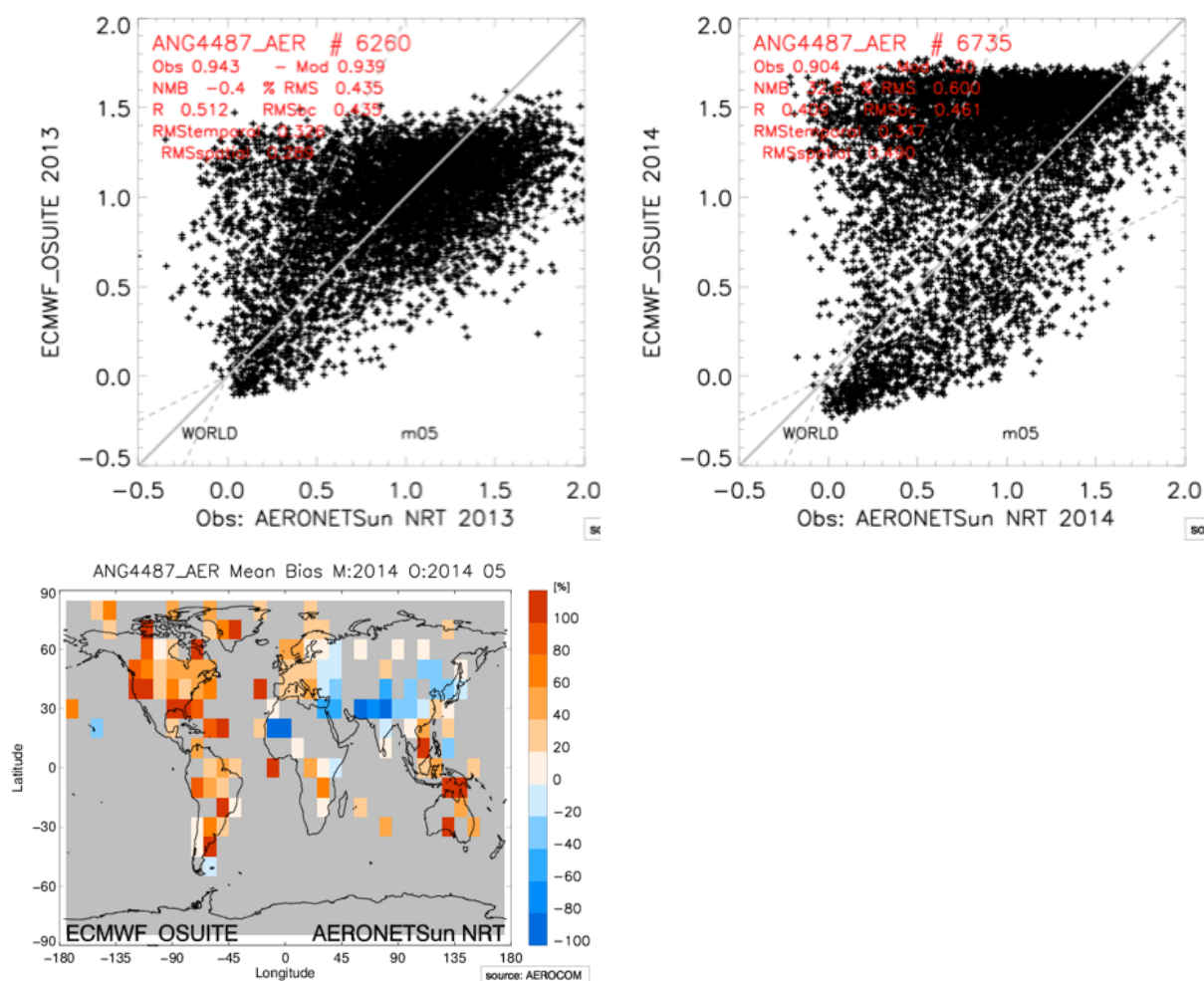


Figure 3.5.6: Evaluation of aerosol Ångström exponent of o-suite for the months May in 2013 a) and May 2014 b), using matching station daily mean values from NRT Aeronet level 1.5 data: c) shows bias map in May 2014.

underestimation over East Asia and the overestimation during latest SON period in North America(3.5.3 b)).

The latitudinal display of model and Aeronet AOD in the period investigated here (Fig. 3.5.4) shows that a significant part of the apparent negative bias against Aeronet NRT comes from tropical and sub-tropical regions.

The simulated aerosol size distribution may be validated to first order using the wavelength dependent variation in AOD, computed as Ångström exponent, with higher Ångström exponents indicative of smaller particles. Figure 3.5.5 a) shows the temporal evolution of simulated and observed mean Ångström exponent, while the correlation is found in figure 3.5.5 b). Recent model version changes in October 2013 have brought a shift in the exponent to higher values, compared to observations. We find a positive bias of +40% (against -5% in before October 2013) (Figure 3.5.5 and 3.5.6). Temporal and spatial variability is rather high and correlation is lower than for AOD (Figure 3.5.5 b), being persistently lower now than in MAM 2013. Figure 3.5.6 c) shows that a high bias in Ångström values is modelled now basically everywhere, except in dusty

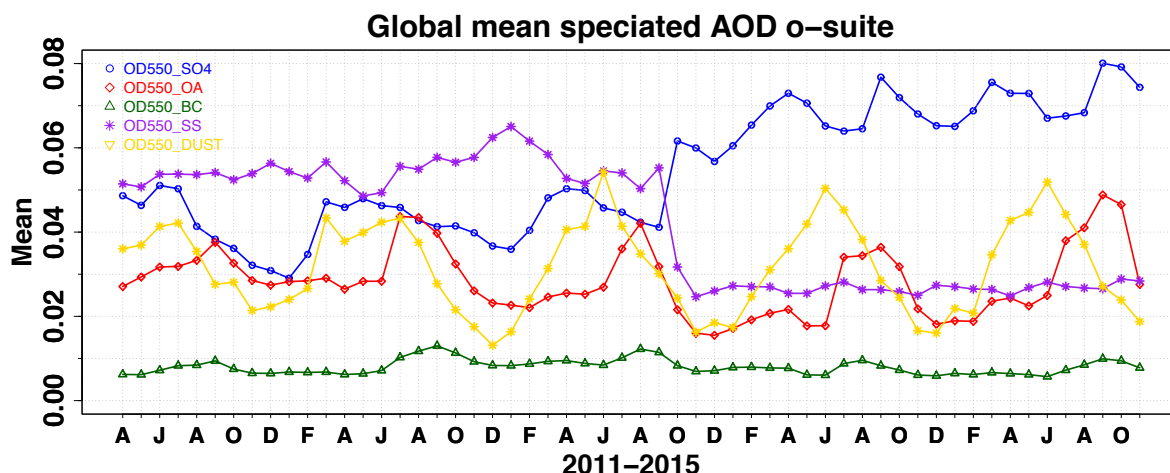


Figure 3.5.7: Evolution of aerosol component's AOD@550nm [OD550_SO4 = sulphate(blue); OD550_OA = organics(red); OD550_BC = black carbon(green); OD550_SS = sea salt(purple); OD550_DUST = dust(yellow)].

Table 3.5.1: Mean global total and speciated AOD in the o-suite for the last two periods covered by the VAL report and change after 3 forecast days.

	o-suite		o-suite	
	Mean JJA 2015 0-24h	Change wrt to first day on day 4	Mean SON 2015 0-24h	Change wrt to first day on day 4
AOD@550	0.181	-11%	0.179	-15%
BC-OD@550	0.007	-17%	0.009	-22%
Dust-OD@550	0.044	4%	0.023	13%
OA-OD@550	0.035	-8%	0.048	-17%
SO4-OD@550	0.068	-23%	0.078	-25%
SS-OD@550	0.027	-7%	0.028	-7%

regions of central Africa and Asia. Figure 3.5.7 shows that the Oct 2013 model changes are responsible for this shift in Ångström exponent. Less sea salt and more sulphate shift the size distribution to smaller sizes. AOD due to sea salt decreased by 50%, that to due organics decreased by 25%, while that of sulphate increased by 40%.

The o-suite uses data assimilation to obtain a first guess aerosol field. In the forecast period, however, a-priori model parameterisations and emissions (except fire emissions, which repeatedly use the latest GFAS values) determine more and more the shape and amplitude of the aerosol fields. The forecasted AOD fields have been used to establish global mean aerosol optical depth and forecast performance after three days (see comparison to first guess in Figure S3 in summary) at Aeronet sites. Table 3.5.1 shows an average global decrease

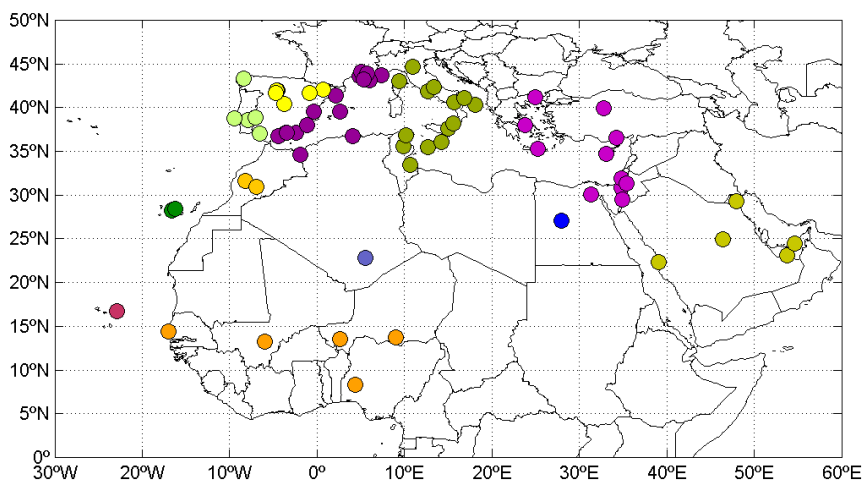


Figure 3.5.8: Map of 71 AERONET level-1.5 stations used in this analysis.

in total aerosol optical depth of 15% during the first four forecast days. The contributions to this reduction stem from almost all aerosol components, except from sea salt and dust. Against Aeronet, correcting for the NRT bias in Aeronet AOD, the o-suite forecast for day three has little overall bias in AOD in summer 2015 (see figure S3).

3.5.2 Dust forecast model intercomparison: Validation of DOD against AERONET, and comparisons with Multimodel Median from SDS-WAS.

Daily dust aerosol optical depth (DOD) from the CAMS o-suite and its control experiment have been validated against 71 AERONET stations grouped in twelve regions for the period 1 September 2015 – 30 November 2015 (Figure 3.5.8).

Here we analyze DOD from CAMS o-suite and control over dust source and transport regions in autumn season when the minimum dust activity is observed over the entire region. We use AERONET (Holben et al., 1998) observations as reference, and compare with daily Multi-model DOD (at 550 nm) Median from nine dust prediction models. The Multi-model Median product is processed at the Sand and Dust Storm Warning Advisory and Assessment System (SDS-WAS) Regional Center for Northern Africa, Middle East and Europe.

We used AOD observations at 550 nm from 61 AERONET whose locations are depicted in Figure 3.5.8. Cloud-screened direct-sun data (Level 1.5) between 440 and 870nm, which contain an uncertainty about 0.01 for AOD under cloud-free conditions, are used. Quantitative evaluations of the modelled dust AOD are conducted for dust-dominated conditions; i.e. when the Ångström exponent (AE) is less or equal to 0.75. All data with AE larger than 1.2 are considered free of dust (DOD = 0 is assumed). Values of AE between 0.75 and 1.2 are associated with mixed aerosols and are not included in the analysis. The AOD at 550 nm is derived from data between 440 and 870 nm following the Ångström's

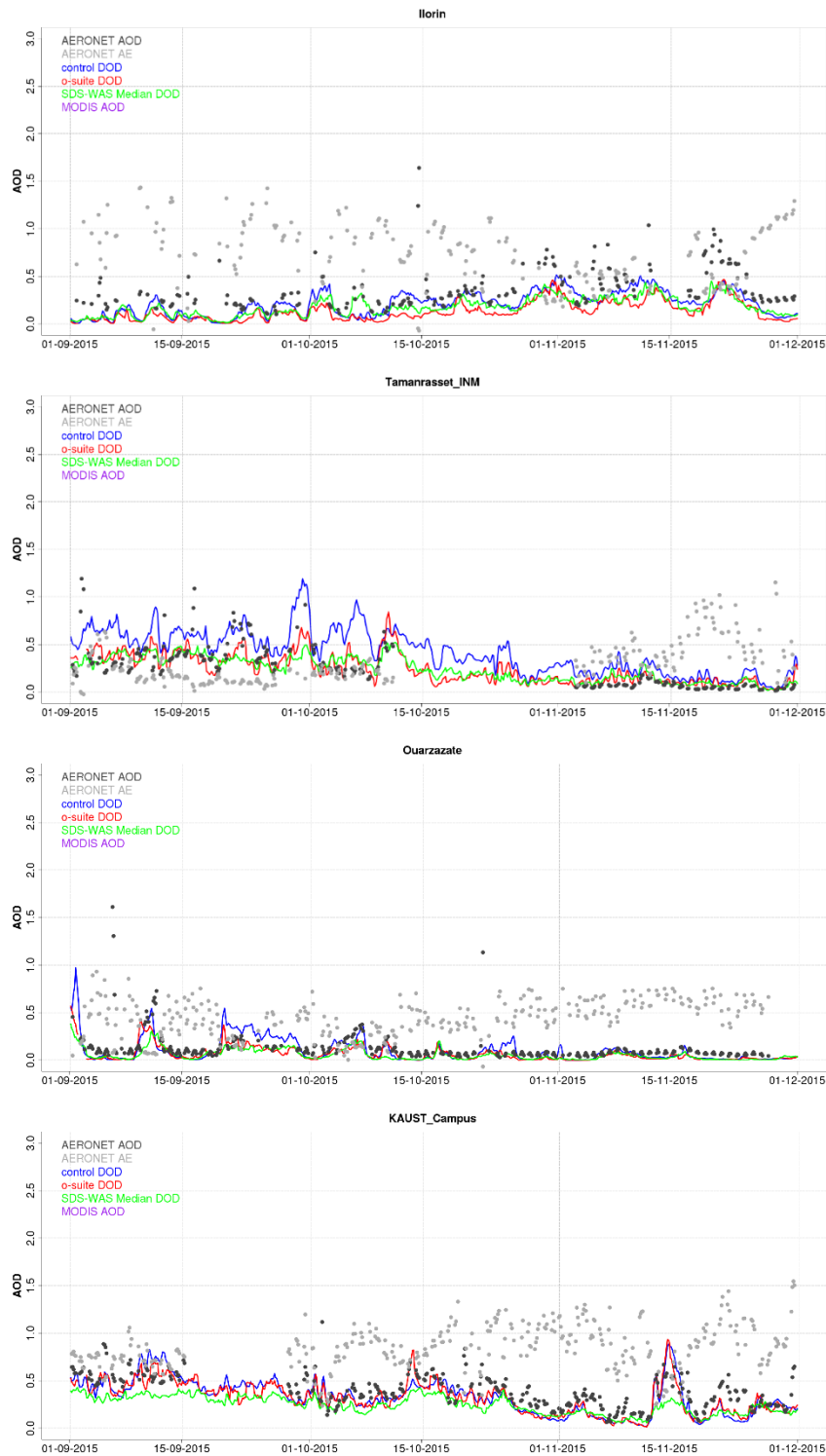


Figure 3.5.9: AOD from AERONET (black dots), DOD o-suite (red line), DOD control (blue line) and DOD Multimodel SDS-WAS Median (green line) for the period September 1st to November 30th, 2015, Ilorin (Sahel), Tamanrasset INM (Sahara), Ouarzazate (NW Maghreb) and Kaust Campus (Middle East).

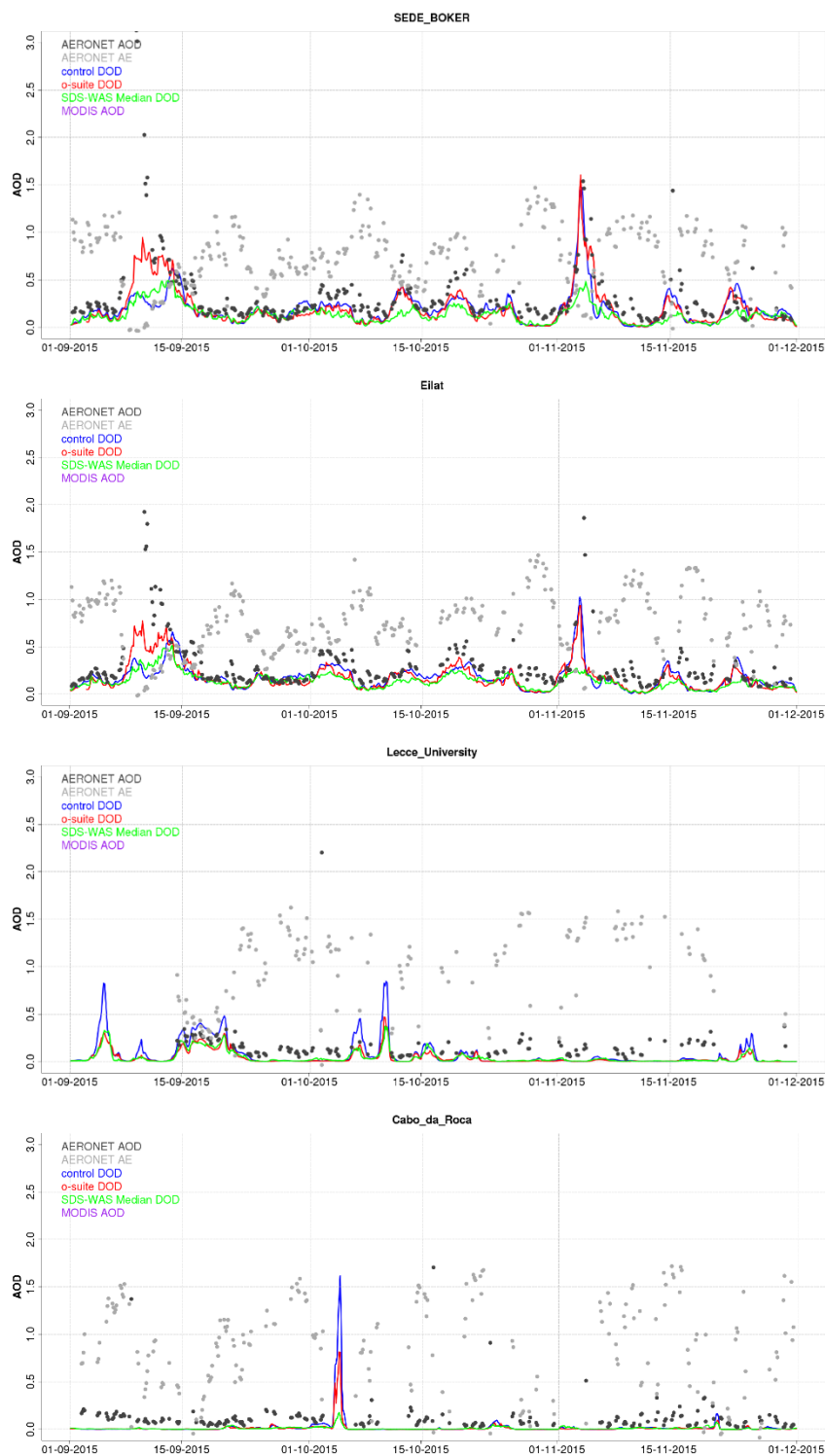


Figure 3.5.10: AOD from AERONET (black dots), DOD o-suite (red line), DOD control (blue line) and DOD Multimodel SDS-WAS Median (green line) for the period September 1st to November 30th, 2015 Sede Boker, Eilat and Cairo EMA in E. Mediterranean, Lecce University (Central Mediterranean) and Cabo da Roca in Western Iberian Peninsula.

Table 3.5.2: Skill scores (MB, FGE, RMSE and r) for CAMS o-suite, CAMS control and SDS-WAS Multi-model Median for the study period, and the number of data (NDATA) used. Dust AOD (DOD) from AERONET is the reference.

	NDATA	o-suite DOD				control DOD				SDS-WAS Median DOD			
		MB	FGE	RMSE	r	MB	FGE	RMSE	r	MB	FGE	RMSE	r
Central Mediterranean	1701	-0.06	1.45	0.19	0.58	-0.01	1.43	0.19	0.56	-0.05	1.41	0.19	0.56
Eastern Mediterranean	1140	-0.10	1.21	0.38	0.74	-0.10	1.22	0.43	0.51	-0.14	1.31	0.45	0.62
Eastern Sahara	270	-0.09	0.48	0.35	0.72	-0.04	0.59	0.39	0.34	-0.08	0.43	0.38	0.49
Iberian Peninsula	837	-0.04	1.97	0.19	0.06	-0.04	1.97	0.19	0.02	-0.04	1.98	0.19	-0.01
Middle East	604	-0.06	0.67	0.25	0.62	-0.08	0.72	0.35	0.44	-0.12	0.73	0.36	0.53
North Western Maghreb	435	-0.09	1.05	0.29	0.28	-0.06	0.95	0.29	0.26	-0.10	1.04	0.29	0.32
Sahara	226	-0.01	0.39	0.14	0.72	0.16	0.66	0.24	0.66	-0.01	0.38	0.16	0.69
Sahel	725	-0.23	0.57	0.47	0.43	-0.07	0.49	0.44	0.33	-0.19	0.49	0.46	0.35
Subtropical North Atlantic	471	0.01	1.54	0.14	0.69	0.07	1.58	0.21	0.65	-0.00	1.55	0.13	0.71
Tropical North Atlantic	224	-0.07	0.35	0.33	0.63	0.11	0.54	0.36	0.54	-0.11	0.44	0.37	0.51
Western Iberian Peninsula	676	-0.05	1.93	0.22	0.15	-0.05	1.93	0.22	0.15	-0.05	1.93	0.22	0.15
Western Mediterranean	1928	-0.04	1.80	0.17	0.40	-0.03	1.79	0.17	0.40	-0.04	1.80	0.17	0.41

law. Because AERONET data are acquired at 15-min intervals on average, all measurements within ± 90 min of the models' outputs are used for the 3-hourly evaluation.

3-hourly values of DOD from AERONET, o-suite, control and SDS-WAS Multi-model Median for the period 1 September 2015 to 30 November 2015 have been computed for 11 study regions shown in Figure 3.5.9. Mean Bias (MB), Fractional Gross Error (FGE), Root Mean Square Error (RMSE), Pearson correlation coefficient (r), and the number of data (NDATA), averaged over the study period for o-suite, control and SDS-WAS Multi-model Median, and for the 11 regions of study are shown in Table 3.5.2.

Over desert dust sources (i.e. Sahara and Middle East), in general, Control tends to overestimate the AERONET observations as indicated by higher MB values than o-suite (one order of magnitude in the Sahara) in Table 3.5.2. Additionally, o-suite reproduce the observed daily variability better than control and the SDS-WAS multimodel median over these regions. Correlation increases from 0.66 for Control to 0.72 for o-suite in the Sahara and from 0.44 for Control to 0.62 for o-suite in the Middle East (see Table 3.5.2). However, in the Sahel is o-suite which significantly overestimates.

Iberian Peninsula shows very low correlations $< \pm 0.1$ for all the models included the SDS-WAS multimodel median. Otherwise, in Western Iberian Peninsula, Control behaves quite similar than o-suite in terms of correlation for the study period (from 0.20 for Control to 0.04 for o-suite, see Table 1). This is explained by very low DOD values (close to 0) over the entire region. The CAMS experiments only predict a strong event in this area in early-November 2015

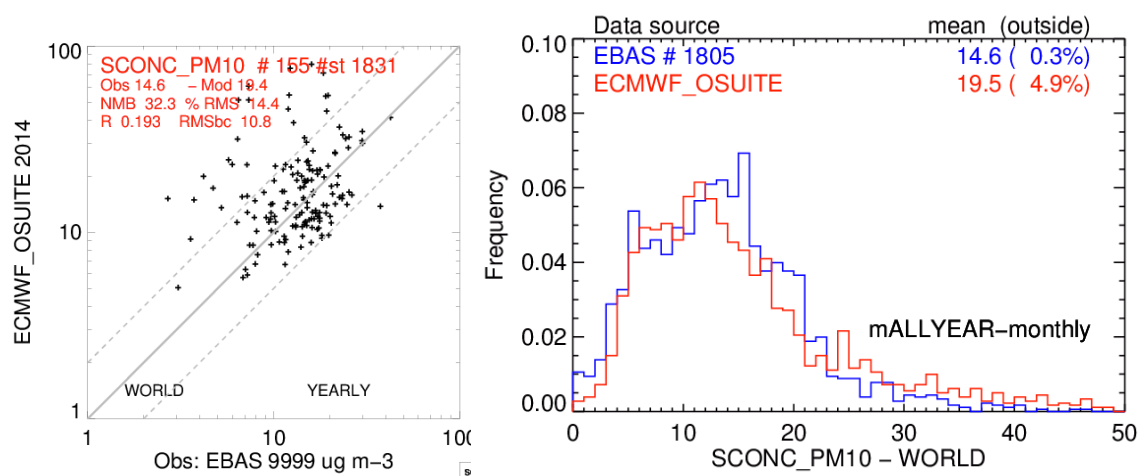


Figure 3.5.11: Histogram of monthly mean and scatterplot of yearly mean PM 10 concentrations at EMEP and IMPROVE sites, simulated o-suite versus climatological average (2000-2009). Data are collected and hold in the EBAS database at NILU.

(see Cabo de Roca in Figure 3.5.10). The maximum DOD predicted by CAMS experiments (up to 1.6 for Control and 0.8 for o-suite at Cabo da Roca) highly overestimates the DOD values from the SDS-WAS multimodel median (up to 0.2 at Cabo da Roca).

In the Eastern Mediterranean (see Figure 3.5.10), correlation increases from 0.51 for Control to 0.74 for o-suite (see Table 3.5.2). Two strong events are observed in this region. On 8-10 September 2015, Control and o-suite underestimate, as well as SDS-WAS multimodel median, compared with the AERONET maximum DOD values (see Figure 4). However, o-suite achieved higher DOD values than Control and SDS-WAS multimodel median. On 3-5 November 2015, lower DOD maximum is observed in Eilat than Sede Boker. These stations are very close each other (see Figure 3.5.8) but the maximum is lower in Eilat than in Sede Boker (that is an accurate prediction).

During the period of analysis, dust activity over desert dust sources (Middle East, the Sahara and dust corridor of North Western Maghreb) is relatively low. From September to November, CAMS o-suite is the model that best reproduces the daily variability of AERONET observations (see Table 3.5.2). In general, Control tends to overestimate compared with AERONET observations over Northern Africa, as indicated by systematic higher MB values than o-suite in Table 3.5.2.

3.5.3 PM10 evaluation against a climatology over Europe and North America

Surface concentration of particulate matter below 10 μm (PM10) from the o-suite experiment has been validated against data from 155 remote EMEP and IMPROVE stations for the year 2014 (Figure 3.5.11). A climatological average has been constructed from data in the period 2000-2009 as available in the EBAS database hold at NILU. The data coverage is not the same at all stations,

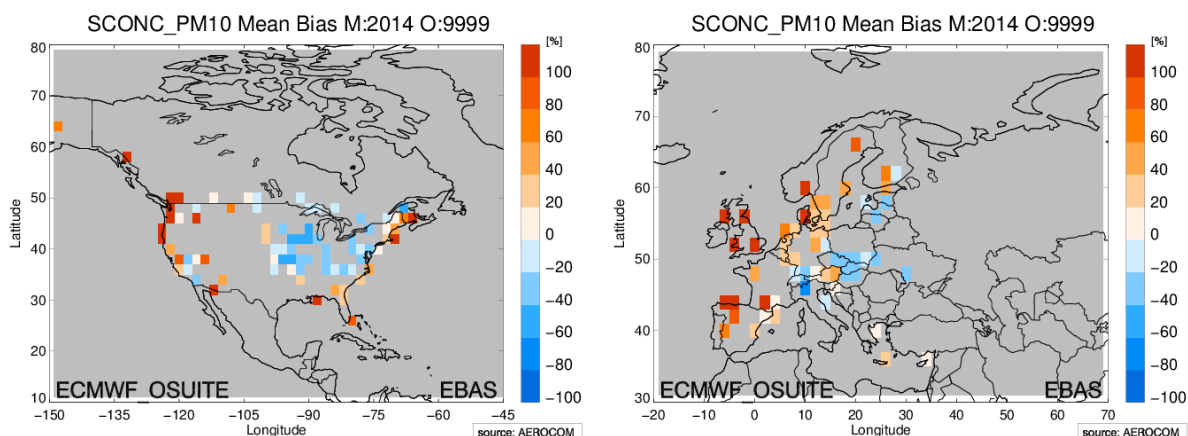


Figure 3.5.12: Bias [%] map of yearly mean PM 10 concentrations at EMEP and IMPROVE sites, simulated o-suite versus climatological average (2000-2009).

and sometimes covers only a few years. Near real time data of that geographical spread are not available at this point. All time series used are documented via the CAMS-AeroCom web interface.

The comparison shows an average positive model bias of 32%. Some stations clearly show high simulated PM concentrations and are responsible for a high bias. Figure 3.5.12. shows that this bias is both in North America and Europe located in regions close to the coastlines. This is an indication that simulated PM10 concentrations are high due to sea salt aerosols. Inner-continental sites have a small negative bias.

3.5.4 Aerosol validation over the Mediterranean

Daily aerosol optical depth (AOD) and surface concentration (PM10 and PM2.5) from CAMS o-suite and its control experiment have been validated against 42 AERONET (Holben et al., 1998) and 125 Airbase stations in the Mediterranean region for the period 1 September 2015 – 30 November 2015 (Figure 3.5.13), to evaluate AOD and surface aerosol concentration (PM2.5 and PM10) from the CAMS system over the Mediterranean. In the autumn season the minimum dust activity is observed over the entire region.

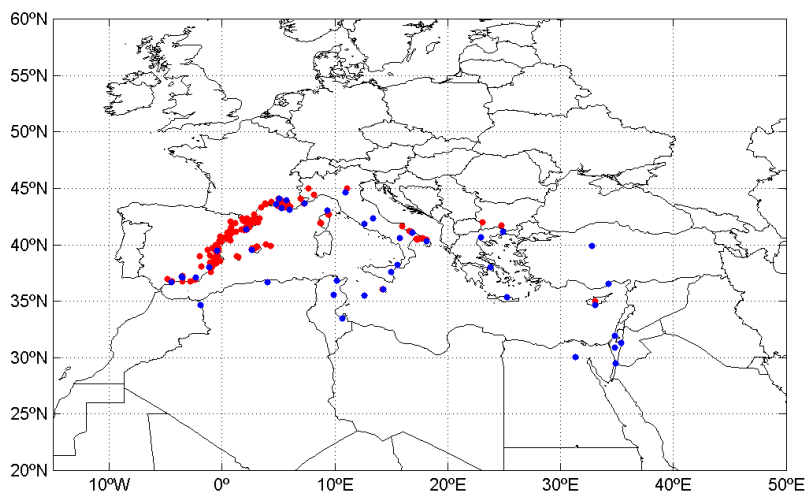


Figure 3.5.13: Map of 42 AERONET (blue points) and 125 Airbase (red points) stations considered in this analysis.

Aerosol optical depth

We used AOD observations at 550 nm from 42 AERONET sites whose locations are depicted in Figure 3.5.13. Cloud-screened direct-sun data (Level 1.5) between 440 and 870nm, which contain an uncertainty about 0.01 for AOD under cloud-free conditions, are used. Quantitative evaluations of the modelled AOD are conducted. The AOD at 550 nm is derived from data between 440 and 870 nm following the Ångström's law. Because AERONET data are acquired at 15-min intervals on average, all measurements within ± 90 min of the models' outputs are used for the 3-hourly evaluation.

3-hourly values of AOD from AERONET, o-suite and control for the period 1 September 2015 to 30 November 2015 over selected sites are shown in Figure 3.5.14 and Figure 3.5.15. Mean Bias (MB), Fractional Gross Error (FGE), Root Mean Square Error (RMSE), Person correlation coefficient (r), and the number of data (NDATA), averaged over the study period for o-suite and control, and for the 38 available stations are shown in Table 3.5.3.

The highest peaks on CAMS AOD simulations are linked to natural sources (mainly desert dust, see Figure 3.5.14 and Figure 3.5.15), except in Eastern Mediterranean on September, 13 (see Sede Boker and Cairo EMA in Figure 3.5.15). From September to November, CAMS o-suite is the model that best reproduces the daily variability of AERONET observations (see Table 3.5.3). In general, Control tends to underestimate the background levels compared with AERONET observations over Southern European sites (more influenced by urban/industrial aerosol sources), as indicated by systematic lower MB values than o-suite in Table 3.5.3.



Table 3.5.3: Skill scores (MB, FGE, RMSE and r) for CAMS o-suite and CAMS control for the study period, and the number of data (NDATA) used. AOD from AERONET is the reference.

Site Name	Region	NDATA	o-suite AOD				control AOD			
			MB	FGE	RMSE	r	MB	FGE	RMSE	r
IMAA_Potenza	C.Med	126	-0,07	0,60	0,21	0,47	-0,10	0,74	0,22	0,49
Modena	C.Med	95	-0,12	0,59	0,25	0,38	-0,16	0,92	0,28	0,04
Lampedusa	C.Med	227	0,04	0,41	0,12	0,77	0,04	0,38	0,14	0,75
Rome_Tor_Vergata	C.Med	227	-0,02	0,40	0,19	0,28	-0,05	0,56	0,20	0,31
Lecce_University	C.Med	137	-0,00	0,43	0,19	0,23	-0,02	0,52	0,20	0,27
ETNA	C.Med	6	0,06	0,48	0,08	0,65	0,02	0,29	0,05	0,89
Messina	C.Med	139	0,00	0,35	0,10	0,66	0,02	0,54	0,16	0,62
Ersa	C.Med	173	0,03	0,48	0,20	0,29	-0,03	0,45	0,21	0,15
Bari_University	C.Med	164	-0,01	0,45	0,12	0,36	-0,04	0,57	0,14	0,34
Gozo	C.Med	38	0,00	0,21	0,02	0,76	-0,03	0,43	0,05	0,31
Ben_Salem	C.Med	294	0,03	0,36	0,12	0,78	0,03	0,45	0,15	0,72
Tunis_Carthage	C.Med	232	0,01	0,34	0,16	0,58	0,01	0,48	0,17	0,60
LAQUILA_Coppito	C.Med	201	0,04	0,66	0,09	0,42	-0,00	0,47	0,08	0,56
Medenine-IRA	C.Med	240	0,03	0,40	0,16	0,63	0,07	0,51	0,20	0,60
SEDE_BOKER	E.Med	320	0,02	0,36	0,35	0,67	-0,08	0,39	0,42	0,45
Xanthi	E.Med	-	-	-	-	-	-	-	-	-
IMS-METU-ERDEMLI	E.Med	54	0,00	0,31	0,07	0,75	-0,05	0,54	0,09	0,68
Nes_Ziona	E.Med	245	0,03	0,28	0,23	0,85	-0,08	0,33	0,36	0,58
ATHENS-NOA	E.Med	195	-0,02	0,31	0,10	0,65	-0,04	0,46	0,12	0,56
FORTH_CRETE	E.Med	36	0,00	0,37	0,06	0,48	-0,02	0,44	0,06	0,47
Eilat	E.Med	318	-0,02	0,27	0,29	0,71	-0,09	0,41	0,36	0,42
TUBITAK_UZAY_Ankara	E.Med	15	0,02	0,36	0,07	0,53	-0,02	0,37	0,03	0,80
CUT-TEPAK	E.Med	95	0,02	0,34	0,10	0,87	-0,00	0,48	0,14	0,75
Cairo_EMA_2	E.Med	276	-0,15	0,46	0,43	0,56	-0,24	0,72	0,53	0,19
KITcube_Masada	E.Med	-	-	-	-	-	-	-	-	-
La_Crau	W.Med	-	-	-	-	-	-	-	-	-
Barcelona	W.Med	83	0,02	0,43	0,07	0,38	-0,02	0,57	0,12	0,17
Villefranche	W.Med	196	-0,01	0,44	0,20	0,29	-0,07	0,52	0,22	0,16
Carpentras	W.Med	237	0,01	0,62	0,14	0,25	-0,04	0,46	0,15	0,18
Toulon	W.Med	168	-0,04	0,62	0,24	0,45	-0,08	0,55	0,27	0,19
Granada	W.Med	248	0,00	0,39	0,07	0,36	-0,05	0,73	0,09	0,32
OHP_OBSERVATOIRE	W.Med	243	0,03	0,71	0,10	0,40	-0,02	0,44	0,09	0,34
Burjassot	W.Med	226	0,02	0,51	0,10	0,47	-0,05	0,53	0,11	0,46
Malaga	W.Med	56	0,04	0,60	0,08	0,90	0,01	0,42	0,07	0,94
Frioul	W.Med	180	0,01	0,55	0,21	0,17	-0,05	0,47	0,22	0,06
Oujda	W.Med	213	0,01	0,38	0,08	0,72	-0,02	0,57	0,09	0,68
Tabernas_PSA-DLR	W.Med	247	0,03	0,50	0,13	0,34	-0,03	0,46	0,14	0,22
Palma_de_Mallorca	W.Med	238	0,02	0,41	0,08	0,65	-0,03	0,49	0,11	0,51
Tizi_Ouzou	W.Med	149	-0,03	0,29	0,11	0,75	-0,02	0,50	0,12	0,82
Cerro_Poyos	W.Med	-	-	-	-	-	-	-	-	-
Murcia	W.Med	256	-0,00	0,40	0,08	0,72	-0,06	0,60	0,12	0,52

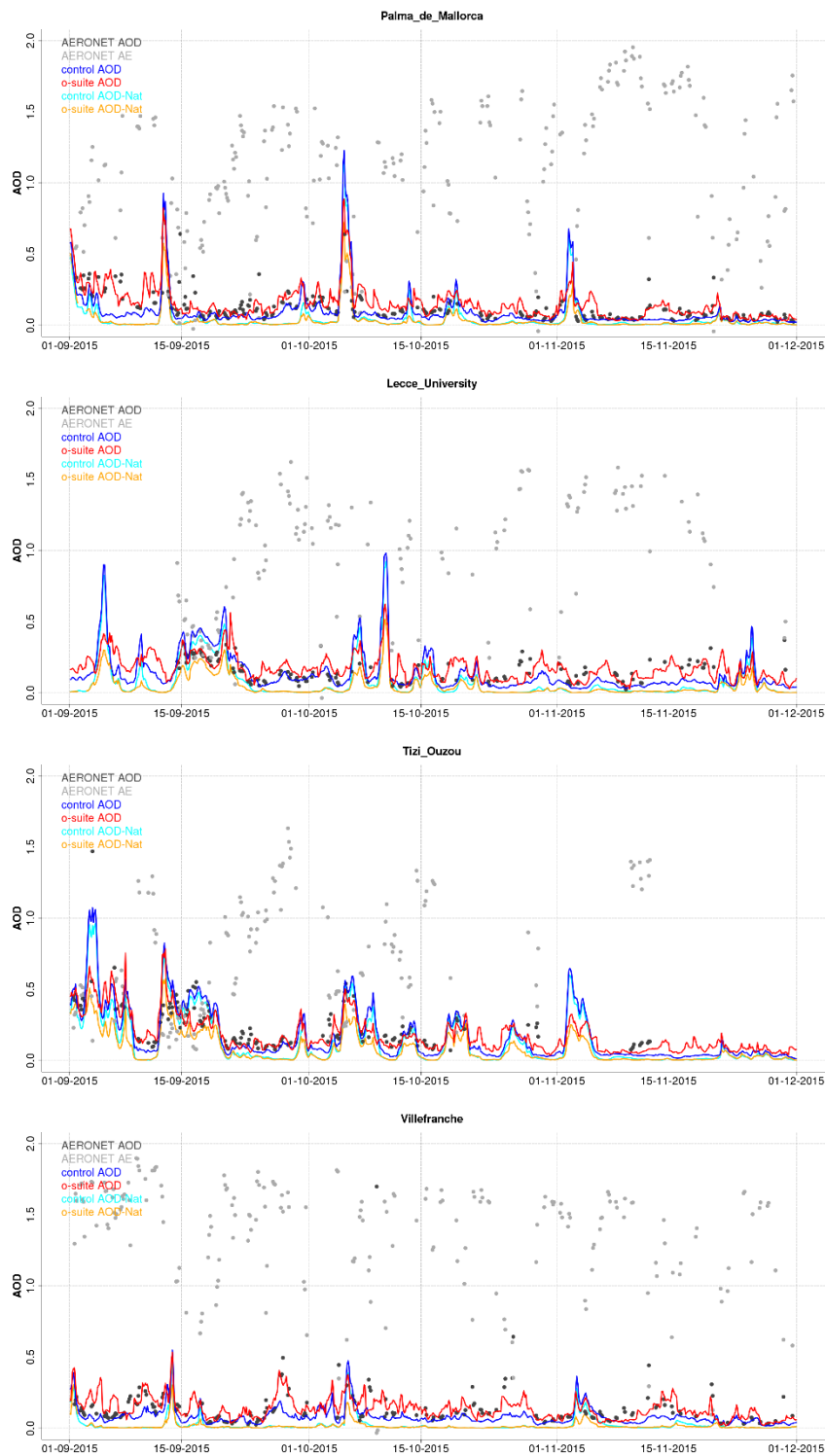


Figure 3.5.14: AOD from AERONET (black dot), AOD o-suite (red line), AOD control (blue line), AOD-Nat o-suite (orange line), AOD-Nat control (cyan line), for the period September 1st to November 30th, 2015 over Palma de Mallorca, Rome Tor Vergata, Tizi Ozou and Villefranche. AOD-Nat corresponds to the natural aerosol optical depth that includes dust and sea-salt.



Figure 3.5.15: AOD from AERONET (black dot), AOD o-suite (red line), AOD control (blue line), AOD-Nat o-suite (orange line), AOD-Nat control (cyan line), for the period September 1st to November 30th, 2015 over Athens NOA, Cairo EMA, and Sede Boker. AOD-Nat corresponds to the natural aerosol optical depth that includes dust and sea-salt.

Surface aerosol concentrations

For ground-level concentrations, we use observations from the European Air quality database (AirBase; <http://acm.eionet.europa.eu/databases/airbase/>) which is the public air quality database system of the EEA. It contains air quality monitoring data and information submitted by the participating countries throughout Europe. The air quality database consists of multi-annual time series of air quality measurement data and their statistics for a representative selection of stations and for a number of pollutants. It also contains meta-information on the involved monitoring networks, their stations and their measurements. Only those stations considered as background sites in

Table 3.5.4: Skill scores (MB, FGE, RMSE and r) for CAMS o-suite and CAMS control for the study period, and the number of data (NDATA) used. PM10 and PM2.5 from Airbase is the reference. Type corresponds



to the environmental description of the measurement site included in Airbase: BU is background urban, BS is background sub-urban and BR is background rural.

Site	Country	Type	NDA TA	o-suite PM10				control PM10				NDA TA	o-suite PM2.5				control PM2.5			
				MB	FG E	RM SE	r	MB	FG E	RM SE	r		MB	FG E	RM SE	r	MB	FG E	RM SE	r
Albacete	Spain	BU	99	-	0.9	22.2	0.62	-	1.1	26.4	0.6	99	0.0	0.7	16.7	0.5	0.09	0.8	22.3	0.5
				13.30	8	4		13.8	7	3	6		6	3	5	1			6	3
Benigánim	Spain	BS	359	-7.97	0.9	23.5	0.16	-	0.9	29.3	0.2	359	-	0.9	21.5	-	-	0.9	27.9	-
				6.11	4	6		6.11	4	6	3		5.2	2	4	0.0	3.70	5	1	0.0
Caudete de las Fuentes	Spain	BR	620	0.19	0.7	23.4	0.23	0.78	0.8	33.7	0.2	620	0.1	0.7	19.7	0.1	0.85	0.8	29.4	0.1
				0.78	9	5		0.78	9	5	5		2	1	8	8		2	1	6
Ontinyent	Spain	BS	96	3.79	0.5	12.3	0.39	0.15	0.5	11.0	0.3	96	4.0	0.5	9.55	0.5	1.12	0.5	8.95	0.4
				0.15	7	5		0.15	7	5	5		3	7	4	4		9	8.95	0.4
Villar Arzobispo	Spain	BR	610	8.77	0.8	28.4	0.12	8.13	0.8	33.5	0.1	610	4.2	0.7	18.5	0.1	4.27	0.8	24.8	0.1
				8.13	6	7		8.13	6	7	8		3	6	1	2		1	8	2
Viver	Spain	BS	218	21.19	0.9	42.1	0.16	20.4	0.9	45.4	0.2	218	9.7	0.8	22.5	0.1	10.0	0.8	28.5	0.1
				20.4	2	2		20.4	2	2	3		1	5	7	4		9	8	6
Zorita	Spain	BR	613	1.29	0.8	20.3	0.07	1.71	0.8	27.9	0.1	613	1.1	0.7	16.3	0.0	1.65	0.8	23.8	0.0
				1.71	8	7		1.71	8	7	0		5	9	7	6		3	5	6
Fos Les Carabins	France	BS	601	-3.97	0.6	16.8	-	-	0.6	17.9	0.1	-	-	-	-	-	-	-	-	-
				3.65	9	9		3.65	9	9	7		-	-	-	-		-	-	-
Gauzy	France	BS	572	-5.33	0.7	15.8	0.17	-	0.7	18.0	0.2	572	2.0	0.6	9.45	0.1	1.09	0.6	13.2	0.1
				4.25	5	8		4.25	5	8	5		5	3	4	1		9	9	4
Aéroport Nice	France	BS	605	-8.12	0.6	14.4	0.15	-	0.7	16.1	0.1	-	-	-	-	-	-	-	-	-
				7.49	2	1		7.49	2	1	9		-	-	-	-		-	-	-
AJACCIO CANETO	France	BS	553	-5.07	0.7	14.0	0.29	-	0.9	16.5	0.3	-	-	-	-	-	-	-	-	-
				5.98	4	2		5.98	4	2	5		-	-	-	-		-	-	-
BASTIA GIRAUD	France	BS	582	-3.43	0.5	11.2	0.40	-	0.6	15.4	0.4	-	-	-	-	-	-	-	-	-
				2.80	9	2		2.80	9	2	5		-	-	-	-		-	-	-

the Airbase catalogue in the Mediterranean region (in red in Figure 3.5.13) are considered in the present validation exercise. All NRT available measurements (i.e. no-validated observations) within ± 60 min of the models' outputs are used for the 3-hourly evaluation.

3-hourly values of PM10/PM2.5 from Airbase, o-suite and control for the period 1 September 2015 to 30 November 2015 over selected sites are shown in Figure 3.5.16 and Figure 3.5.17. Mean Bias (MB), Fractional Gross Error (FGE), Root Mean Square Error (RMSE), Pearson correlation coefficient (r), and the number of data (NDATA), averaged over the study period for o-suite and control, and for the 12 available Airbase stations for the present study period are shown in Table 3.5.4.

Two exceptional events (with PM10 and PM2.5 concentrations above $180 \mu\text{g}/\text{m}^3$), the first from 4th to 6th October 2015 in Western Mediterranean (Figure 3.5.16 and Figure 3.5.17), and the second around 10th October 2015 in Central Mediterranean (Lecce - S. M. Cerrate in Figure 3.5.17) are simulated by CAMS experiments (i.e. control and o-suite). Weaker events (with PM10 and PM2.5 concentrations above $50 \mu\text{g}/\text{m}^3$) are observed over Western Mediterranean (Figure 3.5.16) on 1 September, 1-3 November and 18 November. All these aerosol events are associated to the presence of long-range desert dust transport, except those on 1 September.

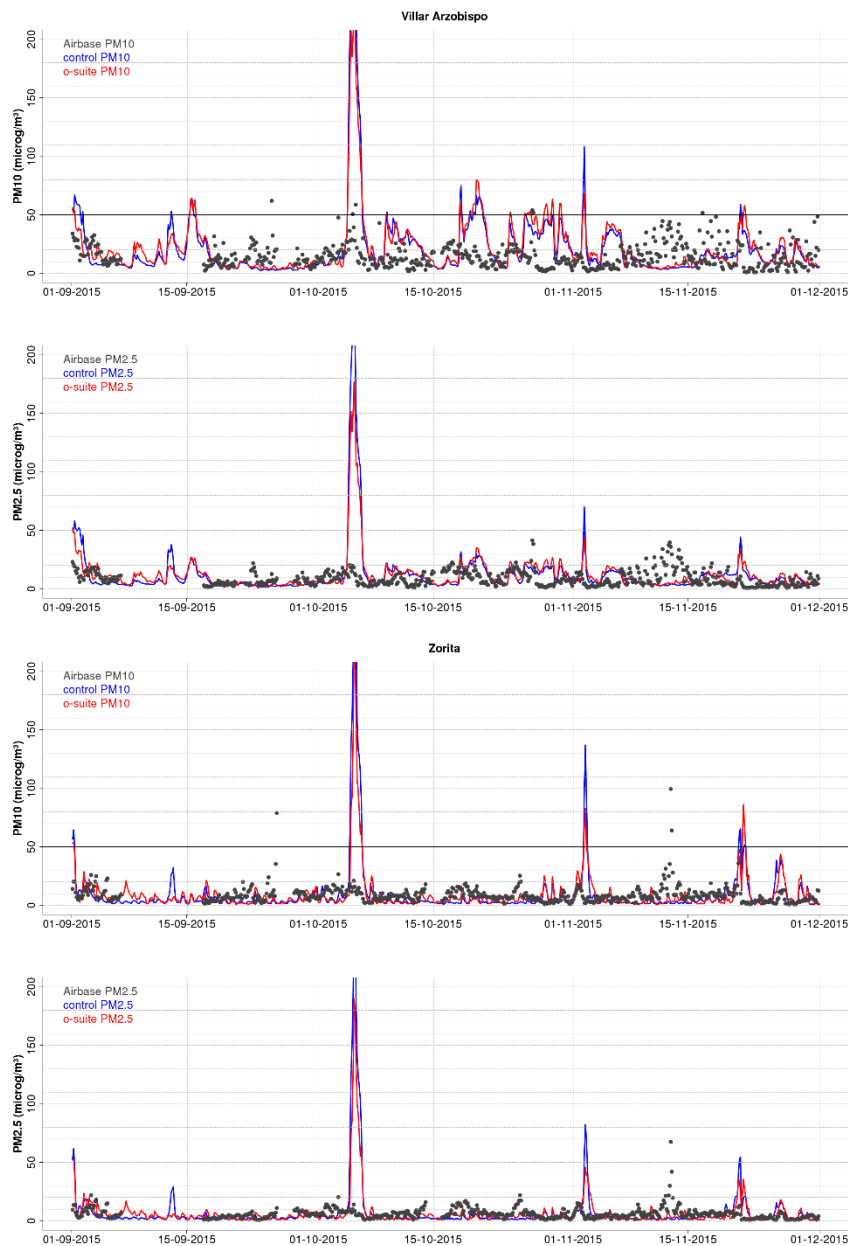


Figure 3.5.16: PM10 and PM2.5 Airbase observations (black dot), PM10 and PM2.5 o-suite (red line) and PM10 and PM2.5 control (blue line) for the period September 1st to November 30th, 2015 over Villar Arzobispo (39.7°N; 0.8°W, Spain) and Zorita (40.73°N; 0.17°W, Spain).

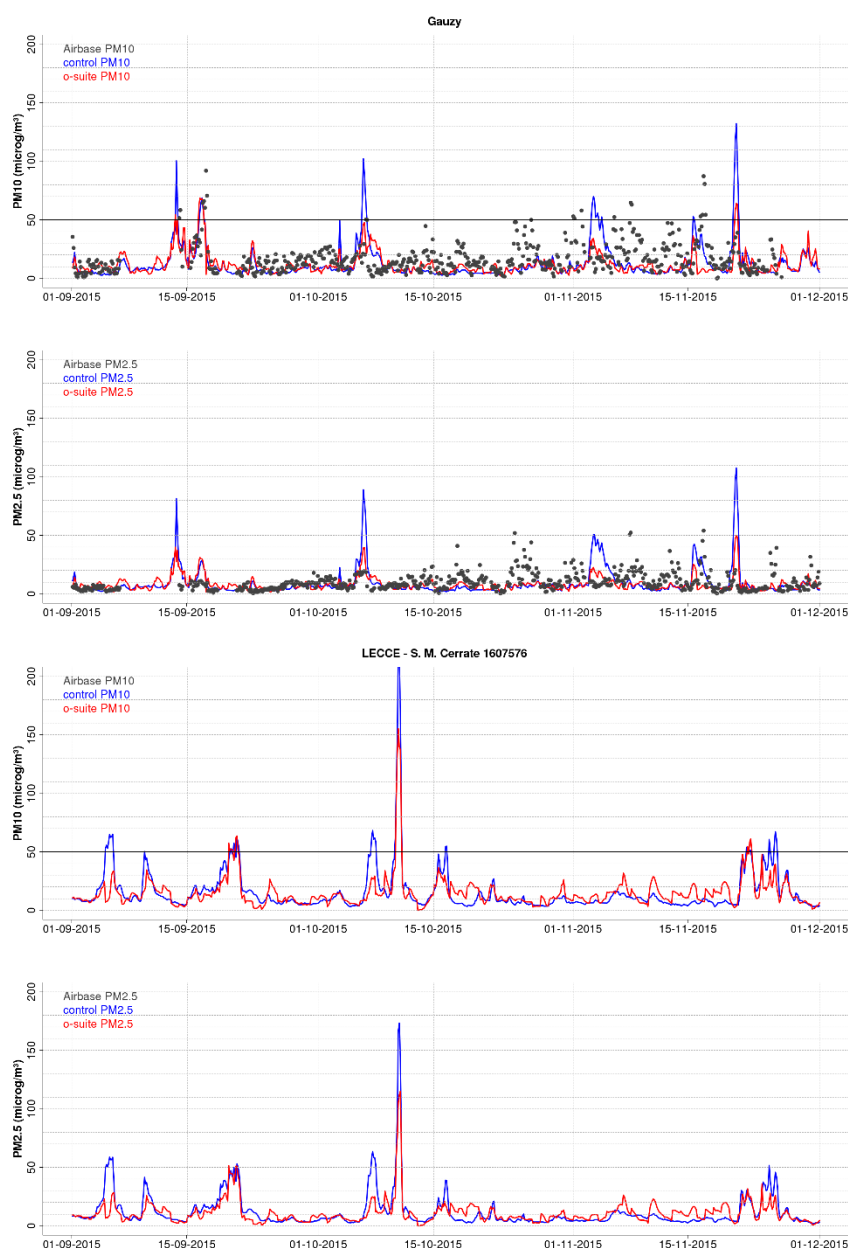


Figure 3.5.17: PM10 and PM2.5 Airbase observations (black dot), PM10 and PM2.5 o-suite (red line) and PM10 and PM2.5 control (blue line) for the period September 1st to November 30th, 2015 over Gauzy (43.83°N; 4.37°E; 40, France) and Lecce - S. M. Cerrate (40.46°N; 18.10°E, Italy).

According to information reported by the CAMS European Air Quality web site (Individual Forecasts), some of the other models also simulated false PM10 peaks on 5th October 2015. This event is associated to a desert dust intrusion over Western Mediterranean. The magnitude predicted by the CAMS simulations (control and o-suite) of these high aerosol events strongly overestimate PM10/PM2.5 air quality measurements over Spain as shown Figure 3.5.16.

The strong aerosol event reproduced in the CAMS simulations on 13 November 2015 in Central Mediterranean (see Figure 3.5.17) is coincident with a high AOD signal observed in the close Lecce University AERONET (see Figure 3.5.14). For



the AOD comparison, both CAMS configurations are able to reproduce the AERONET measurements. Although, the PM₁₀/PM_{2.5} simulated peak by both CAMS experiments looks unrealistic. Further analysis of these episodes are needed in order to find out the reasons behind these discrepancies.

From September to November, CAMS experiments reproduce the daily variability of the most intense aerosol events observed by Airbase sites (see Figure 3.5.16 and Figure 3.5.17). The maximum peaks are associated to long-range desert dust and Control tends to overestimate them compared with Airbase. Otherwise, o-suite better reproduces the background levels that use to be underestimated by Control. In general, CAMS o-suite presents better results in terms of load concentrations (see Table 3.5.4).

3.6 Stratospheric ozone

3.6.1 Validation against ozone sondes

In what follows, we present the results of the stratospheric ozone evaluation against ozone soundings from the NDACC, WOUDC, NILU and SHADOZ databases. The sondes have a precision of 3-5% (~10% in the troposphere for Brewer Mast) and an uncertainty of 5-10%. For further details see Cammas et al. (2009), Deshler et al. (2008) and Smit et al (2007). Model profiles of the o-suite and control are compared to balloon sondes measurement data of 44 stations for the period November 2014 to November 2015 (please note that towards the end of the validation period fewer soundings are available). A description of the applied methodologies and a map with the sounding stations can be found in the Annex 2 of CAMS-VAL report #1. Both runs, the o-suite and the control run, show MNMBs mostly within the range -5 to +10%, for all regions and months, see Fig. 3.6.1-3.6.3.

In order to understand the results for the control run, we would like to remark that at this moment the stratospheric ozone is replaced by ECMWF's operational ozone fields. In order to allow a proper validation of the impact of the assimilation on ozone in the stratosphere, such initialisations have to be removed.

O₃ partial pressures in the stratosphere are mostly slightly overestimated in all latitude bands. MNMBs in Antarctica during the ozone hole season, from August 2015 to November 2015, remain below 10%. The control runs' lower MNMBs in the Northern Midlatitudes and Antarctica result from a combination of over- and underestimation in different pressure levels, which cancel each other out in total, see the profiles in Fig. 3.6.4.

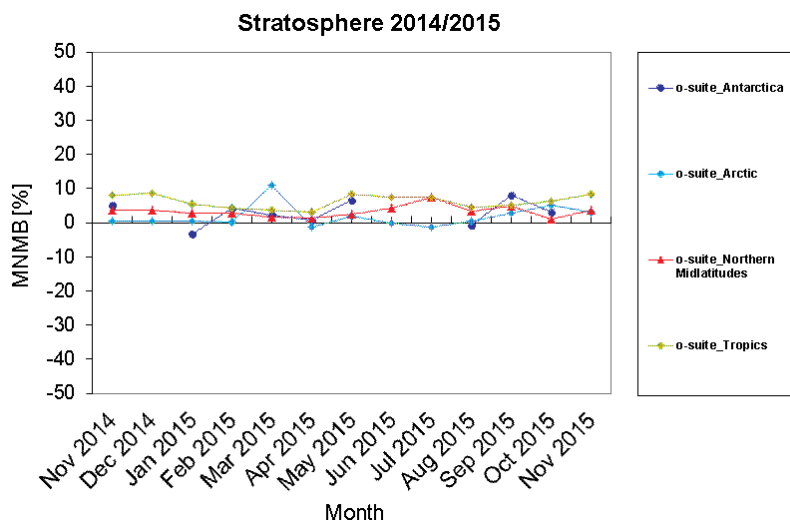


Figure 3.6.1: MNMBs (%) of ozone in the stratosphere from the o-suite against aggregated sonde data in the Arctic (light blue), Antarctic (dark blue) northern midlatitudes (red) and tropics (green).

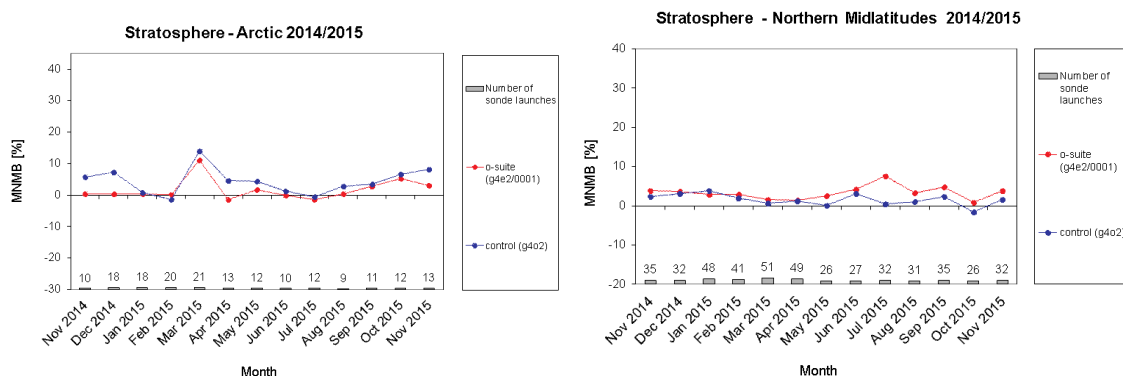


Figure 3.6.2: MNMBs (%) of ozone in the stratosphere from the model runs against aggregated sonde data in the Arctic (left) and the northern midlatitudes (right)

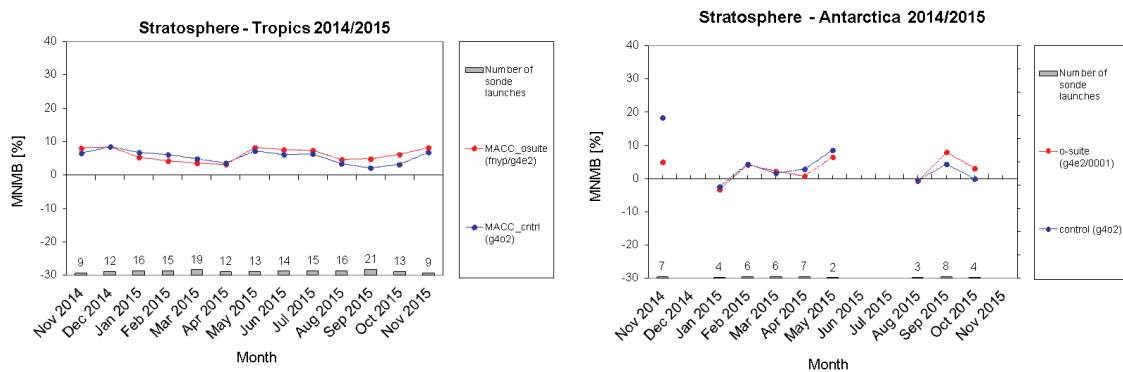


Figure 3.6.3: MNMBs (%) of ozone in the stratosphere from the model runs against aggregated sonde data in the Tropics (left) and Antarctica (right).

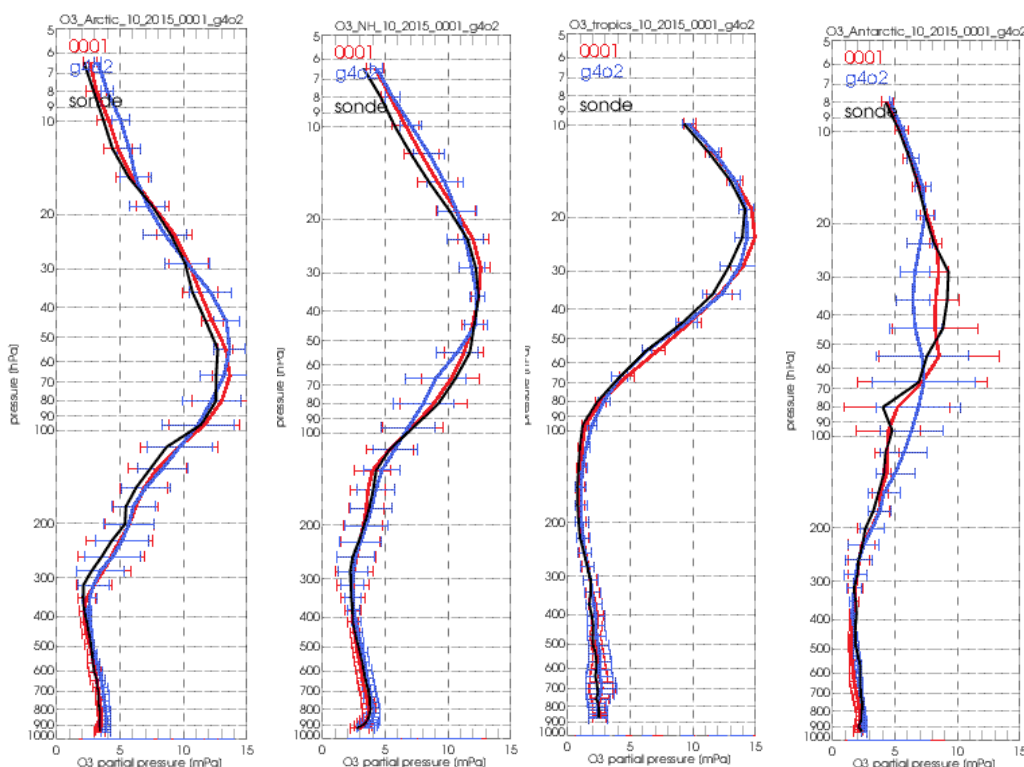


Figure 3.6.4: Comparison between mean O₃ profiles (units: mPa) of o-suite (red), and control (blue) in comparison with observed O₃ sonde profiles (black) for October 2015 for the various latitude bands.

Table 3.6.1: Seasonal relative mean bias (MB, %), standard deviation (STD, %) of the partial (stratospheric) ozone column for the considered period and number of observations used (NOBS), compared to NDACC microwave observations at Ny Alesund and Bern (mean bias and stddev in %).

		DJF			MAM			JJA			SON		
		MB	stddev	nobs									
o-suite	Ny.Ale	8.70	5.88	51	6.56	6.41	41	-0.90	5.03	219	17.53	8.46	206
	Bern	-1.40	2.64	644	-4.05	2.17	641	-4.93	2.50	513	-0.54	2.32	687

3.6.2 Validation against observations from the NDACC network (MWR, LIDAR, and FTIR)

In this section we present a comparison between the CAMS o-suite and MWR and LIDAR observations from the NDACC network. A detailed description of the instruments and applied methodologies for all NDACC instruments can be found in the Deliverable 8.1 report and at <http://nors.aeronomie.be>. MWR (microwave) at Ny Alesund (79°N, 12°E, Arctic station) and Bern (47°N, 7°E, northern midlatitude station). LIDAR at Lauder, New Zealand (46°S, 169.7°E, altitude 370m) and Hohenpeissenberg, Germany (47°N, 11°E, altitude 1km)

From Table 3.6.1, the stratospheric partial column bias at Bern during Sept.-Oct.-Dec 2015 is nearly vanishing (uncertainty on the partial column is 6%). At Ny Alesund, the o-suite overestimates the stratospheric ozone concentration

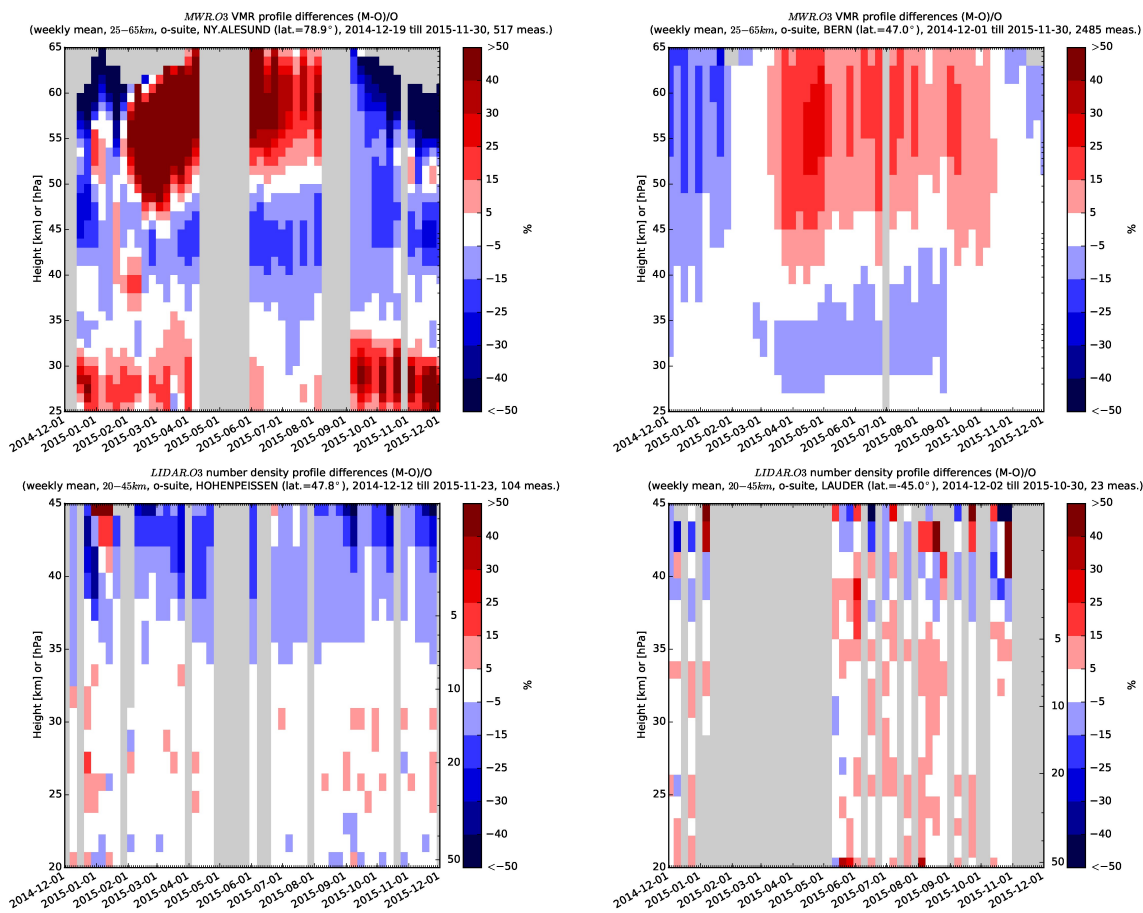


Figure 3.6.5: Comparison of the weekly mean profile bias between the O₃ mixing ratios of o-suite and the NDACC station at Ny Alesund, Bern, Hohenpeissenberg and Lauder. For the LIDAR stations, the measurement uncertainty above 35km is comparable to the observed profile bias.

with 17%. In JJA, both MWR stations observe an overestimation of the ozone content above 50km, and this evolved to an underestimation in SON, reaching values from -5% (Bern) to -15% (Ny Alesund), see also Fig. 3.6.5. Since Sept. 2015, the o-suite strongly overestimates ozone between 25km and 35km at Ny Alesund. At Lauder and Hohenpeissenberg (LIDAR), the o-suite slightly overestimates the observed ozone (<10%) between 25km and 35km. The uncertainty on the LIDAR concentration increases with altitude and above 35km the observed differences are comparable to the measurement uncertainty (>10%, see http://nors.aeronomie.be/projectdir/PDF/NORS_D4.2_DUG.pdf)

3.6.3 Comparison with dedicated systems and with observations by limb-scanning satellites

This section compares the output of the o-suite for the last period, based on the methodology described by Lefever et al. (2015). It also compares the model output with observations by two limb-scanning satellite instruments: Aura-MLS and OMPS-LP. The comparisons with Aura-MLS are only a verification since that dataset is assimilated in both the o-suite and BASCOE. The combination of

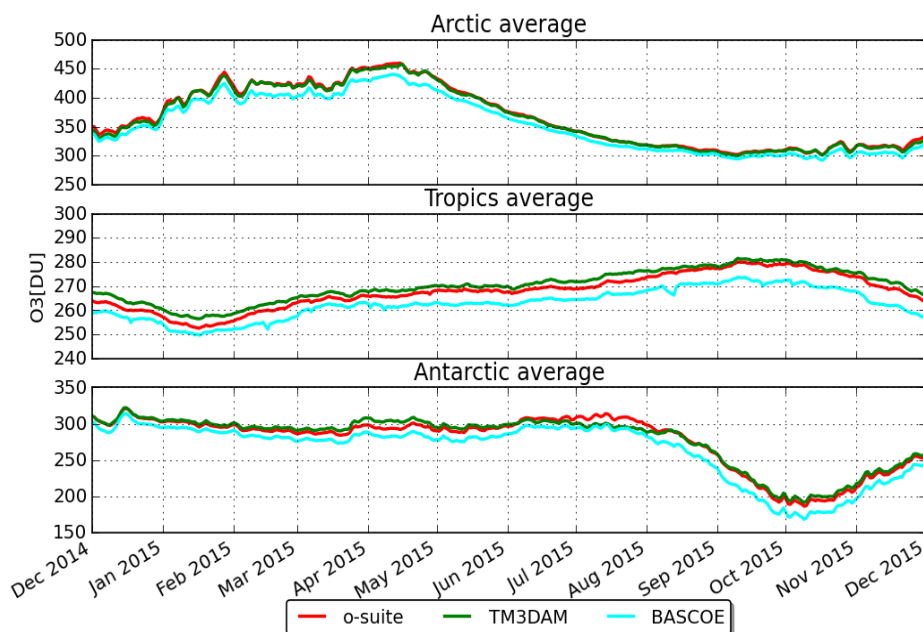


Figure 3.6.6: Zonally averaged ozone total column (Dobson Units) in the Arctic(60°N-90°N), Tropics(30°S-30°N) and Antarctic (90°S-60°S) during the period 2014/12/01-2015/12/01.

these comparisons delivers a good picture of the performance of the CAMS o-suite analyses w.r.t. stratospheric ozone.

All datasets are averaged over all longitudes and over the three most interesting latitude bands for stratospheric ozone: Antarctic (90°S-60°S), Tropics (30°S-30°N) and Arctic (60°N-90°N). In order to provide global coverage, the two mid-latitude bands (60°S-90°S and 60°N-90°N) are also included in some comparisons with satellite observations.

System intercomparison for total columns

Figure 3.6.6 shows the ozone total column over the polar and tropical latitude bands, including results from TM3DAM (green lines) and BASCOE (cyan lines). Since TM3DAM applies bias corrections to the GOME-2 data based on the surface Brewer-Dobson measurements, we use the results from TM3DAM as a “reference” for the ground-truth.

Everywhere there is an underestimation for BASCOE of about 10-20 DU. This is due to the fact that BASCOE does not assimilate any observations of the total ozone column(only Aura-MLS profiles) while the BASCOE model does not account for tropospheric sources of ozone. The o-suite results are much closer to those by TM3DAM:

- In the Arctic, the o-suite gives similar results to TM3DAM.
- In the Tropics, the seasonal maximum of ozone, ranging from 270 to 290 DU, is reached in September. The o-suite presents slight and regular underestimations w.r.t. TM3DAM of about 2-3 DU, i.e. ~1%.

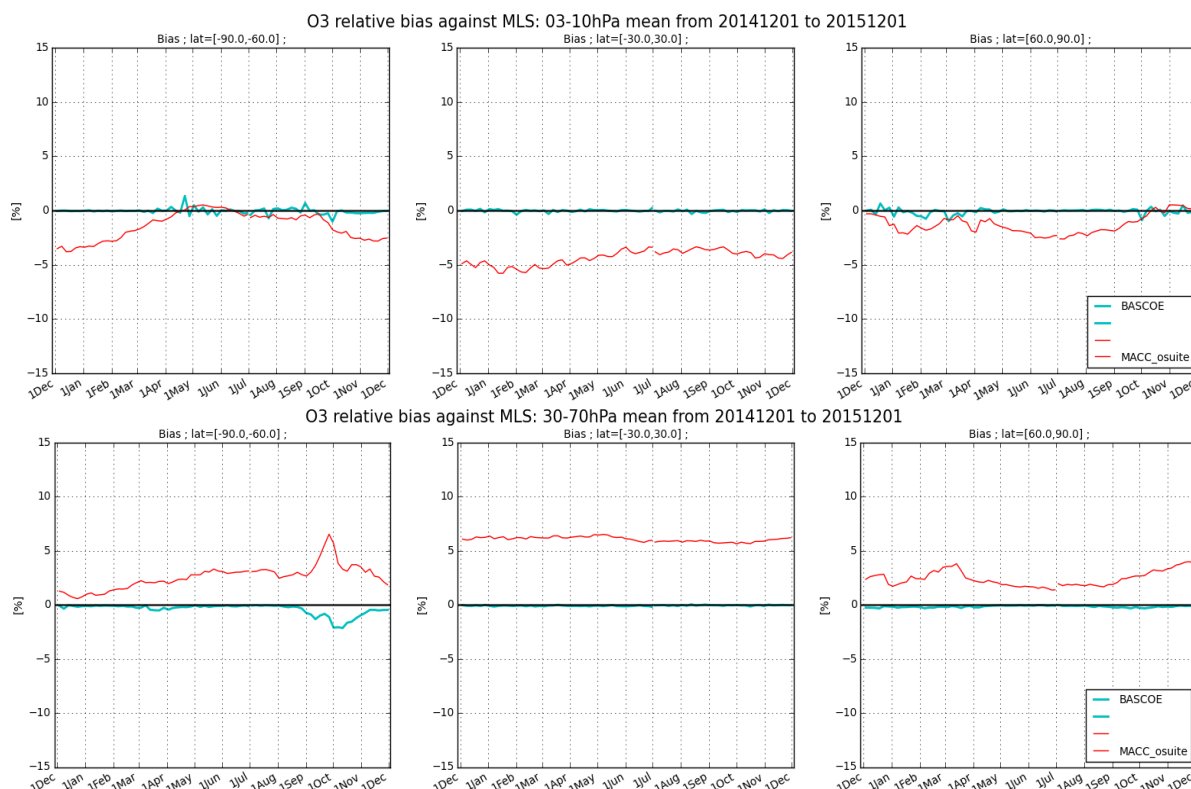


Figure 3.6.7: Relative differences (model-obs)/obs between o-suite (red), BASCOE (cyan) and Aura-MLS, in % of ozone mixing ratio averaged over the 3-10 hPa (top) and 30-70 hPa (bottom) vertical layers.

- In the Antarctic, the o-suite matches TM3DAM during the whole period except for the months of March-April 2015 (underestimation of up to 10DU) and July 2015 (overestimation reaching 15DU in mid-July).

Verification by comparison with the (assimilated) MLS dataset

Figure 3.6.7 shows the annual cycle of the ozone relative differences with respect to *offline* Aura-MLS observations (v3.4 until 30 June 2015; v4 afterwards) averaged over two pressure layers representative of the upper middle stratosphere (3-10 hPa: top) and the lower middle stratosphere (30-70 hPa: bottom). Besides the o-suite which assimilates the *Near Real-Time* Aura-MLS dataset (v3.4 since 20130107) as well as total columns (OMI, GOME-2) and partial columns (SBUV-2), we include in this comparison the analyses by BASCOE (cyan lines) which exclusively assimilates the offline Aura-MLS vertical profiles.

While the bias between the BASCOE analyses and its assimilated observations is negligible, this is not the case for the o-suite. In the Tropics we note slightly oscillating biases, with all year-long underestimation of ~5% in the upper middle stratosphere and overestimation of ~5% in the lower middle stratosphere. In the polar regions, the biases are smaller and depend on the season.

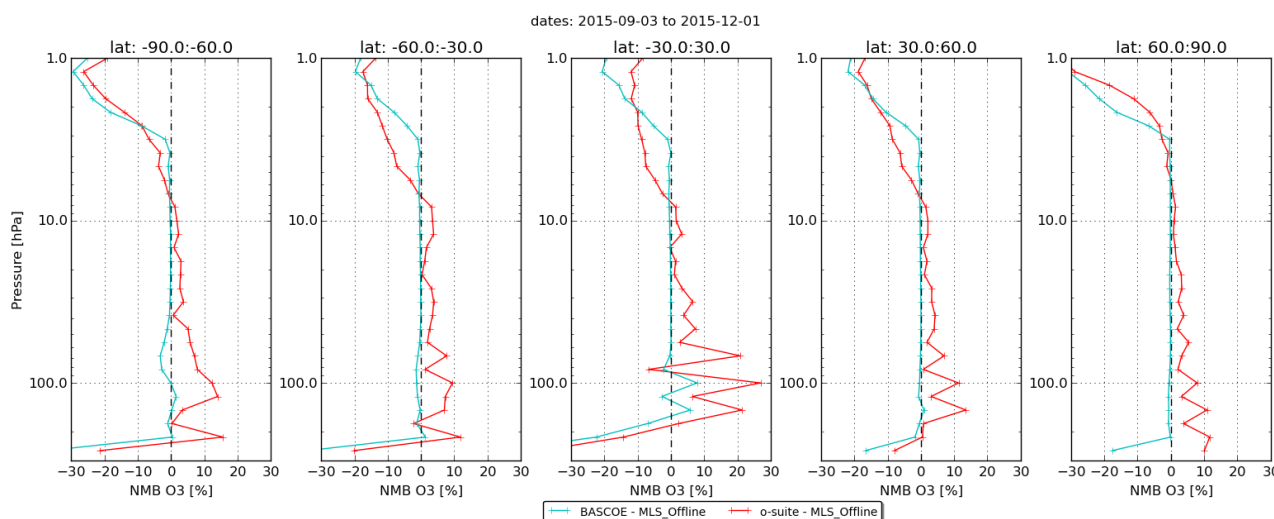


Figure 3.6.8: Normalized mean bias of the ozone profile between o-suite (red line) and BASCOE (cyan line) with MLS observations (offline v4.2) for the period June-July-August 2015.

Fig. 3.6.8 displays vertical profiles of the relative biases between the o-suite or BASCOE and the assimilated MLS satellite retrievals during the most recent 3-month period considered in this validation report, i.e. September-October-November 2015. While on figure 3.6.7 the relative biases were averaged in thick pressure layers, we now display them at each pressure level of the Aura-MLS observational dataset. This figure confirms that the bias of the o-suite w.r.t. MLS could be significant in two regions: the upper stratosphere and the tropical lower stratosphere.

Above 10 hPa, the o-suite analyses underestimate MLS observations with an ozone deficit increasing upwards and exceeding -20% at 1hPa in the polar regions. It should be noted that assimilation is difficult at and above stratopause levels, due to model issues. In the case of the CAMS o-suite, no increments from the O₃ assimilation are applied in the top 5 model levels (roughly above 1 hPa or 50 km) because the model biases are too large to allow useful assimilation of the MLS observations.

In the tropical lower stratosphere, the o-suite overestimates ozone by up to 25% but sharp oscillations are noted between adjacent levels of the Aura-MLS observations. This behavior is found in the o-suite since at least 2013 Sept-Oct-Nov (MACC-III NRT validation report 3, DEL37.3, Fig. 3.6.11).

It must be noted, however, that the o-suite assimilates the NRT version 3.4 Aura-MLS observations, while the dataset used in this report is the offline version 4.2. According to the Aura Microwave Limb Sounder Version 3.4 Level-2 near real-time data user guide (Lambert et al., 2012), the NRT vertical profiles in the UTLS (especially in the tropics) tend to be less oscillatory than the standard product v3.3 profiles, which often exhibit significant artificial oscillations in this region. This will be further investigated in the next quarterly validation report.

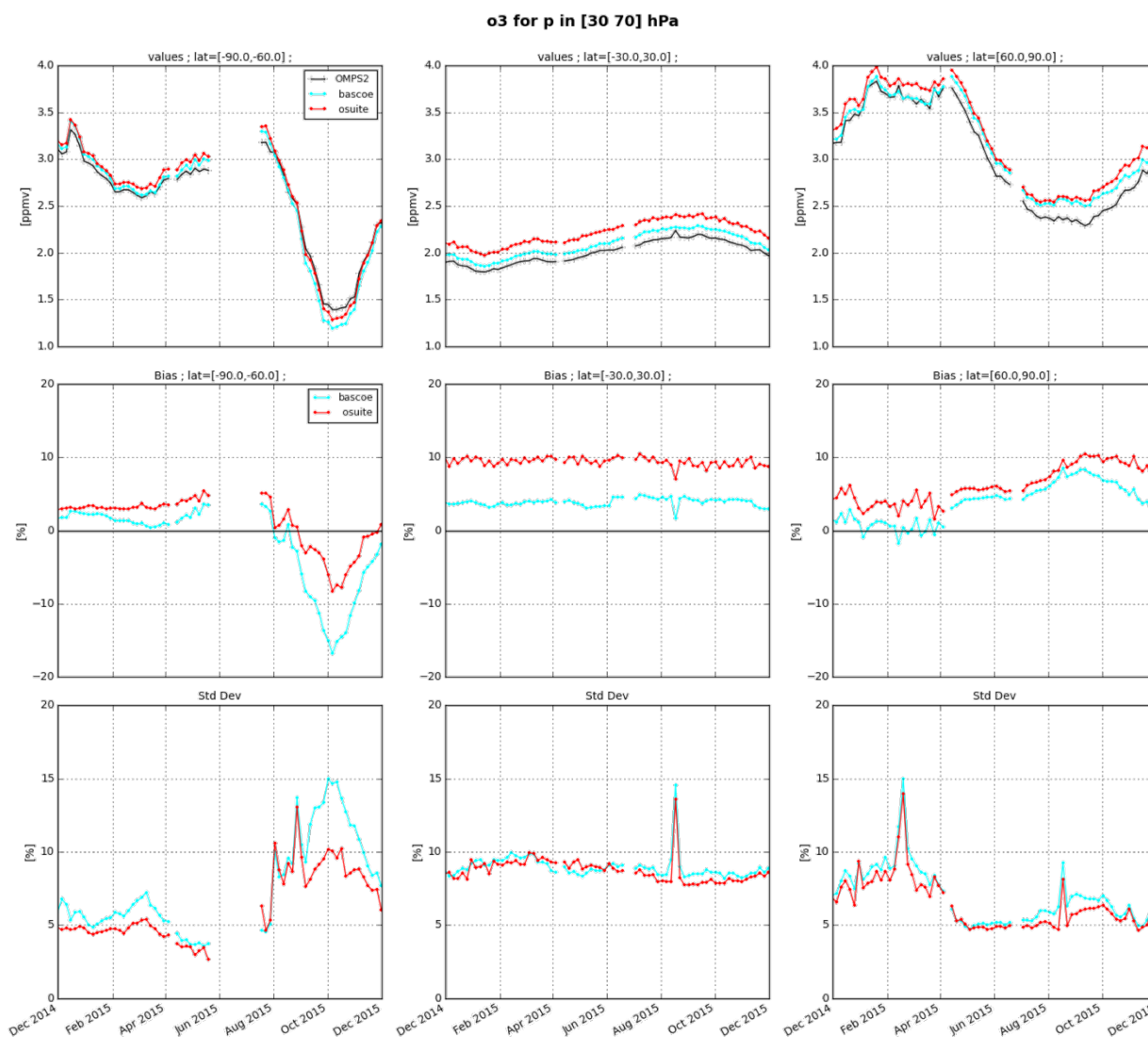


Figure 3.6.9: Time series comparing ozone from o-suite (red), BASCOE (cyan) and OMPS-LP satellite observations (black) for the period 2014-12-01 to 2015-12-01 in the middle stratosphere (30-70hPa averages): top row, mean values (ppmv); middle row, normalized mean bias (model-obs)/obs (%); bottom row, standard deviation of relative differences (%).

Comparison with independent limb satellite datasets: OMPS-LP

In this section, we use the version 2 of OMPS-LP (i.e. the Limb Profiler) for comparison with the o-suite and BASCOE; note that it should not be confused with the nadir profiler (Kramarova et al., 2014; Taha et al., 2014). Figure 3.6.9 shows that in the lower stratosphere (30-70hPa) there is a systematic overestimation by the o-suite (5 to 10%) and to a lesser extent by BASCOE, except over the Antarctic in September-November (i.e. ozone hole season) where the o-suite underestimates ozone by up to 8%. Hence the polar ozone depletion described by the o-suite analyses is stronger than observed by OMPS-LP.

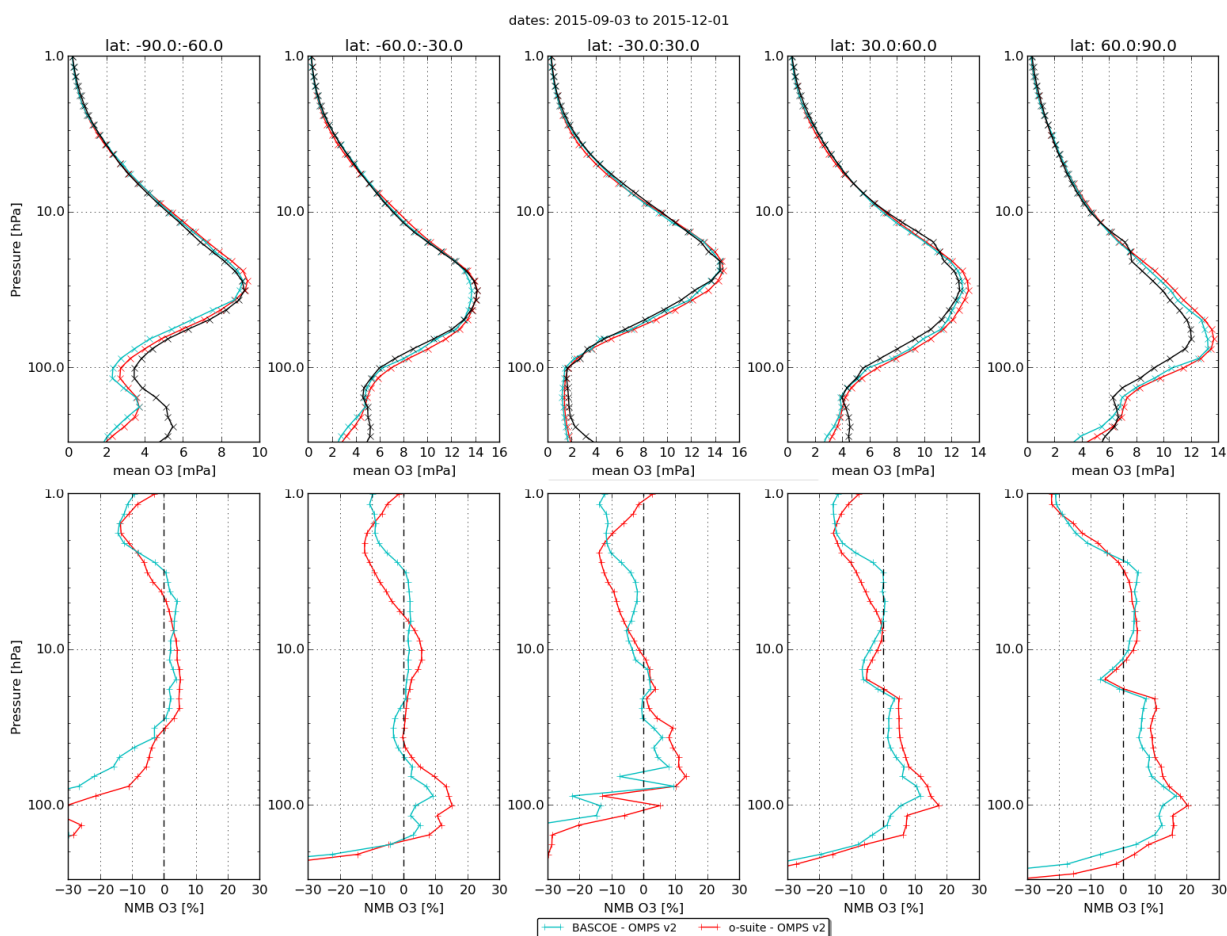


Figure 3.6.10: Mean value expressed in partial pressure (top) and normalized mean bias (bottom) of the ozone profile between o-suite (red line) and BASCOE (cyan line) with OMPS-LP v2 observations for the period June-July-August 2015.

The bottom row of fig. 3.6.9 shows the standard deviation of the differences and can be used to evaluate the random error in the analyses. Hence in the lower stratosphere, the random error of the o-suite is evaluated at 7% to 10% in the Tropics and varies in the polar regions from 5% (summer and fall) to 10% (winter and spring).

Figure 3.6.10 displays vertical profiles of the relative biases between the o-suite or BASCOE and OMPS-LP. The difference is averaged over the most recent 3-month period considered in this validation report, i.e. September-October-November 2015. In the northern hemisphere, a vertical discontinuity of the relative differences is noted at 20 hPa, but this is a spurious feature due to a vertical discontinuity in the OMPS retrievals used here (transition from UV to visible detector).

This quantitative comparison with OMPS-LP confirms the good agreement in the middle stratosphere while the lower stratosphere (< 70hPa) reveals stronger discrepancies. The comparison with BASCOE confirms that the lower stratospheric vertical oscillations seen against Aura-MLS in the Tropical band (figure 3.6.9) are an artifact.



3.7 Stratospheric NO₂

In this section, nitrogen dioxide from SCIAMACHY/Envisat satellite retrievals (IUP-UB v0.7) and GOME-2/MetOp-A satellite retrievals (IUP-UB v1.0) are used to validate modelled stratospheric NO₂ columns. Monthly mean stratospheric NO₂ columns from SCIAMACHY and GOME-2 have relatively small errors of the order of 20% in the tropics and in mid-latitudes in summer and even lower errors at mid-latitudes in winter. As the time resolution of the saved model files is rather coarse and NO_x photochemistry in the stratosphere has a large impact on the NO₂ columns at low sun, some uncertainty is introduced by the time interpolation at high latitudes in winter.

As shown in Fig. 3.7.1, amplitude and seasonality of satellite stratospheric NO₂ columns are very well reproduced by MOZART chemistry without data assimilation (MACC_fcnrt_MOZ), especially northwards of 30°S. However, this is not the case for CB05 chemistry runs and the most recent version of the o-suite. The significant differences between the observations and the CB05 chemistry runs can be explained by the missing stratospheric chemistry for these model runs. The only constraint on stratospheric NO_x is implicitly made by fixing the HNO₃/O₃ ratio at the 10 hPa level. This assumption, in combination with the changing model settings for stratospheric O₃ for control compared to MACC_CIFS_TM5, may explain some of the jumps we see in stratospheric NO₂. In any of these runs the stratospheric NO₂ is poorly constrained. It clearly indicates that stratospheric NO₂ in the latest version of the o-suite is not a useful product and should be disregarded.

Comparison of the o-suite from July 2012 until August 2014 with the other model runs and satellite observations shows that the previous version of the o-suite stratospheric NO₂ columns have a systematic low bias relative to those from MACC_fcnrt_MOZ and satellite observations for all latitude bands. For example, o-suite values are a factor of 2 smaller than satellite values between 60°S to 90°S for October 2013.

Details on the NO₂ evaluation can be found at:

http://www.doas-bremen.de/macc/macc_veri_iup_home.html.

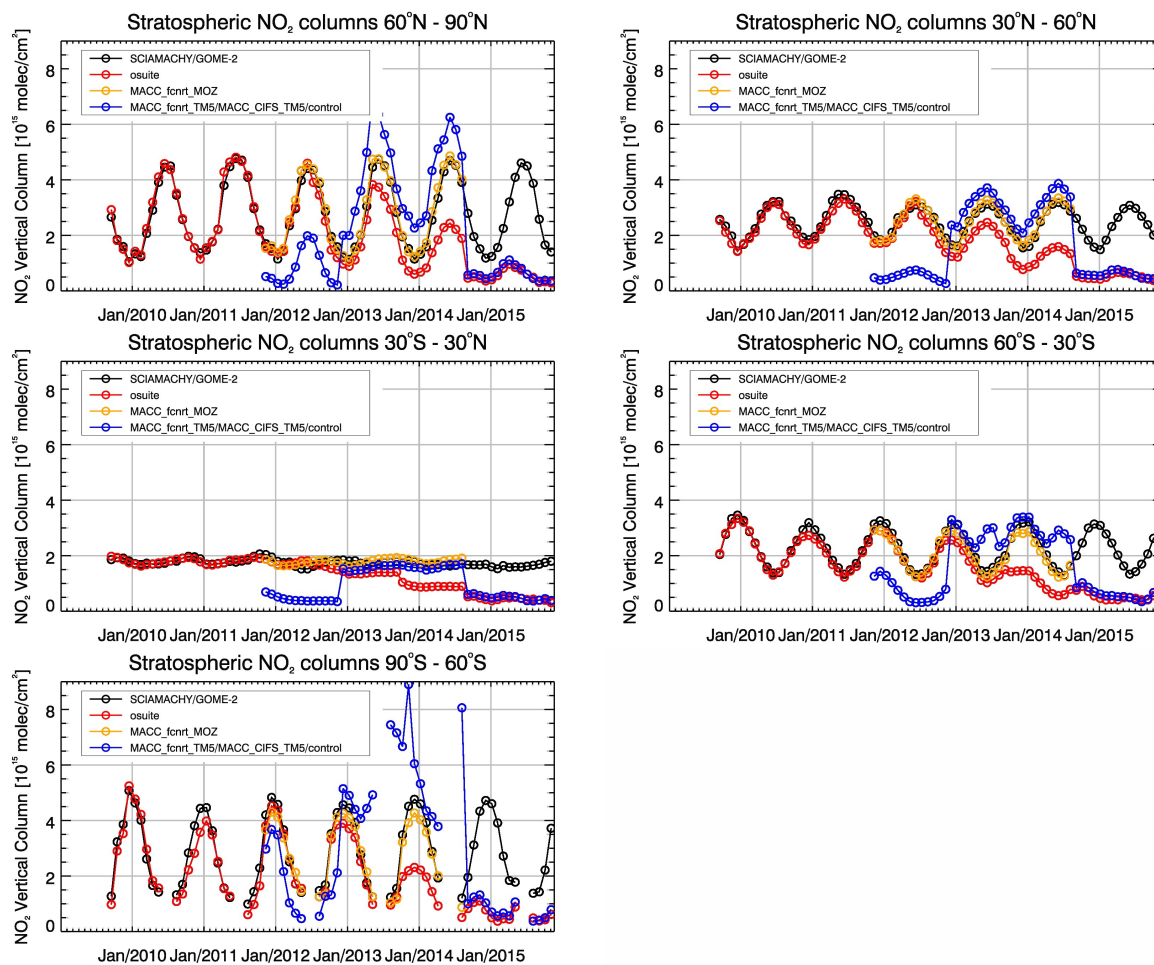


Figure 3.7.1: Time series of average stratospheric NO₂ columns [10¹⁵ molec cm⁻²] from SCIAMACHY (up to March 2012) and GOME-2 (from April 2012) compared to model results for different latitude bands. See text for details. The blue line shows MACC_fcprt_TM5 from November 2011 to November 2012, MACC_CIFS_TM5 results from December 2012 until August 2014 and control results from September 2014 onwards.

4 Events

This section describes the validation results of the CAMS NRT global system for events that took place up to November 2015.

4.1 Fires in Indonesia, September-October 2015

2015 was marked by a strong El Niño event which intensified the dry season over large regions in Indonesia. September and October 2015 were characterized by the largest number of fire events in Indonesia since the start of the CAMS reprocessing for 2003, and the emissions are likely the highest since the last large El Niño event from 1997 (see also <http://atmosphere.copernicus.eu/news-and-media/news/smoke-and-carbon-emission-worsen-south-east-asia%E2%80%99s-fires>). In Figure 4.1.1 the main fire emission regions over Sumatra and Borneo as detected from the MODIS satellite instrument in September and October are shown. The corresponding aerosol alert map for the o-suite for 22 October 2015 shows daily mean aerosol AOD simulated as being significantly larger than climatology, associated with the excessive aerosol loadings during this event.

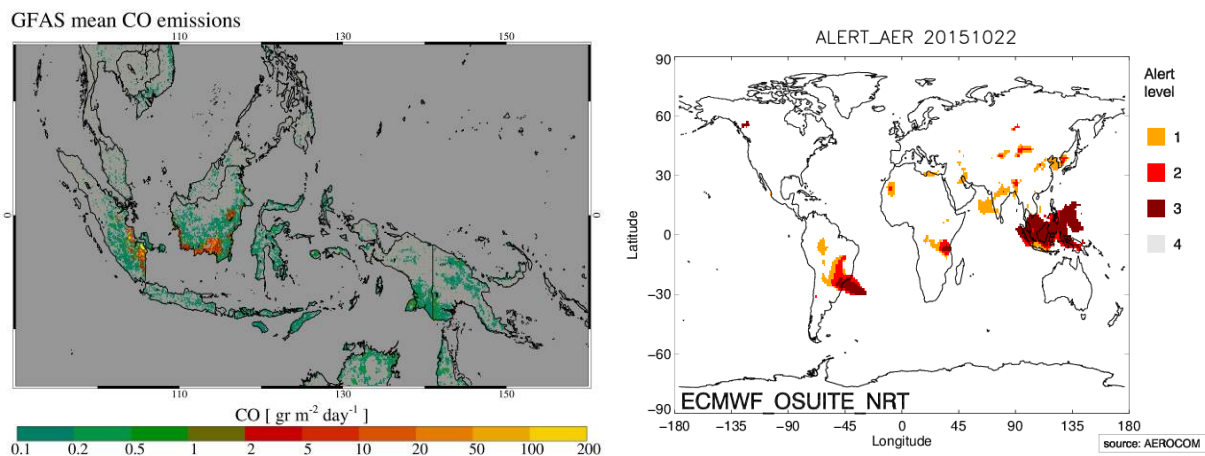


Fig.4.1.1 Left: Mean GFAS CO emissions during September-October 2015. Right: Aerosol alert map for 22 October 2015 derived from the o-suite.

Daily CO total columns from the model simulations over a region covering Indonesia (70°E-150°E and 11°S – 6°N) for September and October 2015 were compared to IASI and MOPITT data. Observations show an area-average increase of CO total column from $\sim 2 \times 10^{18}$ molec cm⁻² in the beginning of September to $\sim 4.5 \times 10^{18}$ molec cm⁻² in IASI and 3×10^{18} molec cm⁻² in MOPITT by the end of October, Figure 4.1.2. Evaluation of model results shows that the o-suite CO total columns are in agreement with both the satellite observations,

considering that model sampling and averaging kernels lead to different model columns for MOPITT and IASI evaluations. The control run shows a growing positive bias by ~ 0.2 to 1.0×10^{18} molec cm^{-2} . At the end of October both o-suite and control runs overestimated IASI CO data, associated with a change in observation density due to growing cloud coverage. In this period also the seasonal rains have started, extinguishing many of the fires. In November the average CO columns decrease again to more normal levels.

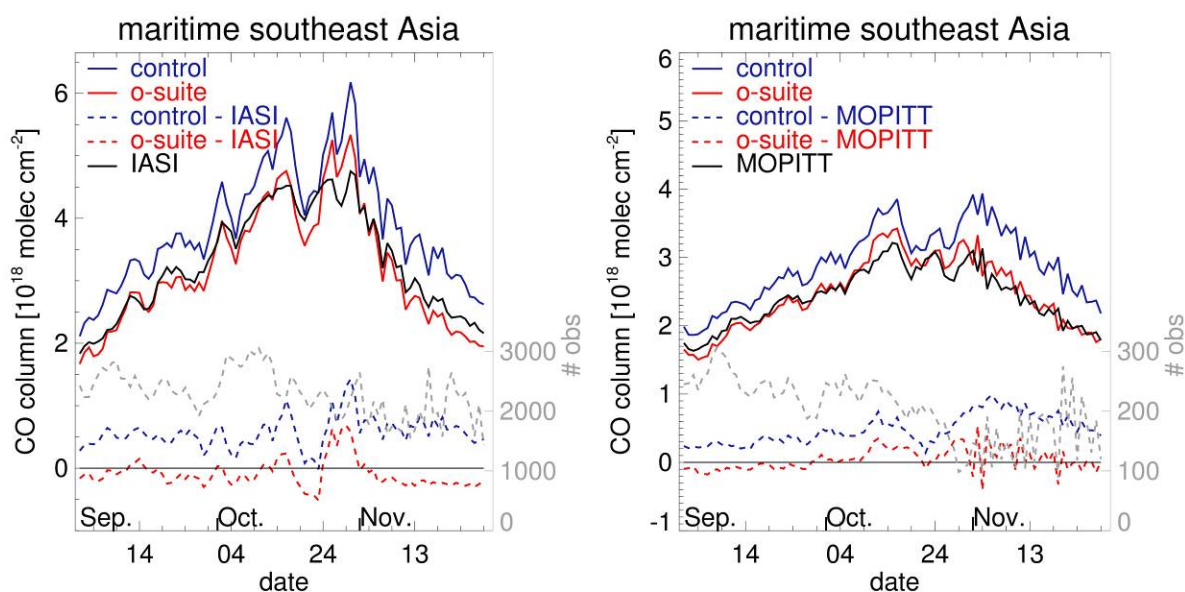


Fig.4.1.2 Time series of three-day running mean CO total column from model simulations and IASI (left) and MOPITT (right) satellite observations over a region including Indonesia and its outflow region over the ocean (70°E-150°E and 11°S - 6°N), and their biases (dashed lines). The scaled daily number of available observations (right axis) is given in gray.

The geographical distribution on 11, 13 September and 22, 25 October 2015 of the CO fire plume can be seen in Fig. 4.1.3. Note that this region is larger than the one shown on Fig.4.1.2. IASI data show a plume with very high values in September, but still largely confined to the Indonesian islands. In October the air parcels with high CO concentrations is more spread, ranging from the Indian Ocean to the Philippine Sea. Both runs captured location of the plume in September. In October, it can be seen that the o-suite is in better match IASI over the land areas and shows underestimation over the Indian Ocean. The control run shows an overestimation over land, but better matches IASI over the Indian Ocean. Figure 4.1.4 suggests a net positive bias in GFAS CO emissions over Indonesia, mostly attributed to Sumatra, while there negative biases in emissions appear over Borneo and West Papua.

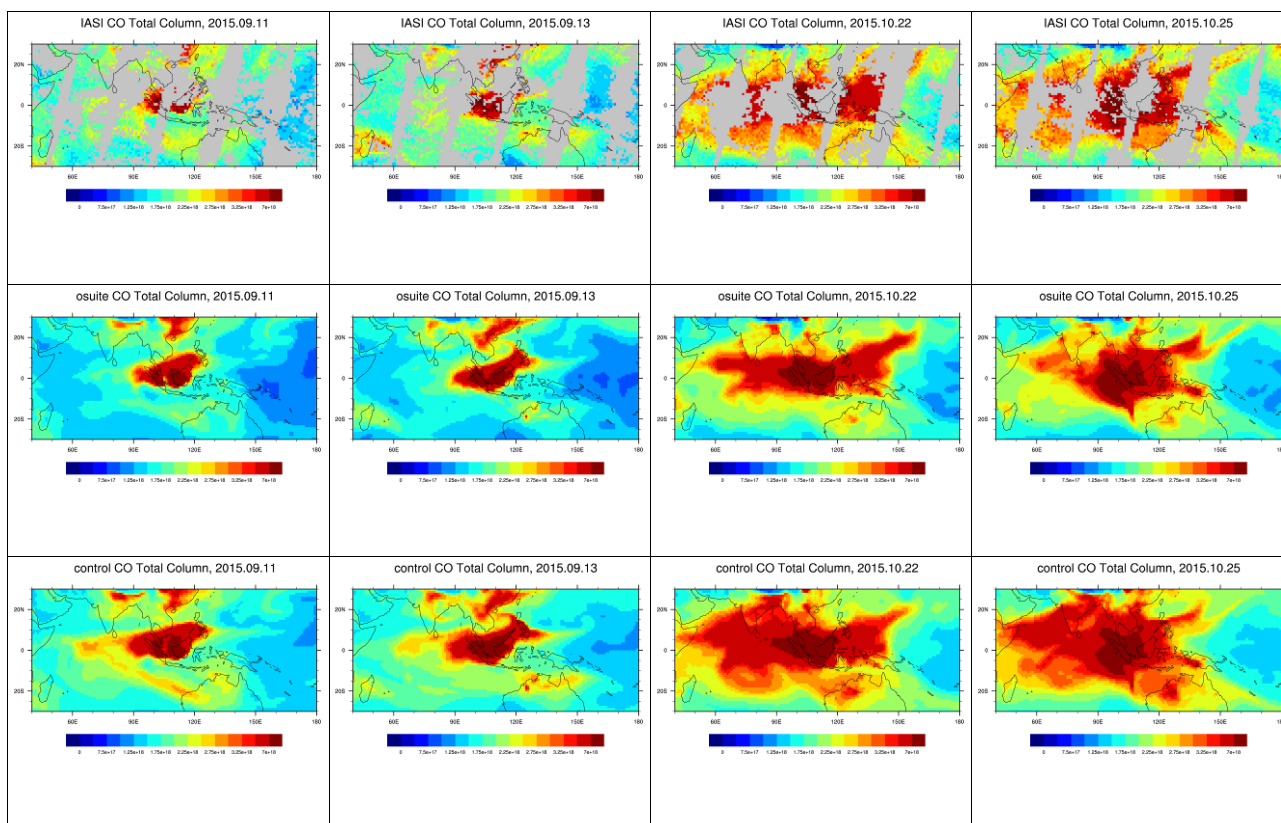


Fig.4.1.3 CO total column from IASI (top), o-suite (middle) and control run (bottom) for 11, 13 September and 22, 25 October 2015 over the selected region.

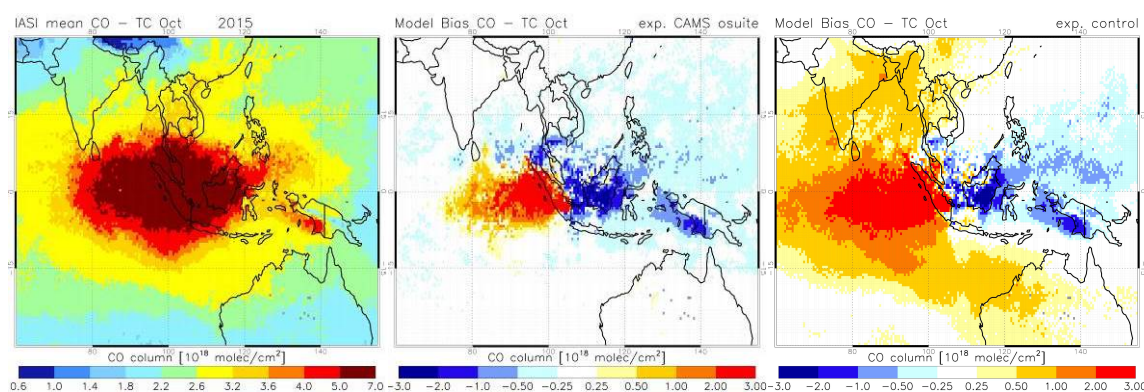


Fig.4.1.4. IASI monthly mean CO TC (left), and corresponding bias for o-suite (middle) and control (right), for October 2015.

Evaluation against HCHO suggests further that emissions used by CIFS-CB05 seem to be largely overestimated, resulting in model simulated HCHO columns which are almost twice as large as those retrieved by GOME-2. Note that a cloud flag (using only data with less than 20% cloud fraction) was applied to satellite retrievals shown in Figure 4.1.5 and model values correspond to these cloud flagged regions only. This may potentially cause an underestimation in

satellite retrieved values, if smoke plumes are incorrectly classified as clouds. However, further investigation using non-cloud-flagged satellite data and corresponding collocated o-suite data (see Figure 4.1.x) also shows the strong overestimation of the peak observed for September and October 2015, with satellite retrieved and o-suite values not very much larger compared to the cloud-flagged case.

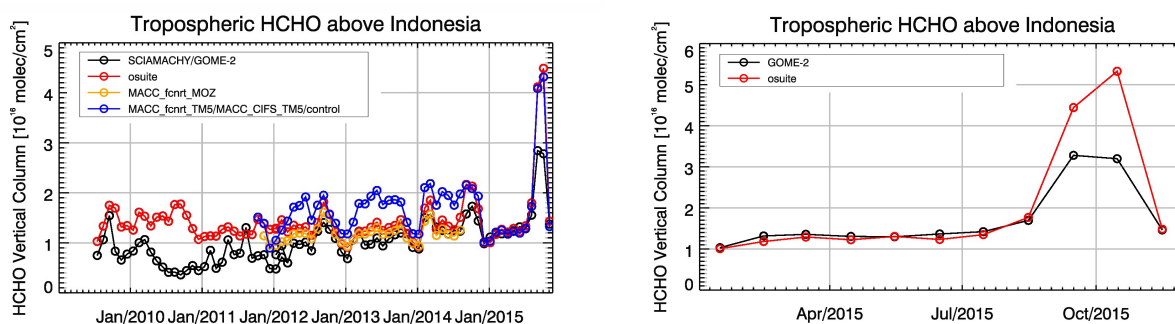


Figure 4.1.5: Left: HCHO time series over Indonesia, filtered for clouds. Right: o-suite HCHO without cloud-flagged data over Indonesia for 2015. See text for further details.

4.2 A dust event over Canary Islands in November 2015

A dust event was selected in the period around 13 November, when a high layer of dust moved from north-western Africa covering the area around the Canary Islands. Three-hourly dust aerosol optical depth (DOD) from CAMS o-suite has been compared with AOD from MODIS in order to see the skill of CAMS o-suite to track the spatio-temporal evolution of the dust plume (Figure 4.2.1). The near-real-time MODIS aerosol product available through the NASA's EOSDIS system (MCDAODHD files), is used for this purpose. It is a level 3 gridded product specifically designed for quantitative applications including data assimilation and model validation. DOD simulated by CAMS o-suite and observed AOD by MODIS from 11th to 15th November 2015 at 12UTC is shown in Figure 4.2.2. Moreover, DOD values from CAMS o-suite have been compared with those from CAMS control, the Multi-Median model generated from the models participating in the WMO SDS-WAS NAMEE Regional Node (<http://sds-was.aemet.es/>), MODIS AOD, and AERONET AOD (Level 1.5) in four AERONET stations strategically located along the path of the dust plume over the Canary Islands (Santa Cruz de Tenerife and Izana sites) and North Western Africa (Capo Verde and Oujda-Morocco sites). Results are shown in Figure 4.2.3.

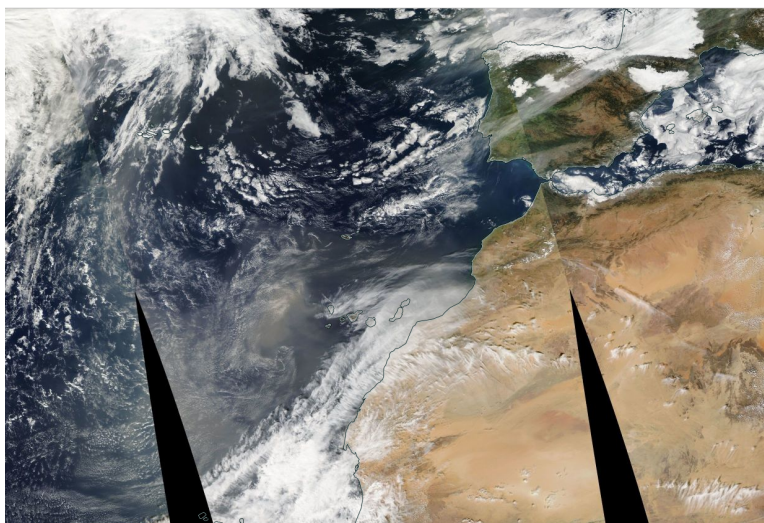


Figure 4.2.1. MODIS-Aqua image, 13 November 14:35 UTC.

Dust mobilization is confined over Mauritania on 9th November caused by an anticyclone over Iberian Peninsula. Over Morocco (see Oujda in Figure 4.2.3), low AOD and high AE are observed during all the study period. The next days, dust is blown over sub-Tropical Atlantic region affecting Canary Islands from 11 to 16 November (see Figure 4.2.2). The two AERONET sites at Tenerife (Santa Cruz de Tenerife and Izana; see Figure 4.2.3) show consecutively an increase in aerosol optical depth (AOD up to 0.5 in Santa Cruz de Tenerife) associated to a sharp decrease of the Ångström Exponent (AE) caused by the arrival of the dust plume. In Santa Cruz de Tenerife some isolated values with AOD ~ 2 , probably are associated to cloud contamination. Dense clouds were present during all the event, see a long cumulus line over the Islands in Figure 4.2.1.

The o-suite is able to timely reproduce the spatial distribution of the dust plume as observed by MODIS (Figure 4.2.2) over the ocean, although the spatial extent of the dust layer is quite low. We can see how CAMS o-suite tracks fairly well the changes in the shape and size of the dust layer throughout the episode. CAMS o-suite, CAMS control and SDS-WAS Multi-Median models show a clear overestimation on the onset of the dust event in both the Santa Cruz de Tenerife and Izana stations. At Izana station, which is at 2,400 m a.s.l., CAMS o-suite, CAMS control and SDS-WAS Multi-Median show a slightly higher overestimation. This is explained by the fact that during this episode the dust layer was confined <4 km a.s.l. over Canary Islands, as confirmed CALIPSO observations. The whole episode is well simulated by CAMS o-suite and CAMS control, although in Santa Cruz de Tenerife and Izana stations (see Figure 4.2.3) on 11nd-16th November CAMS o-suite better reproduces the AOD peak than CAMS control.

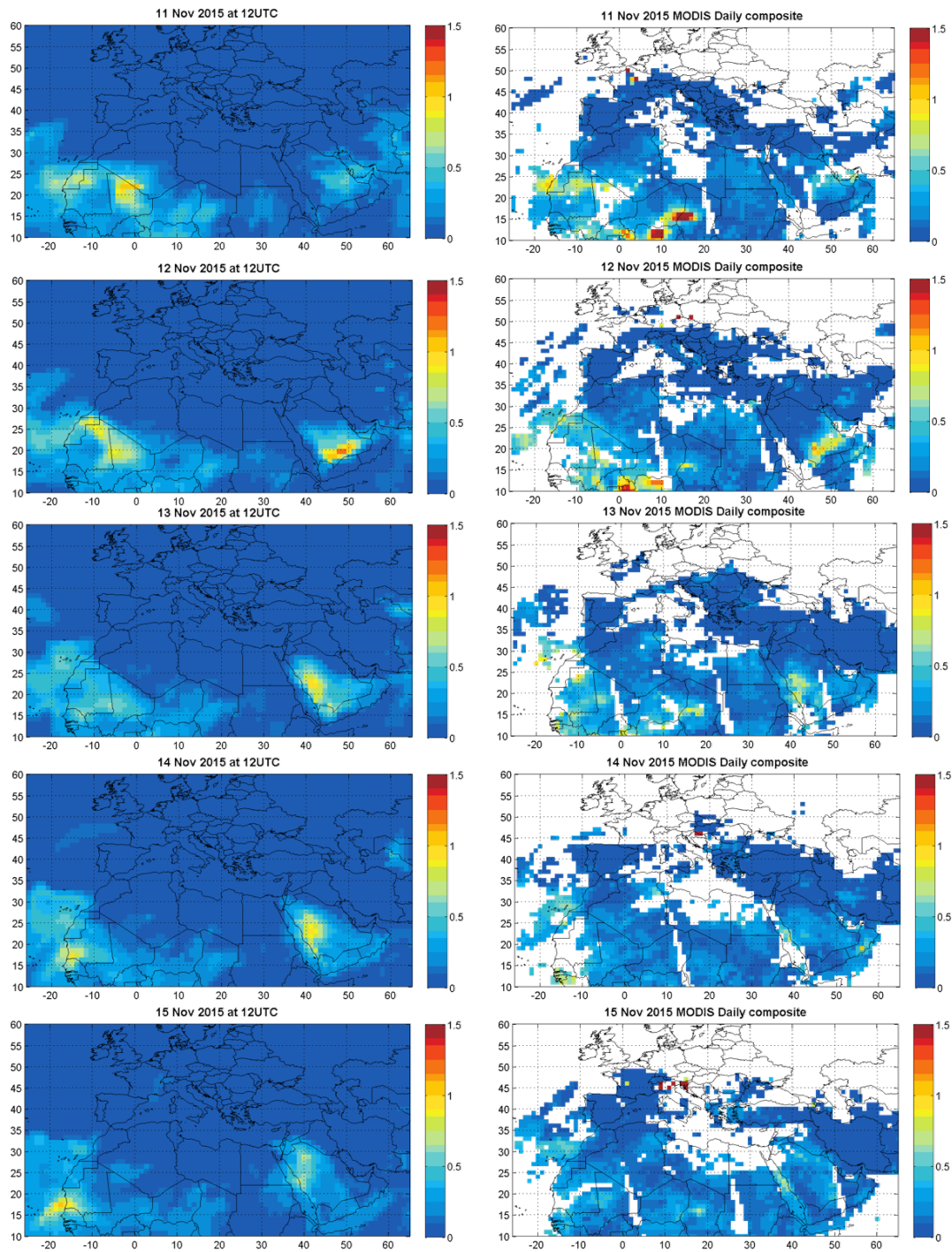


Figure 4.2.2. DOD from o-suite (right column) and AOD from MODIS (left column), for November 11th-15th, 2015 at 12UTC.

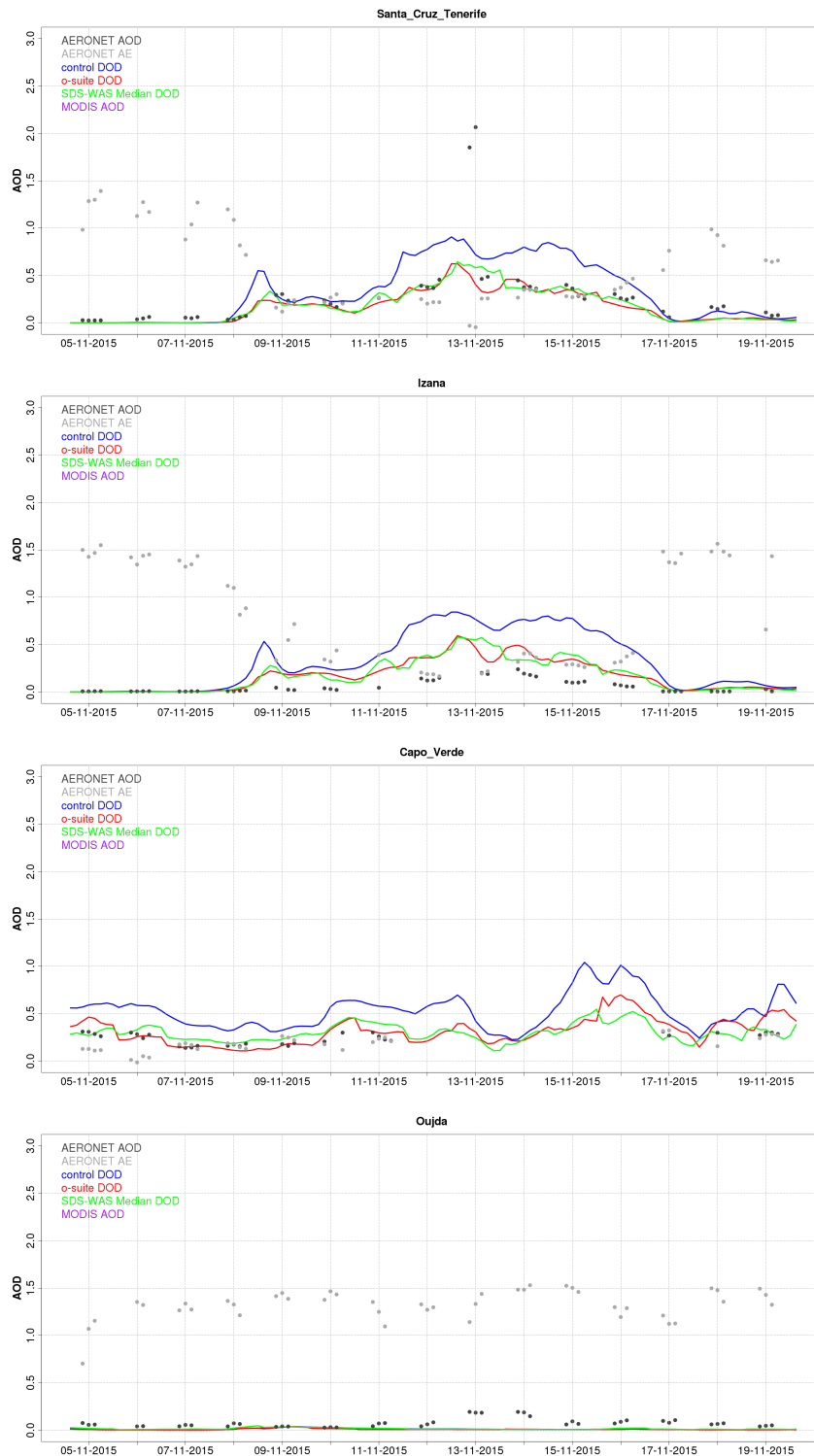


Figure 4.2.3. AOD at 550 nm from AERONET (black), DOD at 550 nm from the o-suite (blue), DOD at 550 nm from the control run (red), AOD retrieved from MODIS-AQUA (purple triangles) and DOD at 550 nm from SDS-WAS Multi-model Median (green) at Santa Cruz de Tenerife, Izana, Capo Verde and Oujda AERONET sites during the case analysis from 5th to 20th November 2015.



5 References

Benedetti, A., J.-J. Morcrette, O. Boucher, A. Dethof, R. J. Engelen, M. Fisher, H. Flentjes, N. Huneus, L. Jones, J. W. Kaiser, S. Kinne, A. Mangold, M. Razinger, A. J. Simmons, M. Suttie, and the GEMS-AER team: Aerosol analysis and forecast in the ECMWF Integrated Forecast System. Part II : Data assimilation, *J. Geophys. Res.*, 114, D13205, doi:10.1029/2008JD011115, 2009.

Cariolle, D. and Teyssède, H.: A revised linear ozone photochemistry parameterization for use in transport and general circulation models: multi-annual simulations, *Atmos. Chem. Phys.*, 7, 2183-2196, doi:10.5194/acp-7-2183-2007, 2007.

Dee, D. P. and S. Uppala, Variational bias correction of satellite radiance data in the ERA-Interim reanalysis. *Quart. J. Roy. Meteor. Soc.*, 135, 1830-1841, 2009.

Deeter, M. N., Emmons, L. K., Edwards, D. P., Gille, J. C., and Drummond, J. R.: Vertical resolution and information content of CO profiles retrieved by MOPITT, *Geophys. Res. Lett.*, 31, L15112, doi:10.1029/2004GL020235, 2004.

Deeter, M. N., et al. (2010), The MOPITT version 4 CO product: Algorithm enhancements, validation, and long-term stability, *J. Geophys. Res.*, 115, D07306, doi:10.1029/2009JD013005.

de Mazière, M., et al., D8.1 NORS Validation server user requirements document, available as NORS deliverable at <http://nors.aeronomie.be/>, 2012

de Mazière, M., et al., D4.2 NORS Data user guide, 2013, available as NORS deliverable at <http://nors.aeronomie.be/>, 2013

Deshler, T., J.L. Mercer, H.G.J. Smit, R. Stubi, G. Levrat, B.J. Johnson, S.J. Oltmans, R. Kivi, A.M. Thompson, J. Witte, J. Davies, F.J. Schmidlin, G. Brothers, T. Sasaki (2008) Atmospheric comparison of electrochemical cell ozonesondes from different manufacturers, and with different cathode solution strengths: The Balloon Experiment on Standards for Ozonesondes. *J. Geophys. Res.* 113, D04307, doi:10.1029/2007JD008975

Dupuy, E., et al.: Validation of ozone measurements from the Atmospheric Chemistry Experiment (ACE), *Atmos. Chem. Phys.*, 9, 287-343, doi:10.5194/acp-9-287-2009, 2009.

Elbern, H., Schwinger, J., Botchorishvili, R.: Chemical state estimation for the middle atmosphere by four-dimensional variational data assimilation: System configuration. *Journal of Geophysical Research (Atmospheres)* 115, 6302, 2010.

Elguindi, N., Clark, H., Ordóñez, C., Thouret, V., Flemming, J., Stein, O., Huijnen, V., Moinat, P., Inness, A., Peuch, V.-H., Stohl, A., Turquety, S., Athier, G., Cammas, J.-P., and Schultz, M.: Current status of the ability of the GEMS/MACC models to reproduce the tropospheric CO vertical distribution as measured by MOZAIC, *Geosci. Model Dev.*, 3, 501-518, doi:10.5194/gmd-3-501-2010, 2010.

Emmons, L. K., D. P. Edwards, M. N. Deeter, J. C. Gille, T. Campos, P. Nédélec, P. Novelli, and G. Sachse, Measurements of Pollution In The Troposphere (MOPITT) validation through 2006 *Atmos. Chem. Phys.*, 9, 1795-1803, 2009

Errera, Q., Daerden, F., Chabrillat, S., Lambert, J. C., Lahoz, W. A., Viscardy, S., Bonjean, S., and Fonteyn, D., 4D-Var Assimilation of MIPAS chemical observations: ozone and nitrogen dioxide analyses, *Atmos. Chem. Phys.*, 8, 6169-6187, 2008.

Errera, Q. and Ménard, R.: Technical Note: Spectral representation of spatial correlations in variational assimilation with grid point models and application to the belgian assimilation system for chemical observations (BASCOE), *Atmos. Chem. Phys. Discuss.*, 12, 16763-16809, doi:10.5194/acpd-12-16763-2012, 2012.

Eskes, H., Huijnen, V., Arola, A., Benedictow, A., Blechschmidt, A.-M., Botek, E., Boucher, O., Bouarar, I., Chabrillat, S., Cuevas, E., Engelen, R., Flentje, H., Gaudel, A., Griesfeller, J., Jones, L., Kapsomenakis, J.,



Katragkou, E., Kinne, S., Langerock, B., Razinger, M., Richter, A., Schultz, M., Schulz, M., Sudarchikova, N., Thouret, V., Vrekoussis, M., Wagner, A., and Zerefos, C.: Validation of reactive gases and aerosols in the MACC global analysis and forecast system, *Geosci. Model Dev.*, 8, 3523-3543, [doi:10.5194/gmd-8-3523-2015](https://doi.org/10.5194/gmd-8-3523-2015), 2015.

Flemming, J., Huijnen, V., Arteta, J., Bechtold, P., Beljaars, A., Blechschmidt, A.-M., Diamantakis, M., Engelen, R. J., Gaudel, A., Inness, A., Jones, L., Josse, B., Katragkou, E., Marecal, V., Peuch, V.-H., Richter, A., Schultz, M. G., Stein, O., and Tsikerdekis, A.: Tropospheric chemistry in the Integrated Forecasting System of ECMWF, *Geosci. Model Dev.*, 8, 975-1003, [doi:10.5194/gmd-8-975-2015](https://doi.org/10.5194/gmd-8-975-2015), 2015.

Franco, B., et al., Retrievals of formaldehyde from ground-based FTIR and MAX-DOAS observations at the Jungfraujoch station and comparisons with GEOS-Chem and IMAGES model simulations, *Atmos. Meas. Tech.*, 8, 1733-1756, 2015

Gielen, C., Van Roozendaal, M., Hendrick, F., Pinardi, G., Vlemmix, T., De Bock, V., De Backer, H., Fayt, C., Hermans, C., Gillotay, D., and Wang, P.: A simple and versatile cloud-screening method for MAX-DOAS retrievals, *Atmos. Meas. Tech.*, 7, 3509-3527, [doi:10.5194/amt-7-3509-2014](https://doi.org/10.5194/amt-7-3509-2014), 2014.

Granier, C. et al.: Evolution of anthropogenic and biomass burning emissions of air pollutants at global and regional scales during the 1980–2010 period. *Climatic Change* (109), 2011

Holben, B. N., Eck, T. F., Slutsker, I., Tanré, D., Buis, J. P., Setzer, A., Vermote, E., Reagan, J. A., Kaufman, Y. J., Nakajima, T., Lavenu, F., Jankowiak, I., and Smirnov A.: AERONET – a federated instrument network and data archive for aerosol characterization, *Remote Sens. Environ.*, 66, 1–16, 5529, 5533, 5537, 5544, 1998.

Huijnen, V., et al.: The global chemistry transport model TM5: description and evaluation of the tropospheric chemistry version 3.0, *Geosci. Model Dev.*, 3, 445-473, [doi:10.5194/gmd-3-445-2010](https://doi.org/10.5194/gmd-3-445-2010), 2010.

Inness, A., Blechschmidt, A.-M., Bouarar, I., Chabrillat, S., Crepulja, M., Engelen, R. J., Eskes, H., Flemming, J., Gaudel, A., Hendrick, F., Huijnen, V., Jones, L., Kapsomenakis, J., Katragkou, E., Keppens, A., Langerock, B., de Mazière, M., Melas, D., Parrington, M., Peuch, V. H., Razinger, M., Richter, A., Schultz, M. G., Suttie, M., Thouret, V., Vrekoussis, M., Wagner, A., and Zerefos, C.: Data assimilation of satellite-retrieved ozone, carbon monoxide and nitrogen dioxide with ECMWF's Composition-IFS, *Atmos. Chem. Phys.*, 15, 5275-5303, [doi:10.5194/acp-15-5275-2015](https://doi.org/10.5194/acp-15-5275-2015), 2015.

Jaross, G., Bhartia, P.K., Chen, G., Kowitt, M., Haken, M., Chen, Z., Xu, Ph., Warner, J., Kelly, T. : OMPS Limb Profiler instrument performance assessment, *J. Geophys. Res. Atmos* 119, 2169-8996, 2014.

Kaiser, J. W., Heil, A., Andreae, M. O., Benedetti, A., Chubarova, N., Jones, L., Morcrette, J.-J., Razinger, M., Schultz, M. G., Suttie, M., and van der Werf, G. R.: Biomass burning emissions estimated with a global fire assimilation system based on observed fire radiative power, *Biogeosciences*, 9, 527-554, [doi:10.5194/bg-9-527-2012](https://doi.org/10.5194/bg-9-527-2012), 2012.

Kramarova, N. A., Nash, E. R., Newman, P. A., Bhartia, P. K., McPeters, R. D., Rault, D. F., Seftor, C. J., Xu, P. Q., and Labow, G. J.: Measuring the Antarctic ozone hole with the new Ozone Mapping and Profiler Suite (OMPS), *Atmos. Chem. Phys.*, 14, 2353-2361, [doi:10.5194/acp-14-2353-2014](https://doi.org/10.5194/acp-14-2353-2014), 2014.

Lahoz, W. A., Errera, Q., Viscardy, S., and Manney G. L., The 2009 stratospheric major warming described from synergistic use of BASCOE water vapour analyses and MLS observations, *Atmos. Chem. Phys.* 11, 4689-4703, 2011

Lambert, A, et al., Aura Microwave Limb Sounder Version 3.4 Level-2 near real-time data user guide, <http://disc.sci.gsfc.nasa.gov/Aura/data-holdings/MLS/documents/NRT-user-guide-v34.pdf>

Lefever, K., van der A, R., Baier, F., Christophe, Y., Errera, Q., Eskes, H., Flemming, J., Inness, A., Jones, L., Lambert, J.-C., Langerock, B., Schultz, M. G., Stein, O., Wagner, A., and Chabrillat, S.: Copernicus stratospheric ozone service, 2009–2012: validation, system intercomparison and roles of input data sets, *Atmos. Chem. Phys.*, 15, 2269-2293, [doi:10.5194/acp-15-2269-2015](https://doi.org/10.5194/acp-15-2269-2015), 2015.



Liu, Z., et al., *Exploring the missing source of glyoxal (CHOCHO) over China*, *Geophys. Res. Lett.*, 39, L10812, doi: 10.1029/2012GL051645, 2012

Logan, J., *An analysis of ozonesonde data for the troposphere: Recommendations for testing 3-D models and development of a gridded climatology for tropospheric ozone*, *J. Geophys. Res.*, 104, pp. 16,115-16,149, 1999.

Morcrette, J.-J., O. Boucher, L. Jones, D. Salmond, P. Bechtold, A. Beljaars, A. Benedetti, A. Bonet, J. W. Kaiser, M. Razinger, M. Schulz, S. Serrar, A. J. Simmons, M. Sofiev, M. Suttie, A. M. Tompkins, and A. Untch: *Aerosol analysis and forecast in the ECMWF Integrated Forecast System. Part I: Forward modelling*, *J. Geophys. Res.*, 114, D06206, doi:10.1029/2008JD011235, 2009.

Oltmans, SJ and Levy II, H, *Surface ozone measurements from a global network*, *Atmos. Environ.*, 28, 9-24, 1994.

O'Neill, N. T., Eck, T. F., Smirnov, A., Holben, B. N. and Thulasiraman, S., *Spectral discrimination of coarse and fine mode optical depth*, *J. Geophys. Res.*, 108, 4559, 2003.

Pumphrey, H. C., M. L. Santee, N. J. Livesey, M. J. Schwartz, and W. G. Read: *Microwave Limb Sounder observations of biomass-burning products from the Australian bush fires of February 2009*, *Atmos. Chem. Phys.*, 11, 6285-6296, 2011

Richter, A., Burrows, J. P., Nüß, H., Granier, C, Niemeier, U.: *Increase in tropospheric nitrogen dioxide over China observed from space*, *Nature*, 437, 129-132, doi: 10.1038/nature04092, 2005

Richter, A., Begoin, M., Hilboll, A., and Burrows, J. P.: *An improved NO₂ retrieval for the GOME-2 satellite instrument*, *Atmos. Meas. Tech.*, 4, 1147-1159, doi:10.5194/amt-4-1147-2011, 2011

Santer, B.D., R. Sausen, T. M. L. Wigley, J. S. Boyle, K. AchutaRao, C. Doutriaux, J. E. Hansen, G. A. Meehl, E. Roeckner, R. Ruedy, G. Schmidt, and K. E. Taylor, *Behavior of tropopause height and atmospheric temperature in models, reanalyses, and observations: Decadal changes*, *JGR*, VOL. 108, NO. D1, 4002, doi:10.1029/2002JD002258, 2003.

Seckmeyer G., A. Bais, G. Bernhard, M. Blumthaler, C.R. Booth, K. Lantz, R.L. McKenzie, P. Disterhoft, and A. Webb (2006), *Instruments to measure solar ultraviolet radiation Part 2: Broadband instruments measuring erythemally weighted solar irradiance*. Draft available at: http://www.wmo.ch/web/arep/reports/gaw164_final_draft.pdf, WMO/GAW No. 164 World Meteorological Organisation, Geneva.

Sindelarova, K., Granier, C., Bouarar, I., Guenther, A., Tilmes, S., Stavrakou, T., Müller, J.-F., Kuhn, U., Stefani, P., and Knorr, W.: *Global data set of biogenic VOC emissions calculated by the MEGAN model over the last 30 years*, *Atmos. Chem. Phys.*, 14, 9317-9341, doi:10.5194/acp-14-9317-2014, 2014.

Smit, H.G.J., W. Straeter, B.J. Johnson, S.J. Oltmans, J. Davies, D.W. Tarasick, B. Hoegger, R. Stubi, F.J. Schmidlin, T. Northam, A.M. Thompson, J.C. Witte, I. Boyd: *Assessment of the performance of ECC-ozonesondes under quasi-flight conditions in the environmental simulation chamber: Insights from the Juelich Ozone Sonde Intercomparison Experiment (JOSIE)*, *J. Geophys. Res.* 112, D19306, doi:10.1029/2006JD007308, 2007.

Stavrakou, T., *First space-based derivation of the global atmospheric methanol fluxes*, *Atm. Chem. Phys.*, 11, 4873-4898, 2013

Taha, G.; Jaross, G. R.; Bhartia, P. K.: *Validation of OMPS LP Ozone Profiles Version 2.0 with MLS, Ozone Sondes and Lidar Measurements*, *American Geophysical Union, Fall Meeting 2014*, abstract #A33J-3322, 2014.

Taylor, K.E.: *Summarizing multiple aspects of model performance in a single diagram*. *J. Geophys. Res.*, 106, 7183-7192, 2001.

van der A, R. J. , M. A. F. Allaart, and H. J. Eskes, *Multi sensor reanalysis of total ozone*, *Atmos. Chem. Phys.*, 10, 11277-11294, doi:10.5194/acp-10-11277-2010, www.atmos-chem-phys.net/10/11277/2010/, 2010



van der A, R., M. Allaart, H. Eskes, K. Lefever, Validation report of the MACC 30-year multi-sensor reanalysis of ozone columns Period 1979-2008, MACC-II report, Jan 2013, [MACCII_VAL_DEL_D_83.3_OzoneMSRv1_20130130.docx/pdf](#)

Vrekoussis, M., Wittrock, F., Richter, A., and Burrows, J. P.: GOME-2 observations of oxygenated VOCs: what can we learn from the ratio glyoxal to formaldehyde on a global scale?, *Atmos. Chem. Phys.*, **10**, 10145-10160, doi:10.5194/acp-10-10145-2010, 2010

Wang, P., P. Stammes, R. van der A, G. Pinardi, M. van Roozendael, FRESCO+: an improved O2 A-band cloud retrieval algorithm for tropospheric trace gas retrievals, *Atmospheric Chemistry and Physics*, **8**, 6565-6576, 2008

Wittrock, F., A. Richter, H. Oetjen, J. P. Burrows, M. Kanakidou, S. Myriokefalitakis, R. Volkamer, S. Beirle, U. Platt, and T. Wagner, Simultaneous global observations of glyoxal and formaldehyde from space, *Geophys. Res. Lett.*, **33**, L16804, doi:10.1029/2006GL026310, 2006

WMO (2010), *Guidelines for the Measurement of Atmospheric Carbon Monoxide*, GAW Report No. 192, World Meteorological Organization, Geneva, Switzerland, 2010.

WMO (2013), *Guidelines for the Continuous Measurements of Ozone in the Troposphere*, GAW Report No. 209, World Meteorological Organization, Geneva, Switzerland, 2013.



Annex 1: Acknowledgements

Listed below are the authors contributing to the sections in this report. The authors contributing to the model description are also provided, as well as acknowledgements to the validation datasets.

Tropospheric reactive gases reactive gases

Hannah Clark, Valerie Thouret, CNRS-LA (IAGOS)
Annette Wagner, Harald Flentje, DWD (O3 sondes, GAW data)
Miha Razinger, Luke Jones, ECMWF (O3 sondes, GAW CO and O3 data)
Anne Blechschmidt and Andreas Richter, IUB Bremen (GOME-2 NO2, HCHO)
John Kapsomenakis, Christos Zerefos, AA (ESRL)
Kaj Hansen, Ulas Im, AU (Arctic theme)
Bavo Langerock, BIRA (NORS / NDACC)

Tropospheric aerosol

Michael Schulz, MetNo (editor, Aerocom, Aeronet)
Anna Benedictow, Jan Griesfeller, MetNo (Aerocom, Aeronet)
Emilio Cuevas, Carlos Camino, AEMET (AERONET, MODIS/Aqua-DeepBlue)
Enric Terradellas and Francesco Benincasa, AEMET/SDS WAS RC NAMEE
José María Baldasano and Sara Basart, BSC-CNS (BSC-DREAM8b)

Stratospheric reactive gases

Simon Chabrillat, BIRA (editor)
Yves Christophe, BIRA (model intercomparisons)
Bavo Langerock, BIRA (NDACC FTIR, MWR, UVVIS DOAS, LIDAR)
Andreas Richter and Anne Blechschmidt, IUB Bremen (SCIAMACHY NO2)

Reactive gases and aerosol modeling

Johannes Flemming (ECMWF), Antje Inness (ECMWF), Angela Benedetti (ECMWF), Vincent Huijnen (KNMI), Johannes Kaiser (KCL/MPIC/ECMWF), Olivier Boucher (LMD), Martin Schultz (FZ Jülich), Richard Engelen (ECMWF)



Acknowledgements for the validation datasets used

We wish to acknowledge the provision of NRT GAW observational data by: Institute of Atmospheric Sciences and Climate (ISAC) of the Italian National Research Council (CNR), South African Weather Service, National Centre for Atmospheric Science (NCAS, Cape Verde), National Air Pollution Monitoring Network (NABEL) (Federal Office for the Environment FOEN and Swiss Federal Laboratories for Materials Testing and Research EMPA), Atmospheric Environment Division Global Environment and Marine Department Japan Meteorological Agency, Chinese Academy of Meteorological Sciences (CAMS), Alfred Wegener Institut, Umweltbundesamt (Austria), National Meteorological Service (Argentina), Umweltbundesamt (UBA, Germany)

We are grateful to the numerous operators of the Aeronet network and to the central data processing facility at NASA Goddard Space Flight Center for providing the NRT sun photometer data, especially Ilya Slutsker and Brent Holben for sending the data.

We wish to acknowledge the provision of ozone sonde data by the World Ozone and Ultraviolet Radiation Data Centre established at EC in Toronto (<http://woudc.org>), by the Data Host Facility of the Network for the Detection of Atmospheric Composition Change established at NOAA (<http://ndacc.org>), by the Norwegian Institute for Air Research and by the National Aeronautics and Space Administration (NASA).

We wish to thank the NDACC investigators for the provision of observations at Ny Alesund, Bern, Jungfraujoch, Izaña, Xianghe, Harestua, Reunion Maito, Uccle, Hohenpeissen, Mauna Loa, Lauder and Haute Provence.

The authors acknowledge the NOAA Earth System Research Laboratory (ESRL) Global Monitoring Division (GMD) for the provision of ground based ozone concentrations.

The MOPITT CO data were obtained from the NASA Langley Research Center ASDC. We acknowledge the LATMOS IASI group for providing IASI CO data.

SCIAMACHY lv1 radiances were provided to IUP by ESA through DLR/DFD.

Index database and especially to the contributors to that database which provided the measurements for comparisons.

We would like to thank the operators of the IASOA Network for access to surface ozone measurements.

We acknowledge the National Aeronautics and Space Administration (NASA), USA for providing the OMPS limb sounder data (<http://npp.gsfc.nasa.gov/omps.html>) and the Aura-MLS offline data (<http://mls.jpl.nasa.gov/index-eos-mls.php>).



ECMWF Shinfield Park Reading RG2 9AX UK

Contact: info@copernicus-atmosphere.eu